8-2018

Enzymatic Activation of Cannabinoid Pro-Drugs

Anna Theresa Margiotta

UNIVERSITY OF NORTHERN COLORADO
Greeley, Colorado
The Graduate School

ENZYMATIC ACTIVATION OF CANNABINOID PRO-DRUGS

A Thesis Submitted in Partial Fulfillment
of the Requirements for the Degree of
Master of Science

Anna Theresa Margiotta

Natural and Health Sciences
Department of Chemistry and Biochemistry

August 2018

This Thesis by: Anna Theresa Margiotta

Entitled: *Enzymatic Activation of Cannabinoid Pro-Drugs*

has been approved as meeting the requirement for the Degree of Master of Science in College of Natural and Health Sciences in Department of Chemistry and Biochemistry.

Accepted by the Thesis Committee:

_____
Richard M. Hyslop, Ph. D. Chair

_____
Corina E. Brown, Ph. D. Committee Member

_____
David L. Pringle, Ph. D. Committee Member

Accepted by the Graduate School

_____
Linda L. Black, Ed.D.
Associate Provost and Dean
Graduate School and International Admissions

ABSTRACT

Margiotta, Anna. *Enzymatic activation of cannabinoid pro-drugs*. Unpublished Master of Science thesis, University of Northern Colorado, 2018.

Cannabinoids have been used throughout history as medical treatments spanning from menstrual cramps in ancient China to enhancing appetite in patients with AIDS or cancer in the modern day. Currently there is research indicating that cannabinoids also have anti-proliferative and pro-apoptotic effects on several strains of cancer cells (Carchman, Harris, & Munson, 1976; Glodde, Jakobs, Bald, Tüting, & Gaffal, 2015; McKallip et al., 2002; Preet, Ganju, & Groopman, 2008; Sánchez, Galve-Roperh, Canova, Brachet, & Guzmán, 1998). The traditional methods for administration of cannabinoids are inhalation or oral; however, for some cannabinoids these may result in undesirable psychoactive side effects. Cell-in-a-Box® technology can be used to develop a new administration process for cannabinoids to avoid these. In theory, it involves administering a cannabinoid pro-drug, which is then activated at the site of the cancer cells via Cell-in-a-Box® encapsulated live cells containing specific enzymes. This administration process is dependent upon the enzymatic activation of the cannabinoid pro-drug. Thus, this study focused on determining a cell line capable of producing an enzyme, which can complete this activation. Five assays of *Pseudomonas putida* were conducted, each showing that the *putida* was not able to activate the specific cannabinoid pro-drug tested. Future research of other cell lines will be needed to complete this novel anti-cancer drug delivery system. Additionally, in this study, two methods of producing

crude cannabinoid extracts from *Cannabis sativa* plant were developed along with two methods of purifying tetrahydrocannabinolic acid from the crude extracts.

ACKNOWLEDGEMENTS

I would first like to thank my thesis advisor Dr. Richard M. Hyslop of the Department of Chemistry and Biochemistry at the University of Northern Colorado. Dr. Hyslop was always available to talk whenever I had an issue or a question about my research or writing. During my thesis project he helped me to grow into a better student, teacher, and scientist. I am also grateful to the other members of my committee, Dr. David Pringle and Dr. Corina E. Brown, for their patience, support, and advice.

I would like to thank PharmaCyte Biotech for their financial support in this project. This truly could not have been accomplished without their support.

I would like to thank Dr. Ann Hawkinson, Tyler Sherman, and all others in the University of Northern Colorado's School of Biological Sciences who assisted in growing the cells used in this study. I would also like to thank Chad Wangeline, Casey Rogers, and Scott Newkirk for helping me solve every one of my instrumentation issues and for making repairs. I am truly appreciative of all the time each of you spent on my project.

I would like to thank my fellow graduate students for their feedback, cooperation, and friendship. I would like to thank my friends for supporting and loving me through the years and distance. Last but not the least, I would like to thank my family: my parents and to my brother and sister for supporting me in my decision to attend the University of Northern Colorado and providing continuous encouragement. This accomplishment would not have been possible without them.

TABLE OF CONTENTS

LIST OF FIGURES

LIST OF TABLES

LIST OF APPENDIX FIGURES

CHAPTER I

INTRODUCTION

Plants of the *Cannabis* genus have been used recreationally throughout history for their euphoric psychoactive effects. The main psychoactive component of *Cannabis sativa* was determined to be Δ^9-tetrahydrocannabinol (Δ^9-THC) (Gaoni & Mechoulam, 1964). Studies investigating the anticancer/antitumor effects of the various plant components began in the 1970s, and since then evidence supporting these effects has been compiling.

This study focused on two major cannabinoid components in plants of the *Cannabis* genus, Δ^9-THC and Δ^9-tetrahydrocannabinolic acid (Δ^9-THCA). Δ^9-THC is responsible for the euphoric, psychoactive effects sought after for recreational use; however, there is research indicating that it also has anti-proliferative and pro-apoptotic effects on several strains of cancer cells (Carchman, Harris & Munson, 1976; Glodde, Jakobs, Bald, Tüting, & Gaffal, 2015; McKallip et al., 2002; Preet, Ganju, & Groopman, 2008; Sánchez, Galve-Roperh, Canova, Brachet, & Guzmán, 1998). Evidence of anticancer activity of Δ^9-THC will be discussed in detail in the literature review. Δ^9-THCA does not exhibit the same psychoactive effects as Δ^9-THC, and it can be converted to Δ^9-THC through a decarboxylation reaction. Thus, administrating Δ^9-THCA to a patient as a pro-drug and converting it to the active drug at the site of the tumor would allow the cannabinoid's anticancer activity to occur while avoiding global activation of cannabinoid receptors by Δ^9-THC. This will avoid Δ^9-THC's undesirable psychoactive

side effects. The site-selective activation of Δ^9-THCA can occur using Cell-in-a-Box® technology.

Cell-in-a-Box®

Cell-in-a-Box® is a new method of treatment delivery, which was developed by Austranova, an Austrian biotechnology company. It involves encapsulating genetically-engineered human cells in a cellulose-based polymeric sphere 0.7-0.8 mm in diameter (Fig. 1), which can convert an inactive chemotherapy drug into its active form. The cells are first genetically engineered to contain the desired enzyme capable of activating a pro-drug, and then they are sent to the Cell-in-a-Box® facilities where they are encapsulated in a cellulose-based sphere through a multi-step process (Fig. 2). This treatment of encapsulation allows for site-specific delivery via injection of the encapsulated cells up stream in the blood from the tumor ("Live Cell Encapsulation Technology", 2017). This is especially helpful when working with cannabinoids with psychoactive side effects because this site-specific delivery would prevent global stimulation of cannabinoid receptors. In addition, target-specific treatment with the cannabinoid would allow for dosage at a lower concentration, which will further minimize the possibility of psychoactive effects common to Δ^9-THC ("Live Cell Encapsulation Technology", 2017). In our application, an engineered human embryonic kidney cell possessing genes for enzymatic decarboxylation of Δ^9-THCA would be encapsulated. Human embryonic kidney cells were chosen for this because the use of human cells would decrease issues of compatibility with the patient; additionally, these cells have no set life span and can divide in the Cell-in-a-Box® capsule. At the delivery site of the encapsulated cells the pro-drug, Δ^9-THCA, would be converted to the active drug, Δ^9-THC.

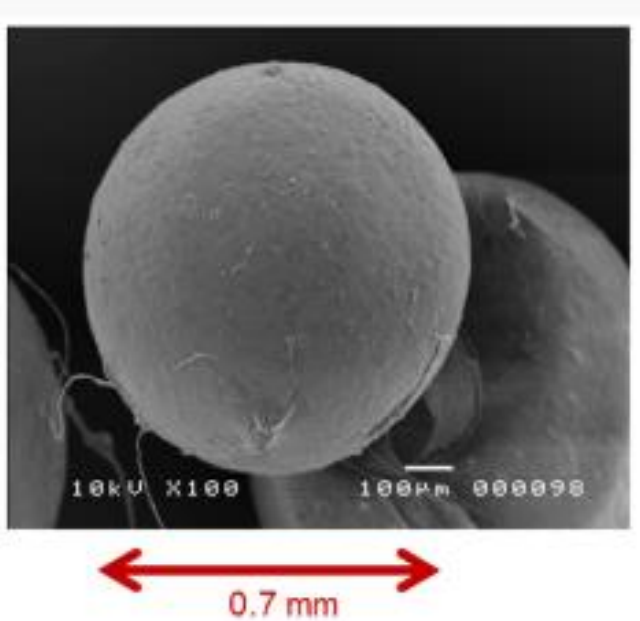

Figure 1: The view of a single Cell-in-a-Box® capsule (From Live Cell Encapsulation Technology, 2017).

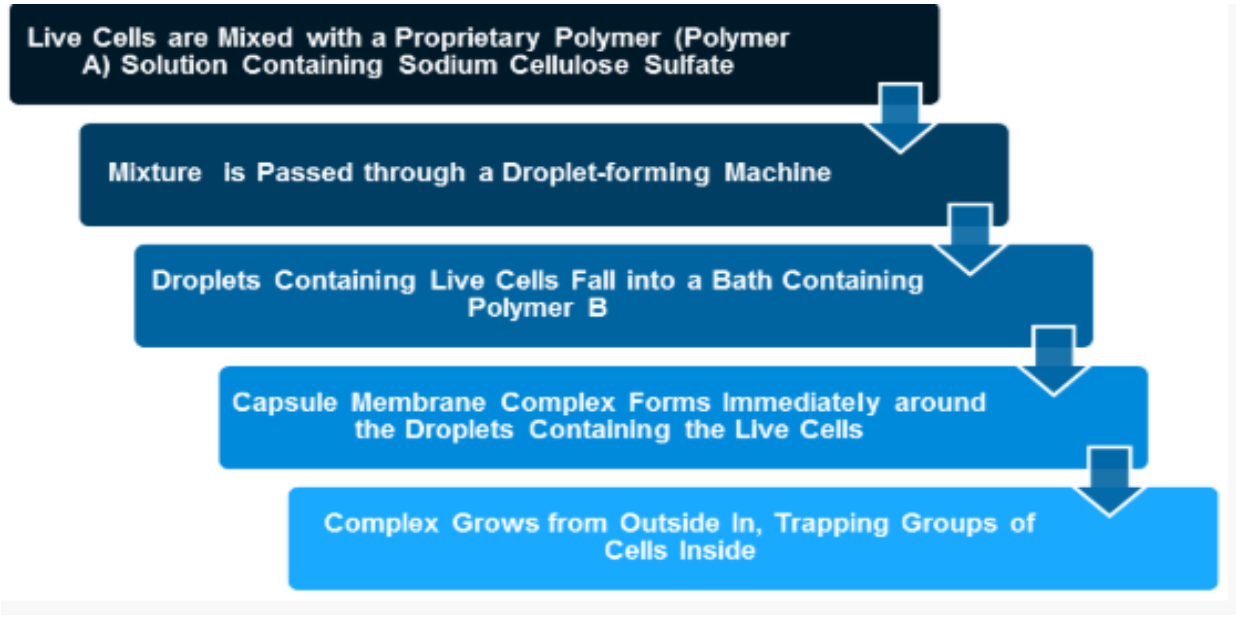

Figure 2: The process for encapsulating live cells in a cellulose sphere by Cell-in-a-Box® (From Live Cell Encapsulation Technology, 2017).

A major benefit of using this type of technology is its site-specific nature. Many anticancer drugs are toxic to human tissues and cause the patients to whom the drug is administered to suffer very serious side effects. Other studies involving the use of

anticancer drugs with the Cell-in-a-Box® technology suggest that the site-specific nature decreases the severity and number of these negative side effects. Dr. Matthias Löhr and his team at the Karolinska Institute in Stockholm, Sweden, have been using the Cell-in-a-Box® technology in administering chemotherapeutic drugs for pancreatic cancer. Dr. Löhr and his research group used encapsulated human 293 cells which were transfected with genes capable of producing CYP2B1, a cytochrome P450 enzyme capable of activating the chemotherapy prodrug ifosfamide to its active anti-cancer form (Löhr et al., 2001). These encapsulated cells were administered to the patient intravenously; the prodrug ifosfamide was then administered and the active chemotherapeutic drug formed at the site of the tumor (Löhr et al., 2001). The median survival time for the patients in this study was doubled when compared to controls. In addition, the one-year survival rate was increased by three times in the patients included in the study (Löhr et al., 2001). In an interview, Dr. Löhr reported that the patients included in the initial trial experienced no side effects, and that the quality of life of the patients was excellent considering their diagnosis (PharmaCyte Biotech, 2016). The results from these studies suggest that the Cell-in-a-Box® technology, when combined with Δ^9-THCA, will result in the active drug, Δ^9-THC, staying localized at the target. Mostly likely, this will prevent the euphoric and altered sensory perception side effects most sought after in recreational use, which result from global cannabinoid receptor stimulation. This should also make this type of treatment more favorable in the public eye.

The compound Δ^9-THC has demonstrated in various studies to have anticancer activity (Carchman et al., 1976; Glodde et al., 2015; McKallip et al., 2002; Preet et al., 2008; Sánchez et al., 1998); however, it also exhibits unfavorable psychotropic effects.

These effects can be avoided through administration of the non-psychoactive Δ^9-THCA combined with Cell-in-a-Box® delivery of a novel human embryonic kidney cell to the site of the cancer. The novel kidney cell would contain a gene for an enzyme capable of converting Δ^9-THCA to Δ^9-THC. The purpose of this study was to determine a cell line which contains this enzyme. Once the screening for decarboxylation activity in the cell lines is complete, the specific gene for the enzyme responsible for the conversion will be identified. This gene will be used to design a novel human embryonic kidney cell line which will be encapsulated via the Cell-in-the-Box® technology for use with Δ^9-THCA.

The Δ^9-THCA used for the cell line assays was isolated from *Cannabis* plant material in-house. This was due to the high cost of Δ^9-THCA standard solution. This study included two preparations of a crude extract of cannabinoids, one using a Soxhlet extractor, and one using sonication and solvent to extract. Additionally, there were two methods developed for isolating Δ^9-THCA from the crude extract: one using preparative high-performance liquid chromatography (HPLC), and one using a Yamazen Smart Flash.

CHAPTER II

LITERATURE REVIEW

This literature section will begin with general background about the plant *Cannabis sativa*, its composition, and how its components interact with the human body through the endocannabinoid system and cannabinoid receptors. Several studies about the effect of Δ^9-THC on various cancer cell lines will be discussed along with the corresponding authors' hypothesized explanations for the effects observed. Finally, the decarboxylation reaction of Δ^9-THCA itself will be discussed along with several cell lines with enzymes capable of catalyzing similar decarboxylation reactions.

Components of *Cannabis*

There are over 421 compounds that can be extracted from the plant *Cannabis sativa*; these include several types of phytocannabinoids and terpeno-phenols (Izzo, Borrelli, Capasso, Di Marzo, & Machoulam, 2009). The most abundant psychotropic component is Δ^9-THC, however there are several non-psychotropic cannabinoids including cannabidiol (CBD), cannabigerol (CBG), cannabichromene (CBC), Δ^9-tetrahydrocannabivarin (Δ^9-THCV), cannabidivarin (CBDV), Δ^9-THCA, and cannabidolic acid (CBDA) (Fig.3). Δ^9-THC is a strong agonist for both types of cannabinoid receptors (to be discussed in a following section). Δ^9-THCV is an antagonist for both receptors at low concentrations and an agonist at high doses (10 mg/kg) *in vivo* in mice. CBDV, CBG, CBD, Δ^9-THC, and Δ^9-THCV can increase the amount of mesenchymal stem cells in bone marrow, which is needed for bone formation and

fracture healing (Izzo et al., 2009). CBG is a transient receptor potential cation channel subfamily M member 8 (TRPM8) receptor antagonist and an agonist for transient receptor potential cation channel, subfamily A, member 1 (TRPA1) receptors (to be discussed in a following section). CBC, Δ^9-THCA, and CBDA are all TRPA1 agonists, and Δ^9-THCA and CBDA are TRPM8 antagonists (Izzo et al., 2009).

Endocannabinoid System

The endocannabinoid system is comprised of endocannabinoids, cannabinoid receptors (CB_1 and CB_2), all the enzymes, and molecules responsible for the synthesis, hydrolysis, and transport of the endocannabinoids (Massi, Solinas, Cinquina, & Parolaro, 2012). Δ^9-THC interacts with the human body through binding to both CB_1 and CB_2 receptors. Endocannabinoids are generally synthesized near the site of the cannabinoid receptor and released on demand (Massi et al., 2012). They participate in many processes including regulation of appetite, motor activity, memory, learning, emesis, and nociception (Fernández-Ruiz et al., 2007). The most bioactive endocannabinoids that humans synthesize are anandamide (arachidonoylethanolamide, AEA), palmitoyl-ethanolamide (PEA), and 2-arachidonoylglycerol (2-AG) (Fig. 3). These are agonists for both types of cannabinoid receptors. Other agonists for these receptors include phytocannabinoids from *Cannabis* plants, such as Δ^9-THC and CBD, and synthetic cannabinoids, such as WIN55212-2, HU-210, and JWH-015 (Battista, Di Tommaso, Bari, & Maccarrone, 2012) (Fig. 3).

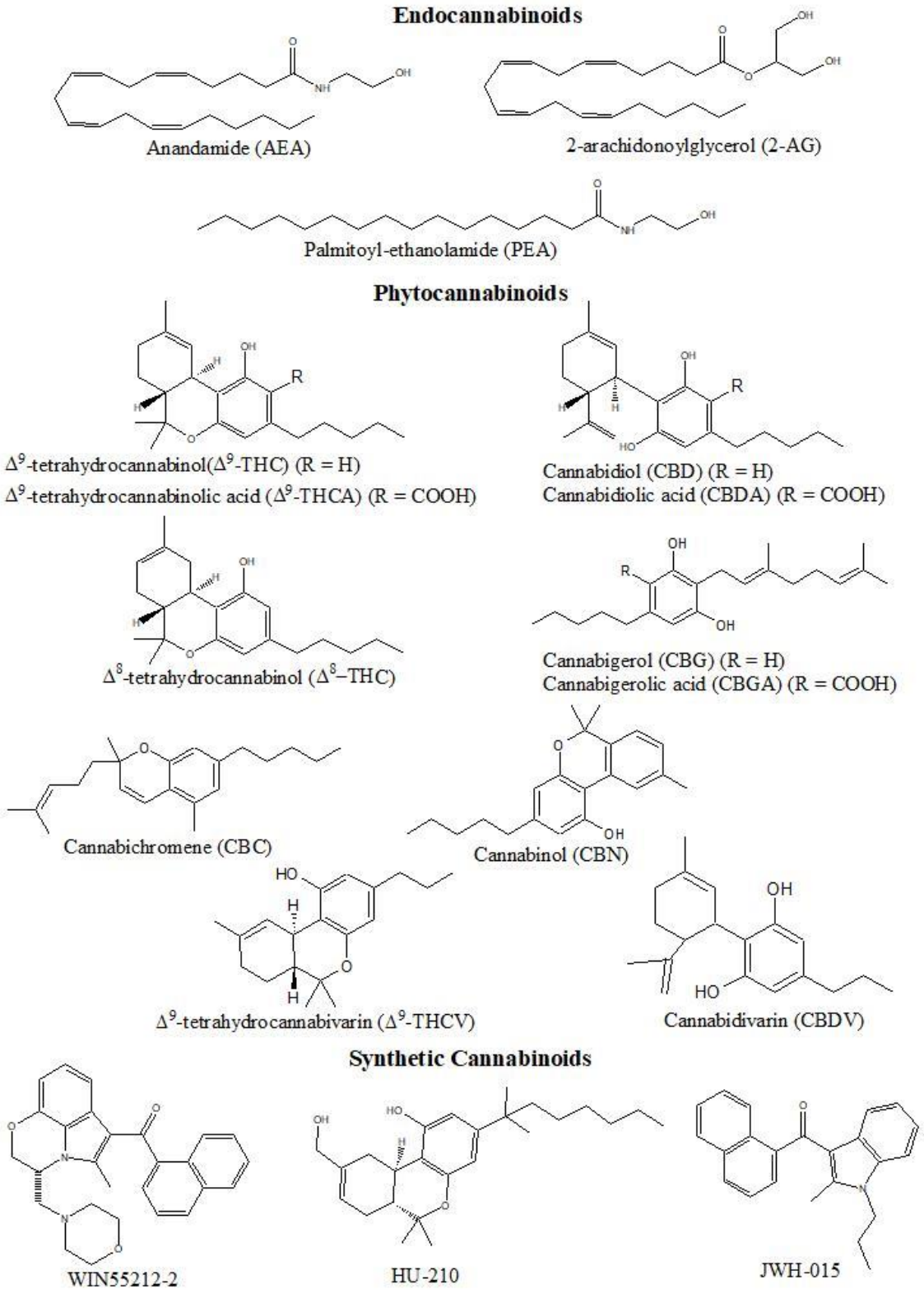

Figure 3: Structures of common cannabinoids.
(Battista et al., 2012; Izzo et al., 2009)

Current clinical use of cannabinoids include treatment for multiple sclerosis, nausea in cancer patients, and loss of appetite in AIDS patients (Grotenhermen & Müller-Vahl, 2012). However, there is therapeutic potential for many other conditions such as mood disorders, pain disorders, obesity, stroke, hypertension, osteoporosis, and cancer (Pacher, Batkai, & Kunos, 2006). Moreover, there are many diseases in which afflicted patients demonstrate an altered endocannabinoid system, necessitating further research into the endocannabinoid system and cannabinoids. These diseases include spinal cord injury, neuropathic pain, atherosclerosis, and myocardial infarction (Massi et al., 2012).

Cannabinoid Receptors

CB_1 and CB_2 receptors are members of the G-protein-coupled family of receptors and thus are mediated by $G_{i/o}$ and G_s proteins (Turu & Hunyady, 2010). There are many signal transduction pathways that are affected due to cannabinoid receptor binding including inhibition of adenylate cyclase and in some cases, stimulation of adenylate cyclase (Fig. 4 & 5A). G-protein-coupled receptors can take several different conformations resulting in these different effects on cAMP production (Turu & Hunyady, 2010). The different conformations are stabilized by the different agonists and antagonists for the receptor. In some cases, the location of the receptor in the human body will influence which conformation the receptor will take and thus which down-stream effects will occur (Turu & Hunyady, 2010). The stimulation of adenylate cyclase results in the formation of cAMP, which regulates many processes, one of which is the activation of protein kinase A (PKA) (Fig. 4).

The CB_2 receptors in rat microglial cells, hamster ovary cells, and mouse neural progenitors have been shown to activate the mitogen-activated protein kinase (MAPK)

cascade via the extracellular-signal-regulated kinases (ERKs) (Fernández-Ruiz et al., 2007) (Fig. 4). Physiological responses to the activation of the MAPK cascade include cell proliferation, differentiation, apoptosis, and cell stress response (Plotnikov, Zehorai, Procaccia, & Seger, 2011). In addition, in human monocyte and leukemia cells the CB_2 receptors have demonstrated the ability to activate the p38 MAPK cascade (Fernández-Ruiz et al., 2007). The p38 MAPK cascade has physiological responses including regulation of immunological effects, apoptosis, cellular senescence, and induction of inflammation (Plotnikov et al., 2011). CB_1 receptors can also activate the p38 MAPK cascade (Fig. 5). Of course, the ability of the endocannabinoid receptor to activate these MAPK cascades represents a certain control of the cell's survival. Further study of CB_2 receptors in rat oligodendroglial cells, rat mast cells, and mouse neural progenitors have shown that stimulation of the receptors can result in activation of the phosphatidylinositol 3-kinase and Akt pathways, which are both pro-survival mechanisms (Fernández-Ruiz et al., 2007) (Fig. 4). Thus, the endocannabinoid system plays a role in controlling the cell's survival or apoptosis.

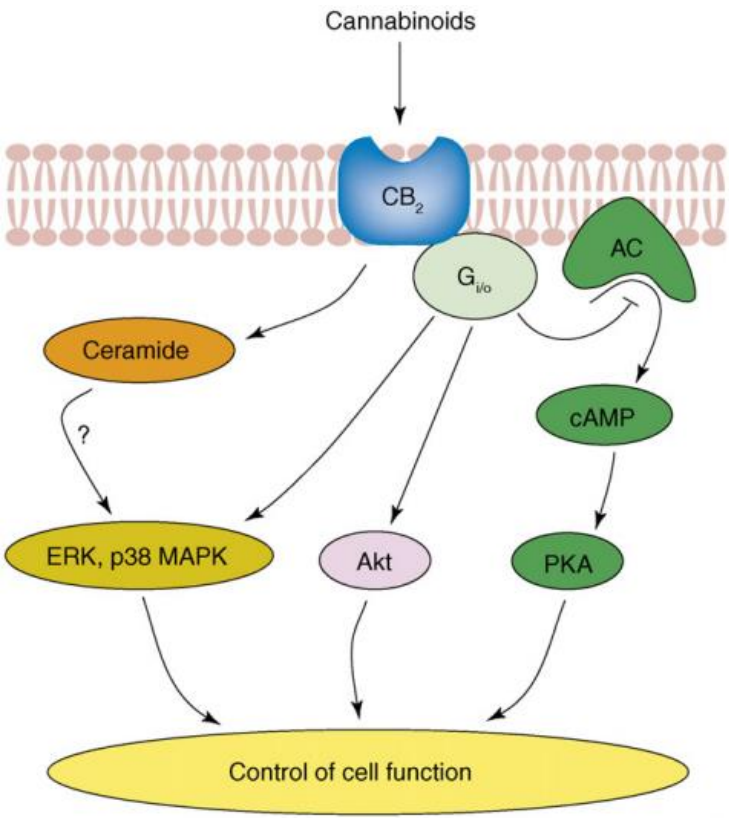

Figure 4: CB_2 receptor signaling pathways
(From Fernández-Ruiz et al., 2007, used with permission).

Stimulation of CB_1 receptors in a variety of cell types have been shown to activate the ERKs (Turu & Hunyady, 2010) (Fig. 5). Downstream physiological effects of the activation of this cascade include proliferation and differentiation of cells, morphological determination of cells, cell survival, and in some conditions cell apoptosis (Plotnikov et al., 2011). Stimulation of CB_1 receptors can also activate c-Jun N-terminal kinase (JNK) (Fig. 5). Stimulation of JNK results in the phosphorylation of many substrates which are involved in gene transcription. Some of the cellular processes resulting from the transcription of these genes include apoptosis, neuronal activity, and insulin signaling (Plotnikov et al., 2011).

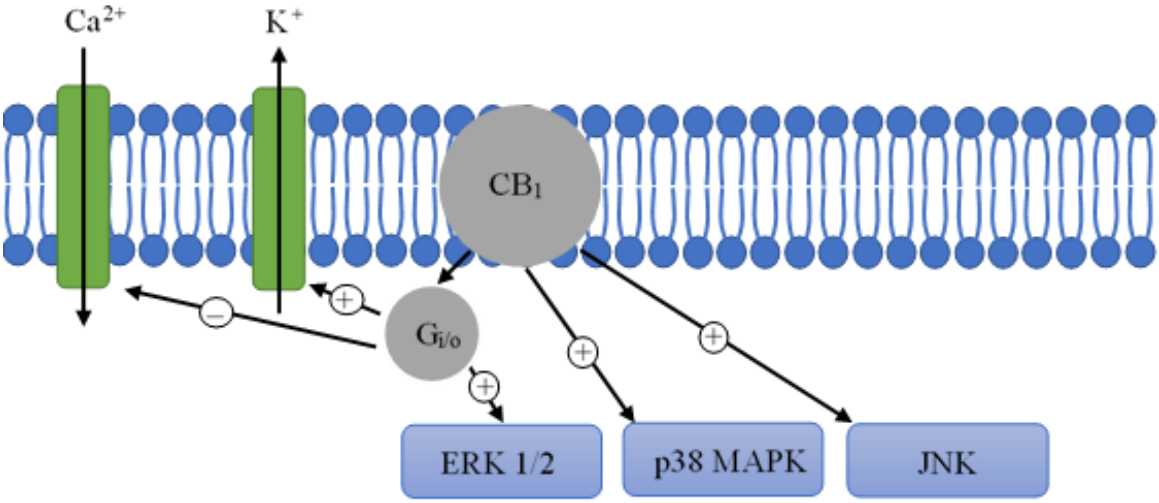

Figure 5: CB_1 receptor signaling pathways.

In addition, cannabinoid receptor binding results in modulation of ion channels (Turu & Hunyady, 2010). In both *Xenopus laevis* oocytes and rat neuronal cells, stimulation of CB_1 receptors resulted in the activation of G-protein-coupled inwardly-rectifying potassium channels (GIRKs) (Turu & Hunyady, 2010) (Fig. 5). CB_1 receptors also influence calcium channels; however, the specific effect depends on the specific cell investigated. Stimulation of the CB_1 receptor can result in inhibition of calcium channels in cerebral vessels, retinal bipolar cells, and neonatal rat solitary tract cells; however, it results in activation of calcium channels in mouse neuroblastoma N18TG2 cells (Turu & Hunyady, 2010) (Fig. 5). In addition, activation of CB_1 receptors inhibit the release of a variety of neurotransmitters including GABA, histamine, serotonin, glutamate, acetylcholine, and dopamine (Grotenhermen & Müller-Vahl, 2012). Overall, the endocannabinoid system has many interactions and physiological effects in the central and peripheral nervous systems, as well as in various peripheral organs and tissues (Turu & Hunyady, 2010).

Transient Receptor Potential Cation Channel Receptors

Some cannabinoids have been observed to interact with TRPM8 receptors and TRPA1 receptors. These include CBG, Δ^9-THCA, and CBDA which are antagonists for TRPM8 receptors. Additionally, CBG, CBC, Δ^9-THCA, and CBDA are agonists for TRPA1 receptors. Both TRPA1 and TRPM8 are involved in the nociceptive process and are transductors of thermal, chemical, and mechanical stimuli (Izzo et al., 2009). Thus, the cannabinoids which interact with these receptors have potential use in analgesia or pain management (Izzo et al., 2009).

Effects of Δ^9-Tetrahydrocannabinol on Various Cancer Cell Lines

Studies exploring the anticancer activity of cannabinoids have focused mainly on cannabidiol and other non-psychoactive cannabinoids. This is due to the psychoactive qualities possessed by some cannabinoids such as Δ^9-THC, which are undesirable at the clinical stage of drug design. However, there is Δ^9-THC in all strains of *Cannabis* plants and there is evidence that CBD and THC have synergistic qualities with each other (Russo & Guy, 2005). In addition, the application of Cell-in-a-Box® technology as suggested in this study negates this issue. The following studies explored the effects of Δ^9-THC on various cancer cell lines.

Carchman et al. (1976) explored the *in vitro* effects of various cannabinoids on DNA synthesis in L1210 leukemia cells and Lewis lung cancer cells. Treatment of the Lewis lung cancer cells with either Δ^9-THC, Δ^8-tetrahydrocannabinol (Δ^8-THC), or cannabinol (CBN) resulted in a dose-dependent inhibition of tumor growth due to inhibition of DNA synthesis in the cell. The inhibition of DNA synthesis was measured by incubating the cancer cells with either one of the cannabinoids or ara-C, a known

inhibitor of DNA synthesis, and then measuring the uptake of radiolabeled thymidine by these cells. Incubating the cells with ara-C resulted in a low uptake of thymidine and an ED_{50} of 1.36×10^{-7} M for Lewis lung cells and 2.53×10^{-8} M for L1210 cancer cells. Incubating Lewis lung cells with Δ^9-THC, Δ^8-THC, ABN Δ^8-THC, or CBN resulted in a low uptake of thymidine, like that of the ara-C, and had ED_{50} values of 4.18×10^{-6} M, 2.99×10^{-6} M, 1.48×10^{-6} M, and 2.3×10^{-6} M, respectively. Incubating L1210 with Δ^9-THC, Δ^8-THC, ABN Δ^8-THC, or CBN resulted in a low uptake of thymidine, and had ED_{50} values of 3.26×10^{-5} M, 8.70×10^{-6} M, 5×10^{-6} M, and 2.2×10^{-6} M, respectively. *In vivo* testing using B6D2F male mice which were inoculated with Lewis lung carcinoma cells occurred. The mice which were treated with either THC or CBN had significantly smaller tumors than those which were not treated (Carchman et al., 1976).

The Carchman study also included treatment of bone marrow cells with the cannabinoids and ara-C to assess their toxicity, and of all the treatments the least toxic was Δ^9-THC. The Δ^9-THC ED_{50} for both types of cancer cells included in this study was about 100 times higher than the ED_{50} of ara-C (Carchman et al., 1976). Ara-C has been shown to cure L1210 *in vivo*, and this study revealed a similar activity caused by the cannabinoids. In addition, the cannabinoids had a lower toxicity to bone marrow than the ara-C.

Preet et al. (2008) investigated the effects of Δ^9-THC on A549 and SW-1573 lung cancer cells both *in vitro* and *in vivo.* They reported that Δ^9-THC inhibited the epidermal growth factor (EGF) receptor, which inhibited migration of the cancer cells *in vivo* that is normally triggered through EGF pathways. Specifically, this was caused through Δ^9-THC inhibition of AKT and MAP kinases which are both important for cancer cell migration.

Δ^9-THC reduced tumor growth and metastasis *in vivo* in the severe combined immunodeficient (SCID) mice tested. In addition, they reported that, after 72 hours of treatment with Δ^9-THC *in vitro,* apoptosis resulted in both A549 and SW-1573 lung cancer cells. They also observed that *in vitro* Δ^9-THC induced EGF-controlled morphological changes which reduced motility of both cell lines.

Glodde et al. (2015) investigated the role of CB1/CB2 receptors in the pathogenesis of HCmel12 melanoma cells, as well as the effect of Δ^9-THC on these cells *in vitro* and *in vivo*. They determined endocannabinoids do not have a role in the pathogenesis of melanoma using chemically-inducing tumors on wild-type mice and CB1/CB2 receptor knock-out mice and monitoring the growth of their tumors. Treatment of melanoma cells with Δ^9-THC during culturing had no effect on their proliferation. However, *in vivo* treatment of HCmel12 cells with Δ^9-THC in mice resulted in a significant decrease in the size of their tumors. They hypothesized that since the Δ^9-THC did not affect the cells *in vitro* their antitumor activity *in vivo* must be due to the Δ^9-THC interaction with the immune system or the angiogenesis of the cancer cells. Cannabinoids as a class have a well-established effect on the immune system, and one characteristic of HCmel12 melanoma cells is an increase of myeloid immune cells in their specific environment. In another related study, the authors displayed Δ^9-THC's ability to both diminish allergic swelling and limit the influx of immune cells to the allergen's contact site (Gaffal, Cron, Glodde, & Tüting, 2013). This combined information supports the hypothesis that Δ^9-THC diminishes tumor cell growth via preventing pro-tumorigenic myeloid immune cells from entering the melanoma cell environment (Glodde et al., 2015).

McKallip et al. (2002) exposed two murine lymphomas (EL-4 and LSA), and a murine mastocytoma (P815) cancer cell line to Δ^9-THC to observe its effect. *In vitro* Δ^9-THC concentrations of at least 10 μM resulted in reduction of the number of cancer cells and an increase in apoptosis for El-4, LSA, and P815 cell lines. The occurrence of apoptosis was confirmed through dying the cells with annexin and propidium iodide (PI). Cells that dye positive with annexin are in early apoptosis, cells that dye with both are in late apoptosis, and cells that dye positive for just PI alone are necrotic. Most of the cells treated with THC tested to be in late apoptosis. *In vivo* testing of Δ^9-THC on the EL-4 cell line in C57BL/6 mice resulted in a reduction of tumor size in most samples (77.3%) and 25% of the mice were cured of their tumors all together (McKallip et al., 2002).

Sánchez et al. (1998) explored the effects of Δ^9-THC on C6.9 glioma cells. Due to the variability and heterogenous nature of C6 glioma cells, a previously characterized sub clone of these cells, C6.9 cells, were used for characterization of apoptosis for this study. *In vitro* administration of Δ^9-THC to these cells in concentrations as low as 0.75 μM resulted in a significant decrease in their optical density assessed via a MTT assay. This is indicative of a significant decrease in metabolic oxidation in the cells. There was eventual cell death. This effect was also shown to be dose-dependent. A fluorescent annexin V binding assay was also performed which showed a loss of plasma membrane asymmetry in cells treated with the Δ^9-THC. DNA fragmentation was seen in the cells treated with Δ^9-THC; both observations are typical results of apoptosis. They hypothesized that the mechanism of the programmed cell death is linked to sphingomyelin breakdown. In the same study, the addition of Δ^9-THC to the cell medium

solution resulted in significant breakdown of sphingomyelin, which resulted in a buildup of ceramide, a widely documented inducer of apoptosis (Sánchez et al., 1998).

Enzymatic Decarboxylation Reaction

Δ^9-THCA can be decarboxylated to produce in Δ^9-THC (Fig. 6). This reaction most commonly occurs through the burning or heating of *Cannabis* plant material containing Δ^9-THCA (Wang et al., 2016). However, there are many types of cells that have enzymes capable of performing decarboxylation reactions. The carboxylic acid group ortho to a phenolic hydroxyl group theoretically could be enzymatically removed from the Δ^9-THCA to form the Δ^9-THC (Fig. 6). Thus, the enzymes that were screened in the current study to determine decarboxylation activity of the Δ^9-THCA were those that have been shown to have this type of activity with compounds that have an ortho hydroxyl group to the targeted carboxylic acid.

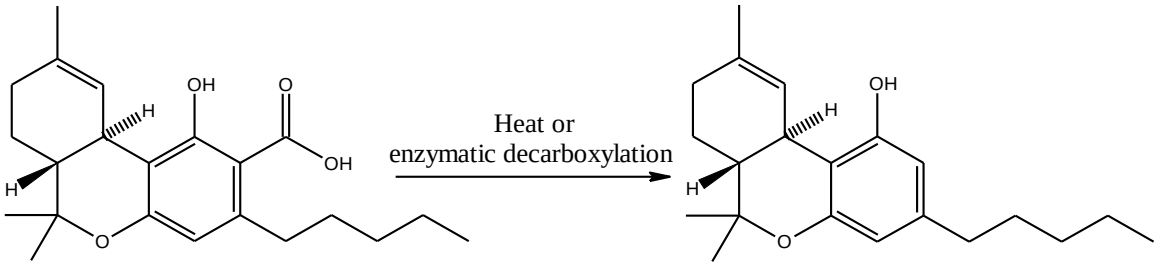

Δ^9-THCA Δ^9-THC

Figure 6: Enzymatic decarboxylation of Δ^9-THCA to produce Δ^9-THC.

6-Methylsalicylic acid decarboxylase is an enzyme coded by the PatG gene, and its substrate is 6-methylsaliylic acid, which has a hydroxyl group ortho to the carboxylic acid that the enzyme catalytically removes (Fig. 7). There are many cell lines that code for this enzymatic activity, including *Aspergillus clavatus, Aspergillus giganteus, Aspergillus longivesica, Byssochlamys nivea,* and *Penicillium expansum* (Snini et al.,

2013). In *Aspergillus clavatus*, the *PatG* gene is responsible for encoding the enzyme which performs this decarboxylation (Snini et al., 2013).

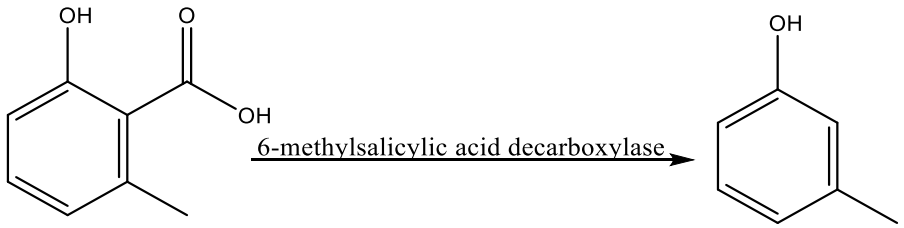

Figure 7: Enzymatic decarboxylation of 6-methylsalicylic acid to produce *m*-cresol.

Another enzyme whose substrate has a hydroxyl group ortho to a carboxylic acid is salicylic acid decarboxylase (Fig. 8). This enzyme is produced by the fungus *Trichosporon moniliiforme*, and it decarboxylates salicylic acid as well as with other carboxylated substrates (Kirimura, Gunji, Wakayama, Hattori, & Ishii, 2010).

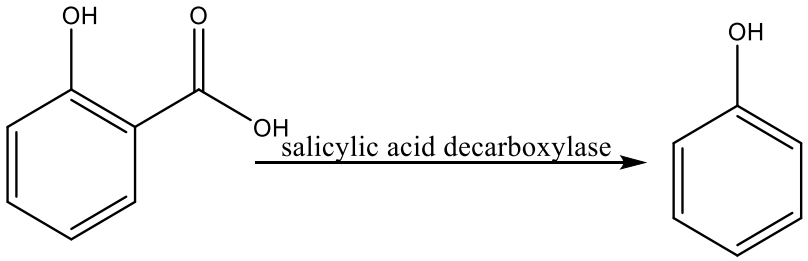

Figure 8: Enzymatic decarboxylation of salicylic acid to produce phenol.

2,3-Dihydroxybenzoic acid is a substrate for 2,3-dihydroxybenzoic acid decarboxylase; it also has a hydroxy group ortho to the carboxylic group to be removed (Fig. 9). This enzyme is produced by several *Aspergillus* fungi including *Aspergillus oryzae* and *Aspergillus niger* (Santha, Rao, & Vaidyanathan, 1996).

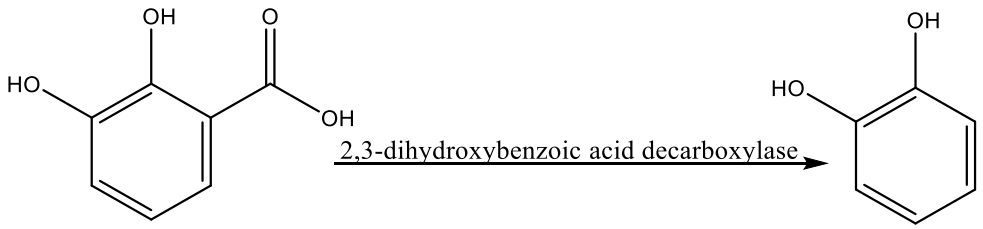

Figure 9: Enzymatic decarboxylation of 2,3-dihydroxybenzoic acid to produce 1,2-dihydroxybenzene (catechol).

1,2-Dihydro-1,2-dihydroxybenzoic acid (DHB) is an intermediate in the formation of catechol from benzoic acid. DHB dehydrogenase is involved in the final step of this reaction, converting the intermediate to catechol (Fig. 10). Like Δ^9-THCA this intermediate has a hydroxyl group ortho to the carbon bearing the carboxylic acid to be removed. This enzyme is produced in *Acinetobacter calcoaceticus, Alcaligenes eutrophus, Pseudomonas cepacia,* and *Pseudomonas putida* (Reiner, 1971).

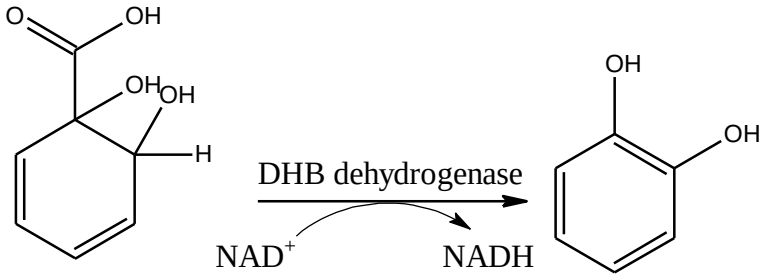

Figure 10: Enzymatic decarboxylation of 1,2-dihydro-1,2-dihydroxybenzoic acid to produce catechol.

Another decarboxylation enzyme synthesized by *Pseudomonas putida* is benzoylformate decarboxylase (Iding et al., 2000). This enzyme catalyzes the decarboxylation of benzoylformate to benzaldehyde (Fig. 11). Like Δ^9-THCA this substrate has an aromatic ring and a carboxylic acid.

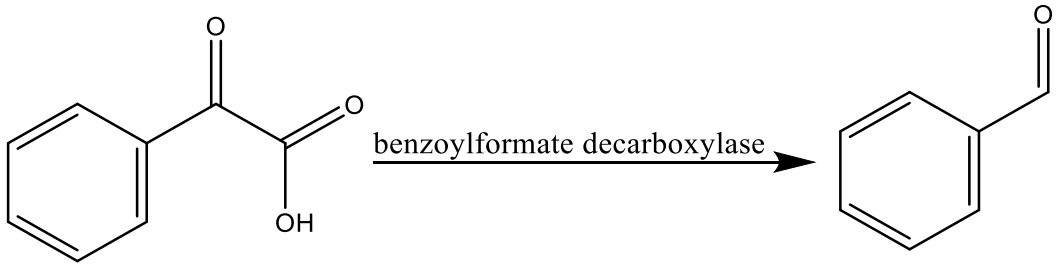

Figure 11: Enzymatic decarboxylation of benzoylformate to produce benzaldehyde.

Pseudomonas putida was used in preliminary studies exploring activation of cannabinoid-like model compounds and succeeded in decarboxylating the model compound (Cribbs, 2016). Thus, *Pseudomonas putida* was used for the microbial cell line assays in this study.

CHAPTER III

METHODS AND MATERIALS

Reagents and Materials

Cannabidiol (CBD) (item number 90080), cannabidiolic acid (CBDA) (item number 14028), and a mixture of cannabinoid standards (item number 18791) were obtained from Cayman Chemical Company. The mixture of cannabinoids contained 100 µg/mL of each of the following: CBDA, cannabigerolic acid (CBGA), cannabigerol (CBG), CBD, tetrahydrocannabivarin (THCV), cannabinol (CBN), Δ^9-tetrahydrocannabinolic acid (Δ^9-THCA), Δ^9-tetrahydrocannabinol (Δ^9-THC), Δ^8-tetrahydrocannabinol (Δ^8-THC), and cannabichromene (CBC). Water was purified in house using a QTUM 000 EX Millipore water purification system to obtain HPLC-grade water. Tryptic soy broth/agar (item number 470015-844), MRS broth/agar (item number 89405-526), and brain heart infusion broth/agar (item number 90000-062) for cell media were purchased from VWR International. Δ^9-THC (item number T2386), HPLC-grade methanol (item number 34860-4L-R), ammonium formate (item number 540-69-2), and HPLC-grade hexane (item number 293253-4L) were purchased from Sigma-Aldrich. HPLC-grade acetonitrile (item number A998-4), HPLC-grade pentane (item number P399-4), absolute ethanol (item number BP2818-4), activated charcoal (item number C170-500), and potassium hydroxide (item number M-10489) were purchased from Fischer Scientific. Formic acid (item number UN1779) and chloroform-d (item number 865-49-6) were purchased from ACROS Organics. Silica gel 60 RP-18F TLC plates with

fluorescent indicator (item number 115685) from Merck were used when producing the Yamazen method. Cell lines containing decarboxylation enzymes were obtained from VWR International. Marijuana plant material (RTI log number 13494-22, reference number SAF 027355, 13.5% Δ^9-THCA) was obtained from the National Institute on Drug Abuse.

Instrumentation

Analytical High-Performance Liquid Chromatography Method

HPLC analysis was used to determine the presence and relative ratios of Δ^9-THC and Δ^9-THCA in samples. The HPLC used was a Shimadzu (Tokyo, Japan) VP equipped with an analytical Luna Omega 5 µm Polar C18 100 LC column 150×4.6 mm with a 4.0×3.0 mm guard column. The HPLC was equipped with a DGU-14A degasser, one LC-10AT pump, and a Rheodyne injector with a 10 µL injection loop. It also had a Shimadzu SCL-10A system controller and a SPD-M10A diode array detector. All solvents were filtered (0.22 µm filter) before being run through the HPLC; all aqueous solvents and methanol were filtered through a nylon filter and all other organic solvents were filtered through a Teflon filter. Solvent A was 20 mM ammonium formate, pH 3.20, and solvent B was HPLC-grade acetonitrile. A twenty-minute-long gradient method was used with the analytical column; this started with 60% B raised to 95% B over nine minutes, held at 95% B for three minutes and then reduced back to 60% B over four minutes and held at 60% until the twenty-minute mark. This was run with a flow rate of 1.2 mL/min. The HPLC system used the CLASS-VP 7.2.1 SP1 software program to generate all chromatograms.

Preparative High-Performance Liquid Chromatography Method

A preparative method for purifying Δ^9-THCA from a crude cannabinoid extract used a Shimadzu VP HPLC equipped with a preparative Luna Omega 5 µm Polar C18 100 LC column 150×21.2 mm with a polar C18 SecurityGuard prep cartridge, 15×21.2 mm. The HPLC was equipped with a DGU-14A degasser, two LC-10AT pumps, and a Rheodyne injector with a 1.0 mL injection loop. The HPLC also had a CBM-10AW communications bus module and a SPD-10A UV-VIS detector. A Gilson FC-100 Micro Fractionator was used with the preparative column to collect the compounds separated by the HPLC. Solvent A was 20 mM ammonium formate, pH 3.20, and solvent B was HPLC-grade acetonitrile. A 120-minute-long gradient method was used with the preparative column, starting with 25% B for five minutes then raised to 95% B over 65 minutes; the concentration was held at 95% B for ten minutes before being decrease to 25% B over 30 minutes. The concentration was held at 25% B until the 120-minute mark. This was run with a flow rate of 5.0 mL/min. The CLASS-VP 7.2.1 SP1 software program was used to generate all chromatograms.

Yamazen Method

A second method of isolating Δ^9-THCA was developed using a Yamazen Smart Flash EPCLC A1-5808. The Yamazen was equipped with a S W826 silica gel inject column and a 2L ODS-SM 50 µm 120 Å universal column. The solvent system used with the Yamazen was 80% acetonitrile, 10% methanol, and 10% 20 mM ammonium formate, pH 3.20. The chromatographic method was set up using the Yamazen's automatic system and a TLC plate which was spotted with crude cannabinoid extract and developed using

the same solvent system described above. The R_f value for the Δ^9-THCA was 0.25 which was entered in the automatic set-up (Fig. 12). The Yamazen automatic chromatographic method set-up does not have a setting for only a single line to be used, so both lines A and B were placed into a container of the aforementioned pre-mixed solvent system, and the mixing ratio was set to 99:1. Finally, the elution mode was set to isocratic, and the flow rate automatically set to 20 mL/min. The software displayed the approximate time that the target will elute and the volume of solvent used at this time (342 mL in this case) (Fig. 12). Additionally, the UV detector was set at a wavelength of 254 nm.

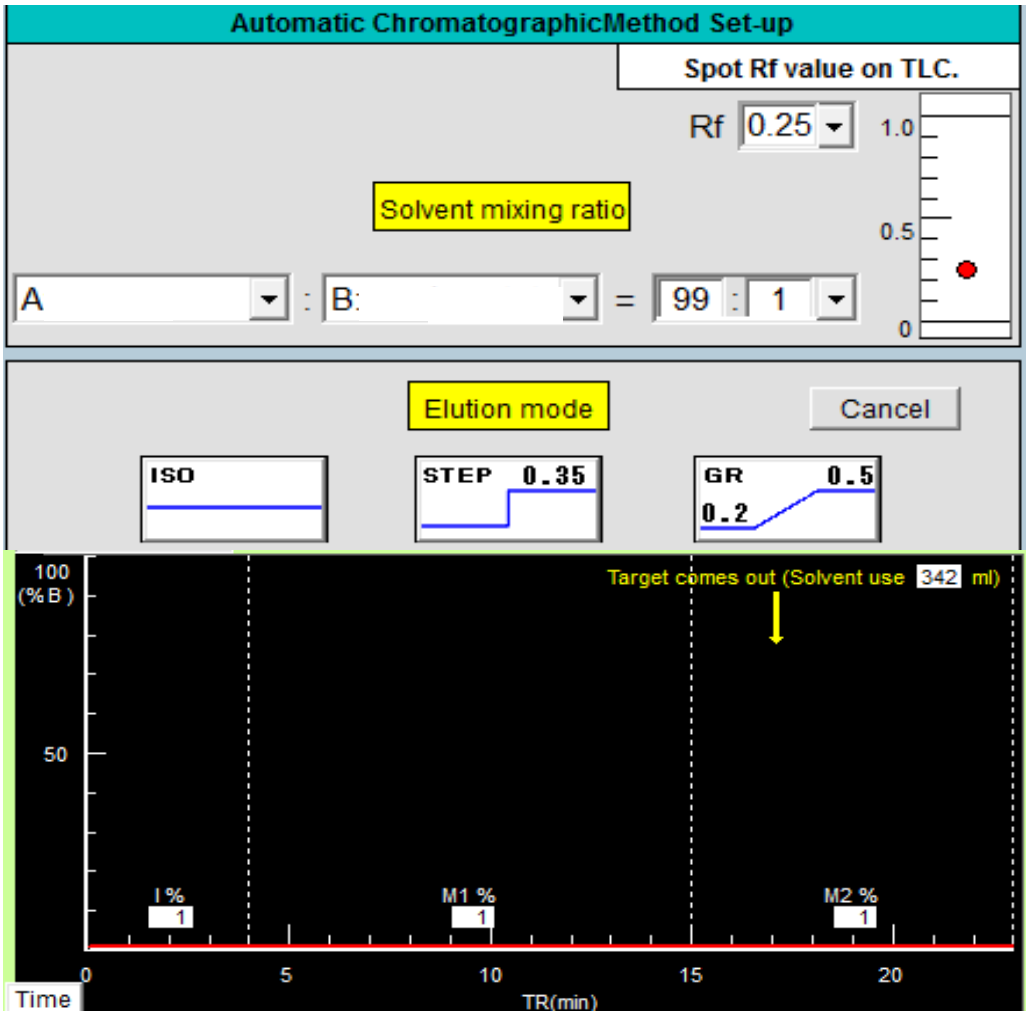

Figure 12: Automatic chromatographic method set-up of the Yamazen Smart Flash EPCLC A1-5808.

Proton and Carbon Nuclear Magnetic Resonance Method

Samples from both the Yamazen method and the preparative HPLC method of purifying crude cannabinoid extract were analyzed via proton NMR. The samples were dried in a stream of N_2 gas, and the residue was dissolved in 600 μL of deuterated chloroform for the analysis. A Bruker 400 MHz NMR was used, and the TOPSPIN 1.3 software program was used to generate all spectra. To determine the identity of the cannabinoids, the spectra were compared to standards of the cannabinoids from literature (Fig. 13). Figure 13 depicts the H-1'' peaks at approximately 2.78 ppm and 2.94 ppm as well as the H-1 doublet at approximately 3.23 ppm and was compared directly to the proton NMR spectrum produced in this study. A study by Hazekamp et al. classify H-5' and H-2 as identifying peaks of Δ^9-THCA, which are located at 6.39 ppm and 6.24 ppm, respectively. Additionally, a carbon NMR of the extract collected via the preparative HPLC method was compared to the carbon NMR of a Δ^9-THCA standard in the Choi et al. study (2004).

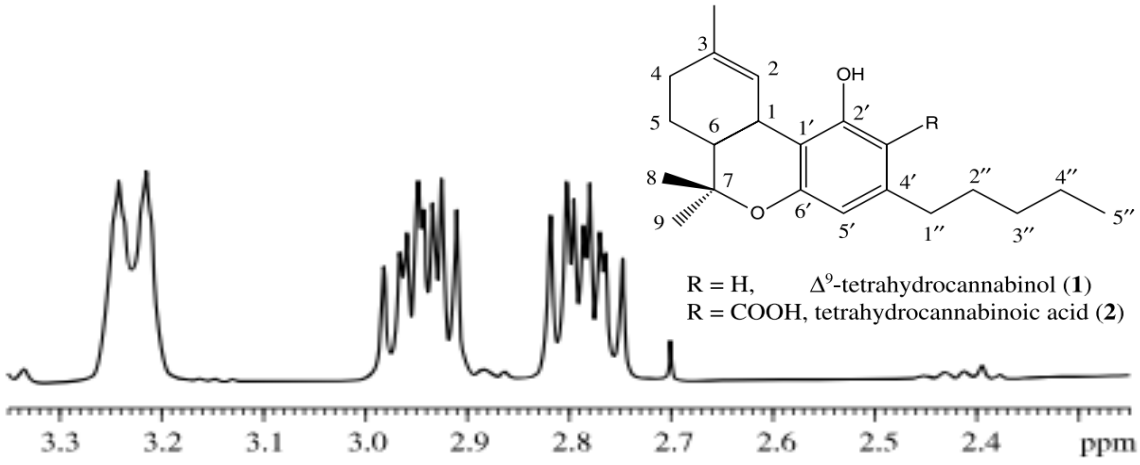

Figure 13: Proton NMR identifying peaks of Δ^9-THCA with numbering of Δ^9-THCA and Δ^9-THC according to Choi.
(From Choi et al., 2004, used with permission).

Infrared Spectroscopy Method

The 4 mg/mL Δ^9-THCA solution prepared after the isolation of Δ^9-THCA via the preparative HPLC method was analyzed using IR. A Nicolet iS5 equipped with a iD5 ATR accessory using the OMNIC software was used for this analysis. This IR spectrum was compared to a spectrum of a Δ^9-THCA standard in a study completed in 2016 by Smith, Lewis, and Mendez.

Additional Instrumentation

Mass measurements were made using either an Ohaus® GA200D balance or a Denver Instrument XE-510 balance. A Cole-Palmer, handheld short/long-wave UV light was used to visualize the spots on developed TLC plates. The pH measurements of the ammonium formate solution were made using a Fisher Scientific Accumet® AB150 pH meter. The pH meter was calibrated using Fisher scientific pH 4.00, pH 7.00 and pH 11.00 buffer solutions. A Büchi Rotavapor® R 110 was used for evaporating solvents. Rainin Pipetman micro pipettes ranging from 20 µL to 5000 µL were used when making sample or standard solutions and transferring cell lines during the decarboxylation assay. During the decarboxylation assay, the cells were incubated with a VWR International constant temperature shaking water bath incubator. When the cells were extracted with pentane, the media and solvent were mixed in a capped test tube using a VWR scientific Bronwill mixer, and then the tubes were centrifuged using an International clinical centrifuge made by International Equipment Company.

Procedures

Preparation of Solutions

Ammonium formate (20 mM) solution was prepared by adding 0.6306 g of ammonium formate to a 500-mL volumetric flask and diluting with HPLC-grade water. A 20 mM solution of formic acid was made to adjust the pH of the ammonium formate solution to a pH of 3.20. The 20 mM formic acid was prepared by adding 0.3835 mL of 96% formic acid to a 500-mL volumetric flask and diluting with HPLC-grade water. The pH of the ammonium formate solution was monitored with the Fisher Scientific Accumet® AB150 pH meter while the 20 mM formic acid solution was slowly added until the solution reached pH 3.20. This ammonium formate buffer solution was used in the solvent system for the analytical HPLC method, preparative HPLC method, and Yamazen Smart Flash method.

During cell growth incubation, *Pseudomonas putida* bacterial cells were treated with 70 mL of 0.011 M salicylic acid to induce the decarboxylation enzymes. The total volume of the bacterial cell in media with the salicylic acid was 770 mL, so the overall concentration of the salicylic acid was approximately 0.0010 M. This salicylic acid solution was prepared by dissolving 0.3798 g of salicylic acid in 25 mL of ethanol with 0.169 mL of 4 M KOH in a 250-mL volumetric flask, and then diluting to volume with water.

The Δ^9-THC standard from Sigma Aldrich was used to make a 1.2 mg/mL solution in ethanol, and a 5.0 mg/mL solution in ethanol. The standard from Sigma Aldrich was a 24 mg/mL solution in ethanol. The 1.2 mg/mL solution was made by taking 0.050 mL of the stock solution, transferring it to a mini vial, and adding 0.95 mL

of ethanol. The 5.0 mg/mL solution was made by taking 0.099 mL of the stock solution, evaporating the ethanol using N_2 gas to obtain 2.38 mg of residue, and then dissolving that in 0.46 mL ethanol.

Crude Extraction of Cannabinoids from Marijuana Plant Material

Sonification method. Initially, 1.0 g of starting plant material, obtained through the National Institute on Drug Abuse, was freeze-dried using a Labconco Freezone 4.5 then pulverized with a mortar and pestle. The dry material was extracted in 20 mL pentane containing 20 μL glacial acetic acid through sonication on ice for two minutes. The sample was sonicated with a Branson digital sonifier for 15-second-long bursts at a time at 10% amplitude and allowed to cool on ice for thirty seconds between bursts, totaling eight bursts. It is possible for the vibration of the sonifier's tip to heat the solution which could cause the Δ^9-THCA to be converted to Δ^9-THC, which is why the solution was sonicated in bursts and on ice to prevent this (Wang et al., 2016). Following sonification this solution was stirred at room temperature on a stir plate for an hour. After one hour, an additional 20 mL of pentane was added, and the solution was stirred for an additional 45 minutes. The extract was filtered through a Fisher Scientific P5 filter paper, treated with 0.5 g activated charcoal, and refiltered. The sample was concentrated using a rotary evaporator at 30 ˚C yielding a brown, viscous residue. This residue was a crude extract of cannabinoids which was further purified using chromatography.

Soxhlet method. A second method of producing a crude extract of cannabinoids was developed using a Soxhlet extractor. This consisted of placing 100 mL of pentane in a 250 mL round-bottom flask and 5.0 g of freeze-dried marijuana plant material in a thimble filter in the Soxhlet attachment. The round-bottom was attached to the Soxhlet

and attached on top was a condenser (Fig. 14). The round-bottom was heated to a gentle boil at 40 ˚C using a variac and a heating mantle. This set up was run for three hours. The round-bottom was then detached, the pentane evaporated using the rotary evaporator, and the remaining brown, viscous residue was the crude extract of cannabinoids.

Figure 14: Image of Soxhlet setup.

Isolation of Δ^9-Tetrahydrocannabinolic Acid

Yamazen Smart Flash. Exploratory TLC silica gel 60 RP-18F plates with fluorescent indicator from Merck were developed with either hexane, acetonitrile, acetone, ethyl acetate, methanol, or dichloromethane using crude cannabinoid extract as the sample. The purpose of TLC was to explore which solvent systems gave an R_f value of approximately 0.2 for the sample Δ^9-THCA to determine which solvent to use with the Yamazen Smart Flash EPCLC A1-5808 when purifying the crude extract. The solvent system determined with the TLC was 80% acetonitrile, 10% methanol, and 10% 20 mM

ammonium formate, pH 3.20. Before the flash chromatography could begin, the Yamazen system was first primed by pumping line A for 2 minutes at a flow rate of 10 mL/min, and then line B for two minutes at a flow rate of 10 mL/min. Then the column was equilibrated by pumping the mobile phase solvent system for ten minutes at a flow rate of 30 mL/min. After this, the automated chromatographic method began, which was 23 minutes long and used 460 mL of mobile phase total (Fig. 12). The method was used with a sample of crude extract (1 mL), which was injected into the Yamazen using the S W826 silica gel inject column onto a 2L reverse phase ODS-SM 50 μm 120Å universal separation column. After this analysis was complete, HPLC-water was pumped through line A for two minutes at a flow rate of 20 mL/min, and then HPLC-water was pumped through line B for two minutes at a flow rate of 20 mL/min. This was done to remove any lingering ammonium formate from the instrument. In total, this method uses 800 mL of mobile phase and 80 mL of water each time it is used.

During the automated chromatographic method, the major peaks were collected from the Smart Flash, and each sample was placed in a 50-mL round-bottom flask and the organic solvent evaporated using a rotary evaporator, leaving behind the aqueous layer. Pentane (7.5 mL) was added to the flask and it was vigorously shaken. The pentane layer was removed with a pasteur pipette, evaporated, and the sample residue re-suspended in 0.1 mL absolute ethanol. Each sample was analyzed with the Shimadzu VP HPLC using the analytical column.

Preparative High-Performance Liquid Chromatography. A second method of purifying the crude extracts was developed using preparative HPLC. A sample of crude extract (0.5 mL) was injected into the HPLC equipped with the preparative Luna Omega

5 μm Polar C18 100 LC column. The peaks were collected using a Gilson FC-100 Micro Fractionator, which was set to shift to a new collection test tube every three minutes. The test tubes were numbered in the order in which they were collected, and the peaks were assigned to which test tube they were in based on their elution time. The major peaks were collected from the fractionator, and each sample was placed in a 50-mL round-bottom flask and the organic solvent evaporated using a rotary evaporator, leaving behind the aqueous layer. Pentane (7.5 mL) was added to the flask and it was vigorously shaken. The pentane layer was removed with a pasteur pipette, evaporated, and the sample residue re-suspended in 0.1 mL absolute ethanol. Each sample was analyzed with the Shimadzu VP HPLC using the analytical Luna Omega 5 μm Polar C18 100 LC column 150×4.6 mm.

Prior to the preparative HPLC chromatographic method being used, an isocratic method of 75 % line A (20 mM ammonium formate, pH 3.20), and 25% line B (HPLC-grade acetonitrile) was run for 20 minutes at a flow rate of 5 mL/min. This was to completely remove the solution in which the column is stored and to achieve a baseline. After the preparative HPLC chromatographic method is complete, an isocratic method of 70% line A (HPLC-grade methanol), and 30% line B (HPLC water) was run for 10 minutes at a flow rate of 5 mL/min. This is the solvent system in which the column is stored. In total, the preparative HPLC chromatographic method uses 750 mL of solvent each time it is used.

Infrared Spectroscopy Method

A sample of the 4 mg/mL solution of Δ^9-THCA obtained via preparative HPLC (0.25 mL) was transferred to a vial, and the ethanol in which the sample was dissolved

was evaporated by running N_2 gas over it. The remaining residue (1 mg) was dissolved in a minimal amount of hexane. The hexane solution was dropped onto the crystal of the iD5 ATR accessory for the Nicolet iS5, and the hexane evaporated. This left behind only the solid Δ^9-THCA residue on the crystal, which was then analyzed.

Cell Growth and Assay

Studies referenced in the literature review section exploring different microbial species capable of decarboxylating aryl carboxylic acids were used to determine the cell lines to screen for their ability to decarboxylate Δ^9-THCA.

Pseudomonas putida was tested for decarboxylation activity. The *Pseudomonas putida* cells were cultured in 500 mL of MRS agar at 37 ˚C. The cells were fed every two days with 200 mL of fresh media. The *Pseudomonas putida* cells grew for five days before being induced with salicylic acid, and then they were incubated for an additional two days. The cells were centrifuged in 50-mL conical tubes at 4000*g* for 10 minutes. The remaining cell pellet was weighed and then resuspended in 25 mL of appropriate culture medium. Lysed cells were used to alleviate any issues there may have been with diffusion or transporting the Δ^9-THCA across membranes. The cells were lysed through sonification with a Branson Digital sonifier. The samples were sonicated at a 10% amplitude for ten seconds, the sonication paused for one second, and then sonicated again for ten seconds. This method was repeated twice for each cell sample.

To evaluate if the cells chosen will decarboxylate the Δ^9-THCA, 16.0 mL of the cell suspension plus 0.10 mL of Δ^9-THCA were incubated and 2.0 mL aliquots of the media were removed at various times to analyze with the HPLC to determine the presence of Δ^9-THC. The concentration of the Δ^9-THCA used is specified in appendices

D-H. Cells were incubated in a water bath at 37 °C with gentle shaking. The 2-mL aliquots were taken at 0, 1, 2, 3, 4, 5 and 6 hr. The cannabinoids were extracted from the 2-mL media aliquot using 5.0 mL pentane containing 0.5 mL ethanol. The extract was evaporated to dryness with N_2, and the residue containing cannabinoids was resuspended in 0.10 mL ethanol and analyzed via HPLC. The second through the fifth assays had an identical control solution of bacteria and Δ^9-THCA which had aliquots taken at the same time as the experimental solution. The only difference between the control and the experimental solution was that the control was autoclaved beforehand to inactivate all enzymatic activity. Thus, if enzymatic decarboxylation activity was observed in the experimental aliquot samples, this would not be seen in the control aliquot samples. The first assay conducted did not have a control.

Comparison of Δ^9-Tetrahydrocannabinolic Acid Yield Between Preparative High-Performance Liquid Chromatography Method and Yamazen Method

The yield of the two methods of isolating Δ^9-THCAwere compared. A Soxhlet extraction was performed, the mass of the crude extract recorded, and then a solution of the crude extract was injected in to the preparative HPLC and the Yamazen Smart Flash. The mass of the residue presumed to contain Δ^9-THCA was measured after it was collected from both the preparative HPLC and the Yamazen Smart Flash. After this each of the residues presumed to contain Δ^9-THCA were dissolved in ethanol to make a 2 mg/mL solution, and then each analyzed via the analytical HPLC method to confirm they contain Δ^9-THCA. The CLASS-VP 7.2.1 SP1 software program was used to determine the percent area under the curve of the Δ^9-THCA peak for the whole

chromatogram in each sample. This was then used to determine the actual mg of Δ^9-THCA in each and then the percent Δ^9-THCA in the total equivalent mass of marijuana plant injected. This percentage was then compared to the percentage of Δ^9-THCA reported on the label (13.5%) of the marijuana plant received from the National Institute on Drug Abuse.

Construction of Calibration Curve for Δ^9-Tetrahydrocannabinolic Acid

Prior to assessing the ability of a cell line to decarboxylate the Δ^9-THCA, a calibration curve was constructed by graphing different concentration samples of Δ^9-THCA against the area under the curve of the peak detected for each with the analytical HPLC. A 4 mg/mL solution of Δ^9-THCA in ethanol was prepared from Δ^9-THCA obtained using the preparative HPLC method. Serial dilution of the 4 mg/mL Δ^9-THCA produced a 2, 1, 0.5, and 0.25 mg/mL solutions. This was repeated using three different starting 4 mg/mL solutions obtained from preparative HPLC runs to make triplicates of each concentration. Each solution was analyzed via the analytical HPLC method, the area under the curve of the peak was obtained using the CLASS-VP 7.2.1 SP1 software program, and the calibration curve constructed by plotting these areas against the corresponding concentration of the sample. Since triplicates of each concentration were analyzed, the area under the curve used for the calibration curve were the average of the triplicates.

Construction of Calibration Curve for Δ^9-Tetrahydrocannabinol

If decarboxylation activity is observed, the concentration of Δ^9-THC produced can be determined through using a calibration curve. The calibration curve was

constructed by plotting different concentration samples of Δ^9-THC against the area under the curve of the peak detected for each with the analytical HPLC. A 5 mg/mL solution of Δ^9-THC in ethanol was obtained by diluting the standard obtained from Sigma-Aldrich. This was used to make three 4 mg/mL solutions of Δ^9-THC. A serial dilution of each of the 4 mg/mL Δ^9-THC solutions was made to produce solutions containing 2 mg/mL, 1 mg/mL, 0.5 mg/mL, and 0.25 mg/mL. Each solution was analyzed via the analytical HPLC method, the area under the curve of the peak was obtained using the CLASS-VP 7.2.1 SP1 software program, and the calibration curve constructed by plotting these areas against the concentration of the sample. Since triplicates of each concentration were analyzed, the area under the curve used for the calibration curve were the average of the triplicates.

CHAPTER IV

RESULTS AND DISCUSSION

Isolation of Δ^9-Tetrahydrocannabinolic Acid

Analytical High-Performance Liquid Chromatography Assessment of Cannabinoid Standards

Standards of cannabinoids were analyzed via the analytical HPLC method to determine their elution times. This was done for Δ^9-tetrahydrocannabidiol (Δ^9-THC), cannabidiol (CBD), cannabidolic acid (CBDA), and a mixture of cannabinoids containing CBDA, cannabigerolic acid (CBGA), cannabigerol (CBG), CBD, tetrahydrocannabivarin (THCV), cannabinol (CBN), Δ^9-tetrahydrocannabinolic acid (Δ^9-THCA), Δ^9-THC, Δ^8-tetrahydrocannabidiol (Δ^8-THC), and cannabichromene (CBC) (Fig. 15 – 18). Some drift of the standard peaks was observed so many assessments of the standards were performed. From this it was determined that the elution time for each of the cannabinoids is dependent on whether they are in a mixture. In addition, the elusion time for a standard may vary depending on the solvent in which it is dissolved and if the gradient method does not have enough time to re-equilibrate after each sample analysis.

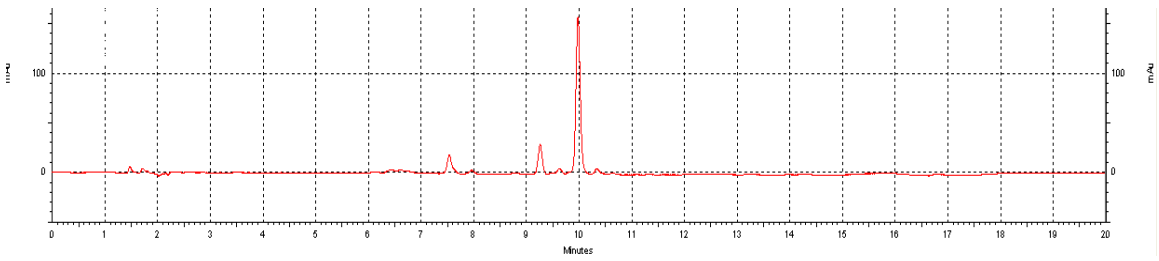

Figure 15: Analytical HPLC method chromatogram of Δ^9-THC standard (1.2 mg/mL in ethanol).

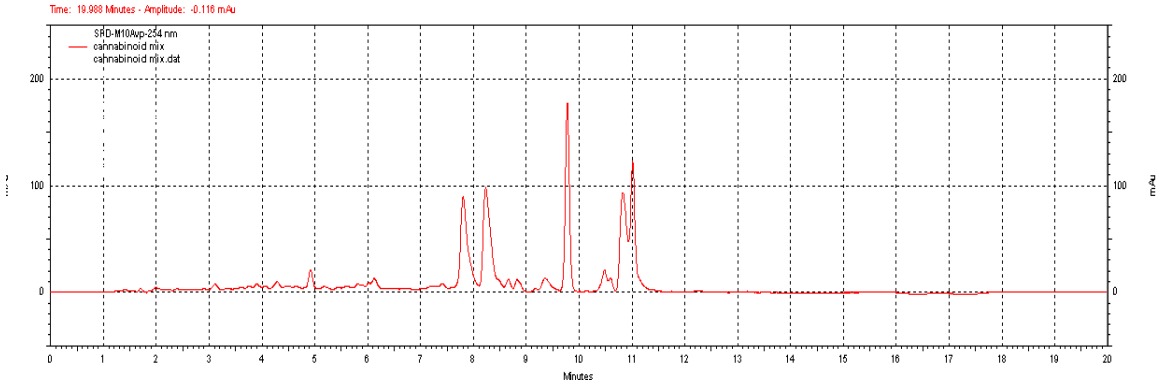

Figure 16: Analytical HPLC method chromatogram of cannabinoid mixture standard containing CBDA, CBGA, CBG, CBD, THCV, CBN, Δ^9-THCA, Δ^9-THC, Δ^8-THC, and CBC (100 µg/mL each in acetonitrile).

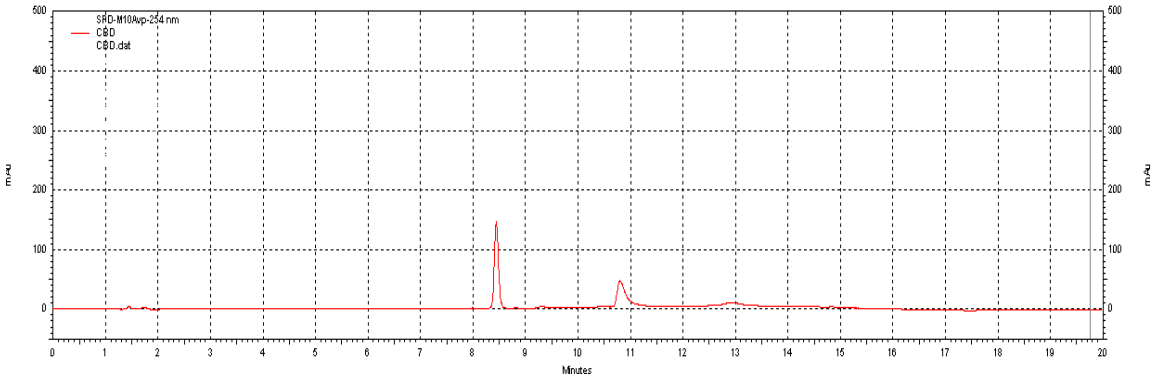

Figure 17: Analytical HPLC method chromatogram of CBD standard (1.2 mg/mL in ethanol).

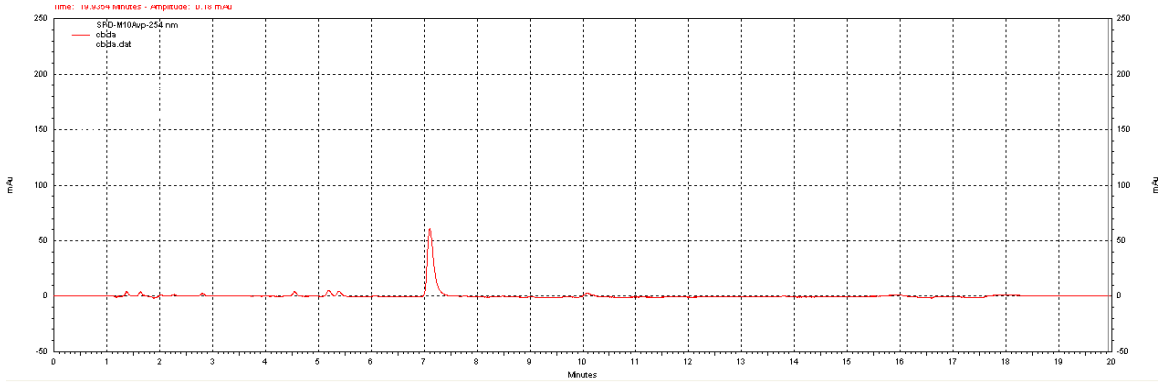

Figure 18: Analytical HPLC method chromatogram of CBDA standard (0.1 mg/mL in ethanol).

Phenomenex, the company which made the analytical column used for the analytical HPLC method, released a chromatogram of a mixture of cannabinoid standards analyzed using the Luna Omega Polar C18 100x2.1 mm column with a similar 20 mM pH 3.20 ammonium formate and acetonitrile method as used in this study. Through comparing their chromatogram (Appendix A) with Figures 16 - 19, the peaks in Figure 16 can be assigned. In Figure 16, the peak at 4.9 minutes is CBDV, the peak at 7.9 minutes is mostly likely both CBD and CBDA, the peak at 8.2 minutes is most likely both CBGA and CBN, the peak at 9.9 minutes is Δ^9-THC, the peak at 10.9 minutes is CBC, and the peak at 11 minutes is Δ^9-THCA (Appendix A; Fig. 15 – 18).

A reverse phase method was used for the analytical HPLC column. Traditionally, reverse phase methods consist of using a polar mobile phase and a non-polar stationary phase. Δ^9-THCA, since it has an extra carboxylic group would be expected to be more polar than Δ^9-THC, and thus have a shorter elution time. However, there is intramolecular hydrogen bonding in Δ^9-THCA which does not exist in Δ^9-THC. This causes Δ^9-THC to behave more polar than Δ^9-THCA and thus it had a shorter elution time than Δ^9-THCA using the analytical HPLC method.

In addition, the solvent in which the sample is dissolved when injected into the analytical HPLC will affect the elution time. This can be seen when comparing the Δ^9-THC standard chromatogram with the mix of cannabinoids chromatogram. The Δ^9-THC standard is dissolved in ethanol and the Δ^9-THC eluted at 10.0 minutes, whereas the mixture of cannabinoids are dissolved in acetonitrile and the Δ^9-THC eluted at 9.9 minutes (Fig. 15 and 16). The CBD standard is dissolved in ethanol and eluted at 8.4 minutes, whereas the CBD in the mixture eluted at 7.9 minutes (Fig. 16 and 17). The

CBDA standard is dissolved in ethanol and eluted at 7.1 minutes whereas the CBDA in the mixture eluted at 7.9 minutes (Fig. 16 and 18). The Δ^9-THCA in the mixture of cannabinoids eluted at 11.0 minutes (Fig. 16). The samples from the microbial cell assay that were injected into the analytical HPLC were dissolved in ethanol, thus the elution time for the Δ^9-THCA in these samples should have a slightly shorter elution time than the Δ^9-THCA in the mixture of cannabinoids.

Crude Extraction of Cannabinoids From Marijuana Plant Material

Both the sonication and the Soxhlet methods of extracting a crude mix of cannabinoids from plant material were successful. Samples of the crude extract were prepared for isolation of Δ^9-THCA by placing 1 mL of absolute ethanol into the round-bottom flask in which the extract was collected at the end of both crude extraction processes and vigorously shaken (see Methods). The 1.0 mL volume of ethanol should be saturated with cannabinoids and then used for the isolation of Δ^9-THCA by injecting into either the Yamazen or the preparative HPLC. Both methods of obtaining crude extract provided an adequate mass of Δ^9-THCA to be isolated and further using in the cell line assays. The Soxhlet method allowed for a greater mass of plant material to be extracted compared to the sonication method; 5.0 g versus 1.0 g, respectively. Further, the Soxhlet method required no human interaction during the three-hour extraction after the initial setup, whereas the sonication method required several steps of interaction during its approximately two-hour long extraction. Thus, comparatively the Soxhlet method was a more useful method of producing the crude extract since it allowed more time for the cannabinoids to dissolve into the solvent, and it was very simple in execution.

Yamazen Chromatography

Chromatograms of the samples of cannabinoids were developed using reverse-phase TLC plates to determine what solvent system would result in a cannabinoid extract having an R_f value for THCA of approximately 0.2. This was done because the Yamazen Smart Flash uses an image of the TLC plate to set up its chromatographic method, and an R_f value of approximately 0.2 for the compound of interest is recommended for this. The final solvent system which was used was 80% acetonitrile, 10% methanol, and 10% 20 mM ammonium formate, 3.20 pH. This gave a R_f value of 0.25 (Fig. 19). The spots on this plate were visualized using an ultraviolet light.

Since there was no available standard of Δ^9-THCA to compare the crude extract via TLC, additional TLC plates were developed which were spotted by a crude cannabinoid extract made from marijuana plant material of high CBD content and a crude cannabinoid extract made from marijuana plant material of high Δ^9-THCA content (both of which were made through the Soxhlet extraction method). This was done to determine where the Δ^9-THCA would appear on the TLC plate through comparing these two extracts. Comparing these, the Δ^9-THCA was identified by observing a larger spot in the cannabinoid extract made from marijuana plant material of high Δ^9-THCA when compared to the cannabinoid extract made from marijuana plant material of high CBDA (TLC plates not pictured). The Δ^9-THCA from this plate was used when developing the TLC plate which was used for the Yamazen chromatography (the spot on the right in Figure 19). The spot on the left in Figure 19 is crude cannabinoid extract (made through the sonication method). In Figure 19 both of these samples have a major spot at an R_f of 0.25, which was presumed to be Δ^9-THCA.

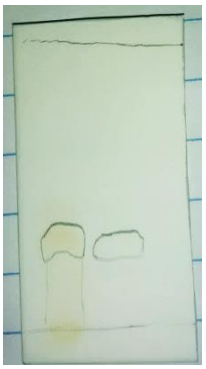

Figure 19: Image of TLC plate used for developing the Yamazen Smart Flash method. Left lane is crude cannabinoid extract, right lane is Δ^9-THCA obtained from an unpictured TLC plate.

Four peaks were collected from the Yamazen (Fig. 20). The first peak was from time 0.25 min to 0.67 min, the second peak was from time 2.75 min to 5.17 min, the third peak was from time 5.17 min to 11.42 min, and the fourth peak was from time 11.42 min to 19.67 min (Fig. 20). The organic solvent was evaporated from each peak using a rotary evaporator and the remaining aqueous layer was extracted with 7.5 mL pentane to collect all cannabinoids. The pentane was evaporated via open-dish evaporation, and the remaining reside was weighed and dissolved in 0.1 mL absolute ethanol to be analyzed via analytical HPLC.

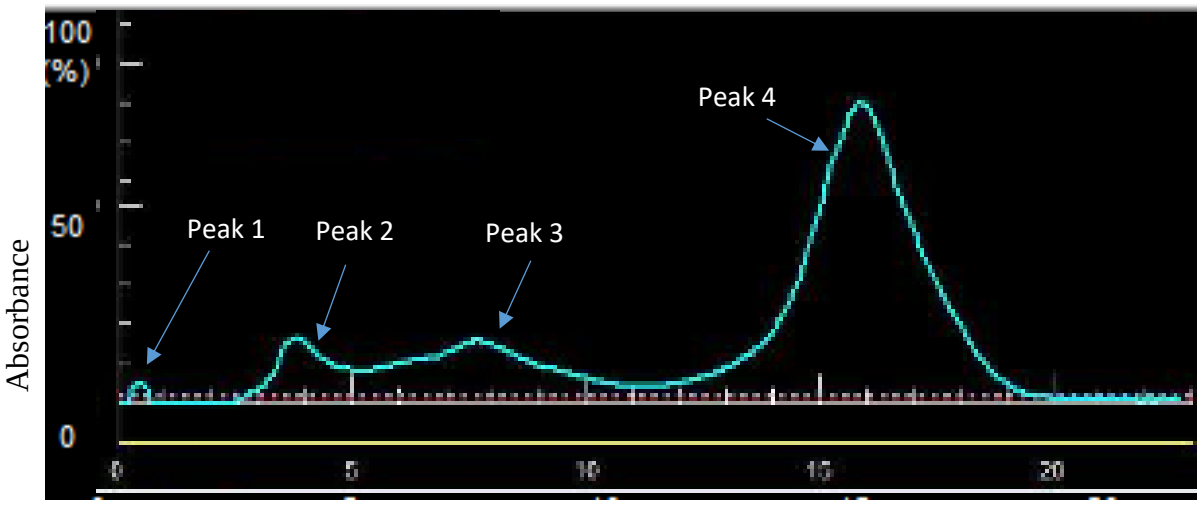

Figure 20: Yamazen chromatogram obtained after injecting 1.0 mL crude cannabinoid extract solution.

The fraction under each of the Yamazen peaks were individually injected into the Shimadzu HPLC equipped with the analytical column. The first two Yamazen fractions (representing peaks 1 and 2) had no significant peaks corresponding to Δ^9-THCA when analyzed with the analytical HPLC method. Fraction 3 had a significant peak at approximately 12.5 minutes (Fig. 21). Fraction 4 had a significant peak at a slightly later elution time (13.5 min). This sample was used as the Δ^9-THCA in the first three microbial cell assays. The solvent was evaporated from this sample and the remaining residue weighed. The residue was dissolved in 5.65 mL of absolute ethanol to produce a 4 mg/mL solution.

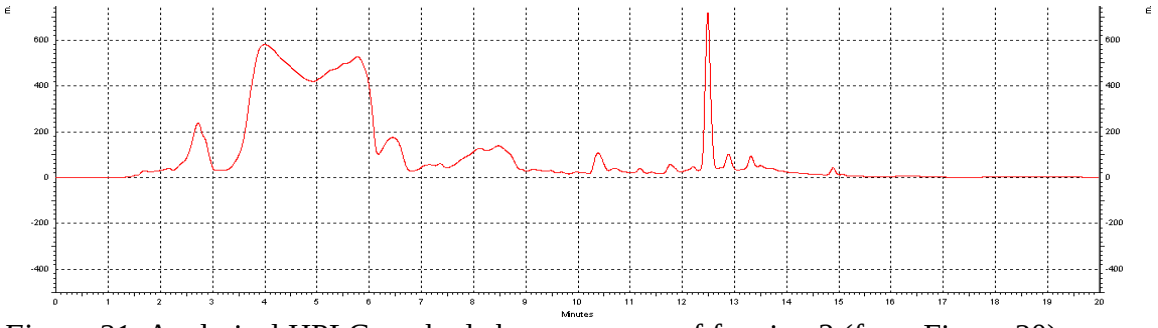

Figure 21: Analytical HPLC method chromatogram of fraction 3 (from Figure 20).

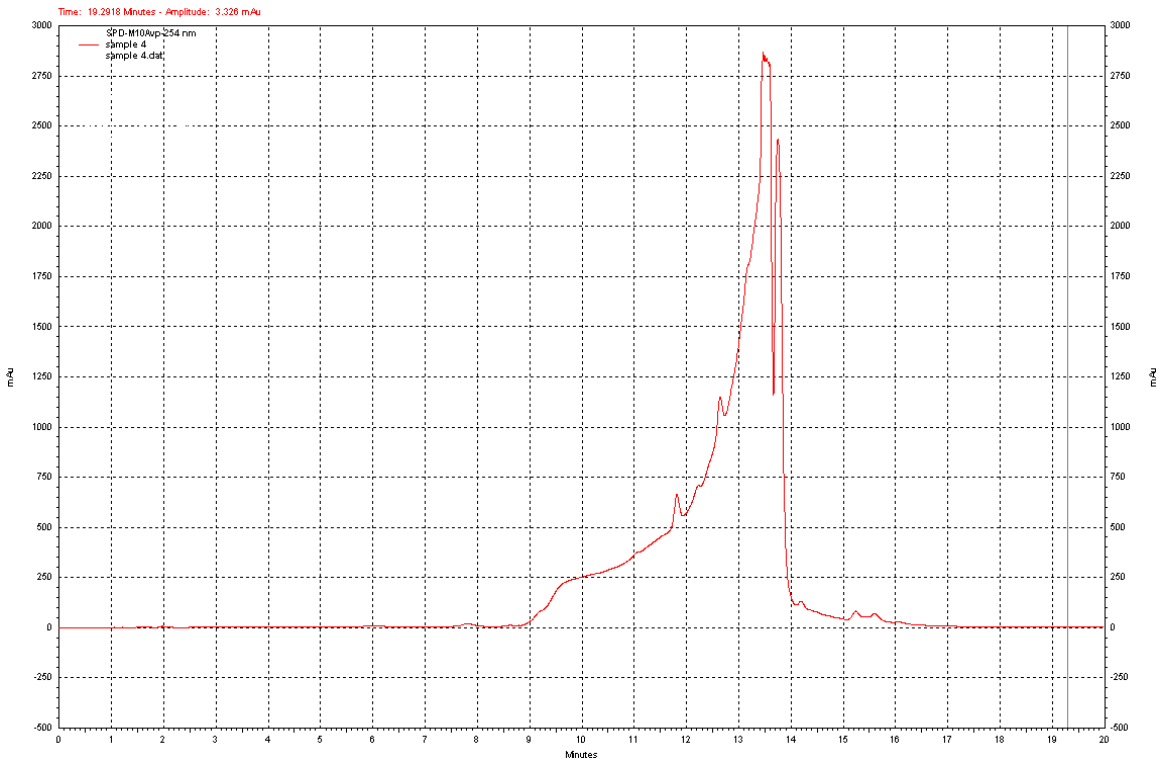

Figure 22: Analytical HPLC method chromatogram of fraction 4 (from Figure 20). The peak at 13.5 min was presumed to be Δ^9-THCA.

In addition to analysis via HPLC, each of the four fractions collected from the Yamazen were also analyzed via proton NMR (Appendix B). Both fraction 3 and fraction 4 from Figure 20 appear to contain Δ^9-THCA when comparing each of their spectra (Fig. 23 & 24, respectively) to the literature Δ^9-THCA NMR spectrum (Fig. 13). Additionally, the NMR spectra (both Figures 24 and 25) have peaks at approximately 6.39 ppm and 6.24 ppm which can be assigned according to Hazekamp et al. as peaks in Δ^9-THCA (2004).

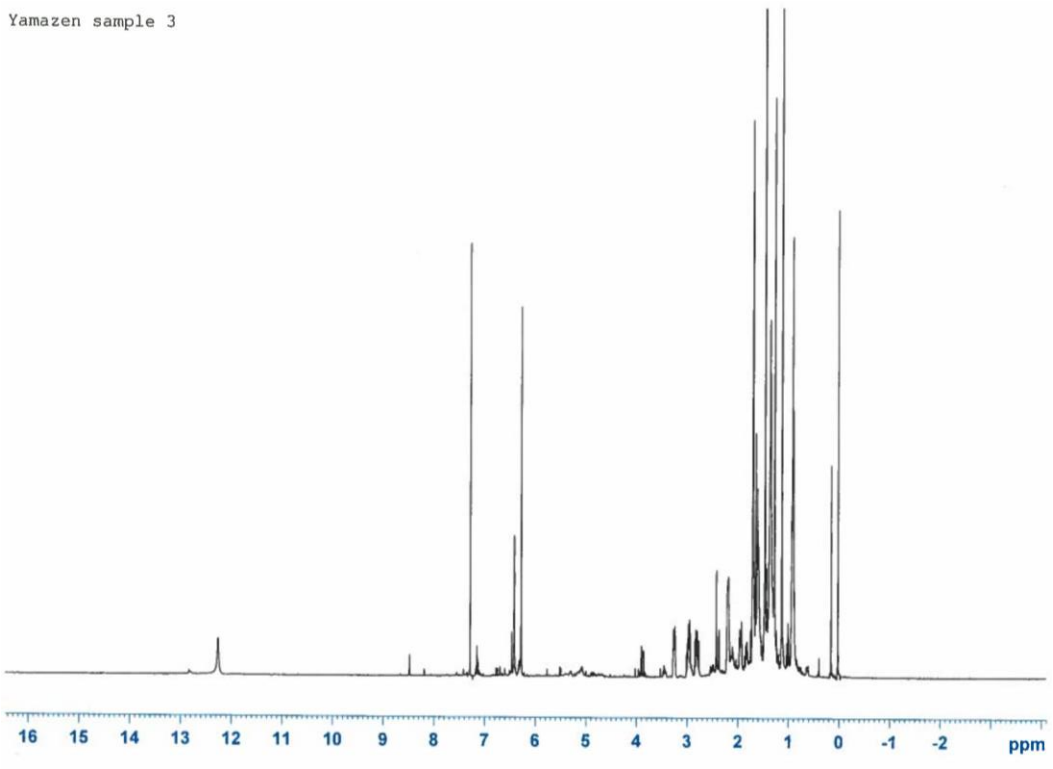

Figure 23: Proton NMR chromatogram of fraction 3 (from Figure 20).

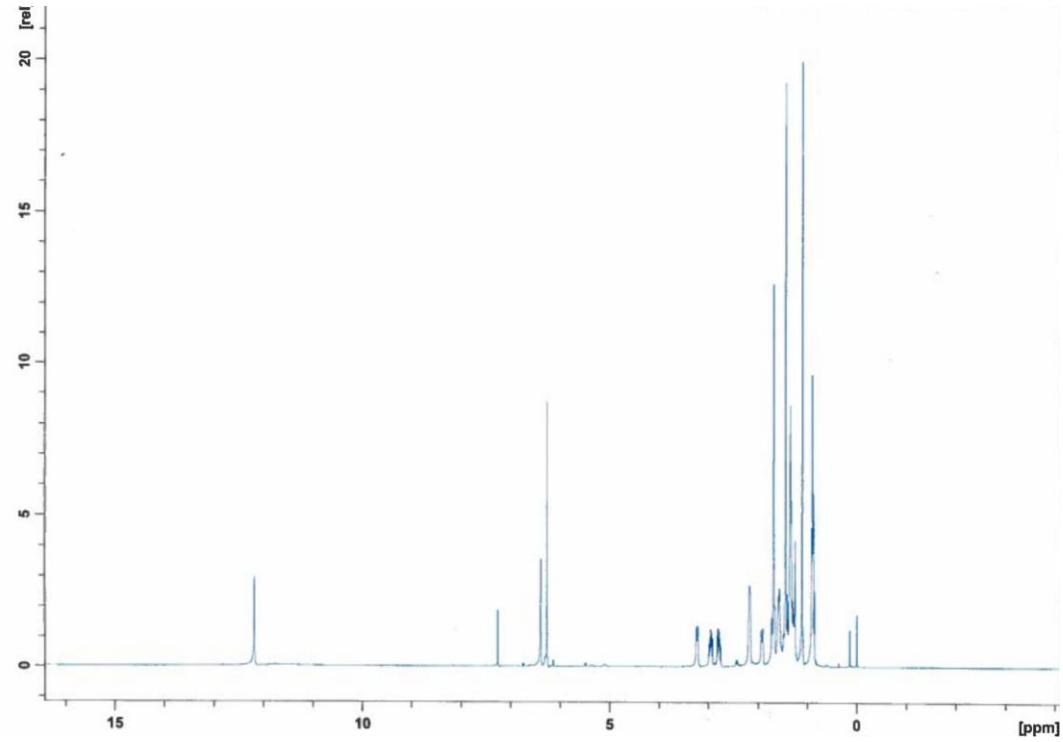

Figure 24: Proton NMR chromatogram of fraction 4 (from Figure 20).

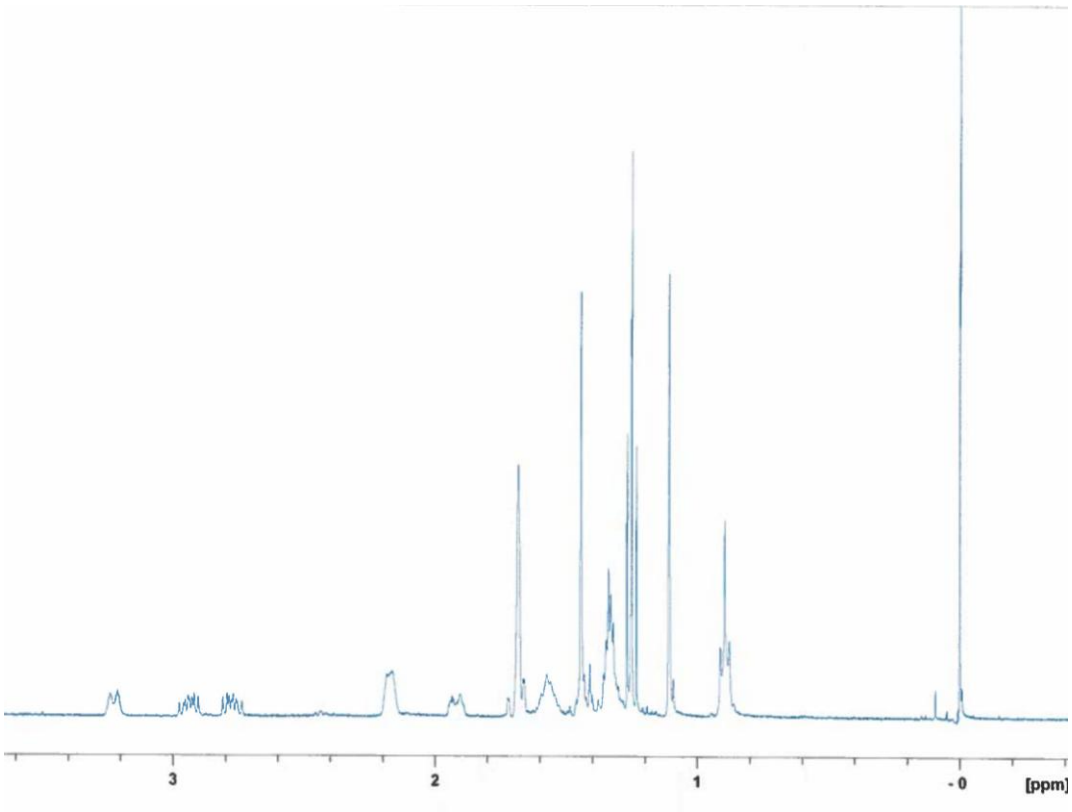

Figure 25: Zoom of proton NMR chromatogram of fraction 4 (from Figure 20).

In Figure 24, a carboxylic acid proton is seen at approximately 12.2 ppm. In addition, when Figure 24 is compared to the literature standard Δ^9-THCA spectra reported by Hazekamp et al. the peaks for H-2 and H-5' at approximately 6.2 and 6.4 ppm, respectively, are visible (2004). Comparing Figure 25 to the literature standard Δ^9-THCA spectra (Fig. 13), both the H-1'' peaks at approximately 2.78 ppm and 2.95 ppm are visible as well as the H-1 doublet at approximately 3.23 ppm are visible. These observations indicate that fraction 4 from Figure 20 collected from the Yamazen chromatography contains Δ^9-THCA. All these peaks are also seen in the NMR spectra for fraction 3 from Figure 20. The major peak at approximately 7.3 ppm is due to a small

amount of chloroform present in the chloroform-d used as the solvent for the NMR (Fig. 23). Fraction 4 was used for some of the microbial cell assays.

Preparative High-Performance Liquid Chromatography

Several components were separated using the preparative HPLC and collected into test tubes using the Gilson FC-100 Micro Fractionator. Figure 26 is the chromatogram for the preparative separation of 0.5 mL of crude extract produced through Soxhlet extraction. Due to the fractionator, each peak seen on the chromatogram was collected in a numbered test tube, which are recorded for the major peaks in Figure 26.

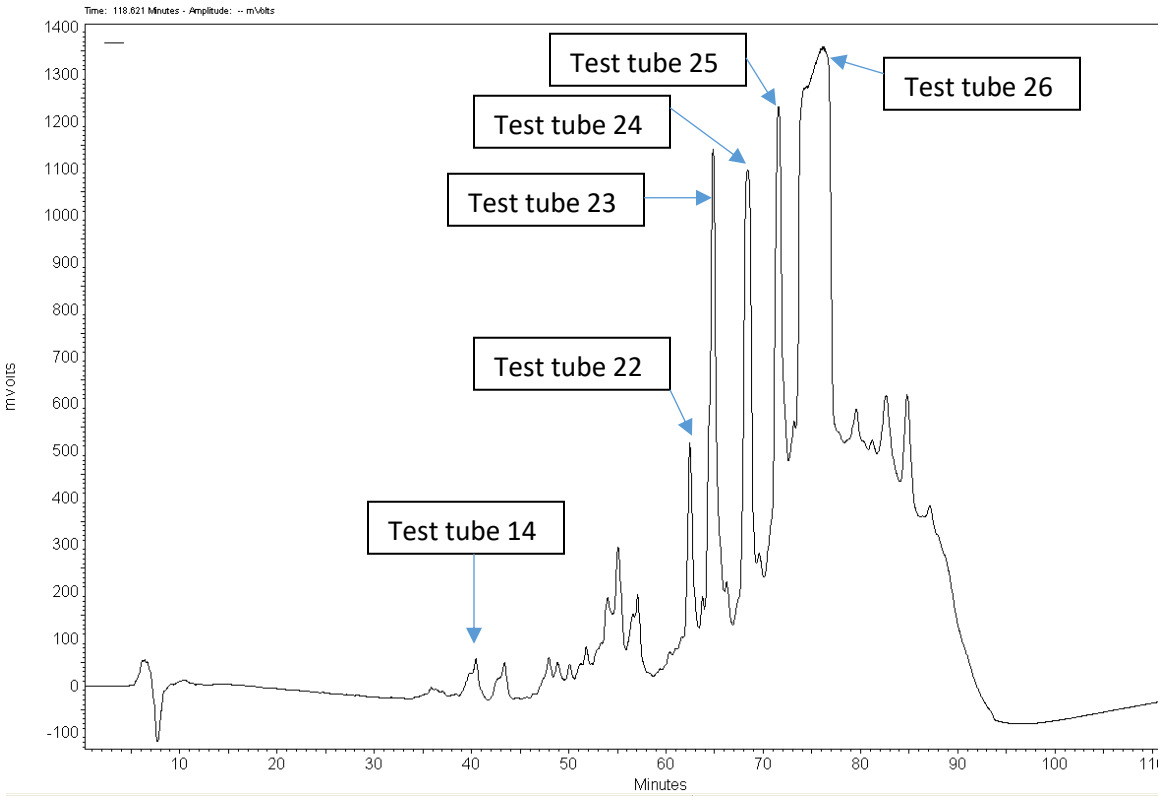

Figure 26: Preparative HPLC chromatogram of 0.5 mL of crude cannabinoid extract.

Each of the major fractions collected from the preparative HPLC method were analyzed via proton NMR and analytical HPLC (Appendix C). The organic solvent was

evaporated from each test tube with a rotary evaporator followed by extraction of the aqueous solvent with pentane, evaporated to dryness, and the mass of the residue was determined. Fraction 14 was from elution time 38.97 to 41.97 min, fraction 22 from 62.97 to 65.97 min, fraction 23 from 65.97 to 68.97 min, fraction 24 from 68.97 to 71.97 min, fraction 25 from 71.97 to 74.97 min, and fraction 26 from 74.97 to 77.97 minutes (Fig. 26). Before being analyzed via NMR, each sample was dissolved in 600 μL of deuterated chloroform. The fraction collected in test tube 26 appeared to contain Δ^9-THCA through comparison of its NMR spectra (Fig. 27 – 28) with the Δ^9-THCA standard literature spectra (Fig. 13). Additionally, the NMR spectrum (Figure 27) has peaks at approximately 6.39 ppm and 6.24 ppm which are identified by Hazekamp et al. as peaks in Δ^9-THCA (2004).

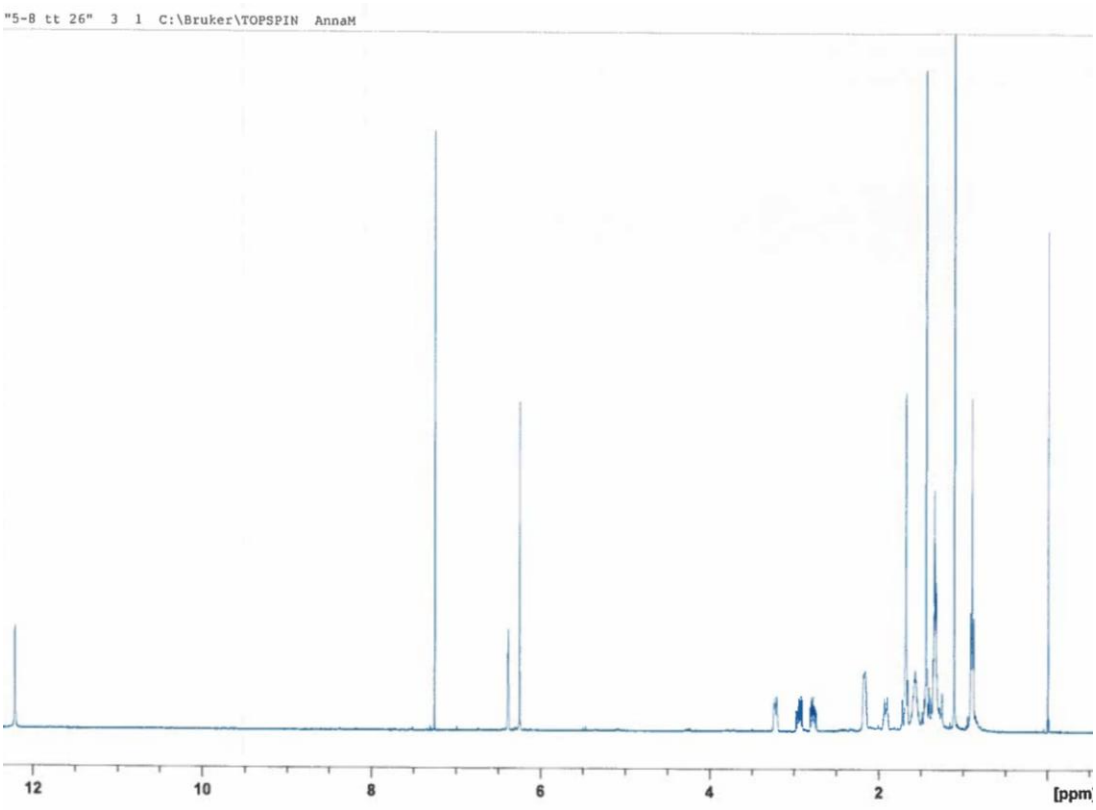

Figure 27: Proton NMR spectra of fraction 26 (from Figure 26).

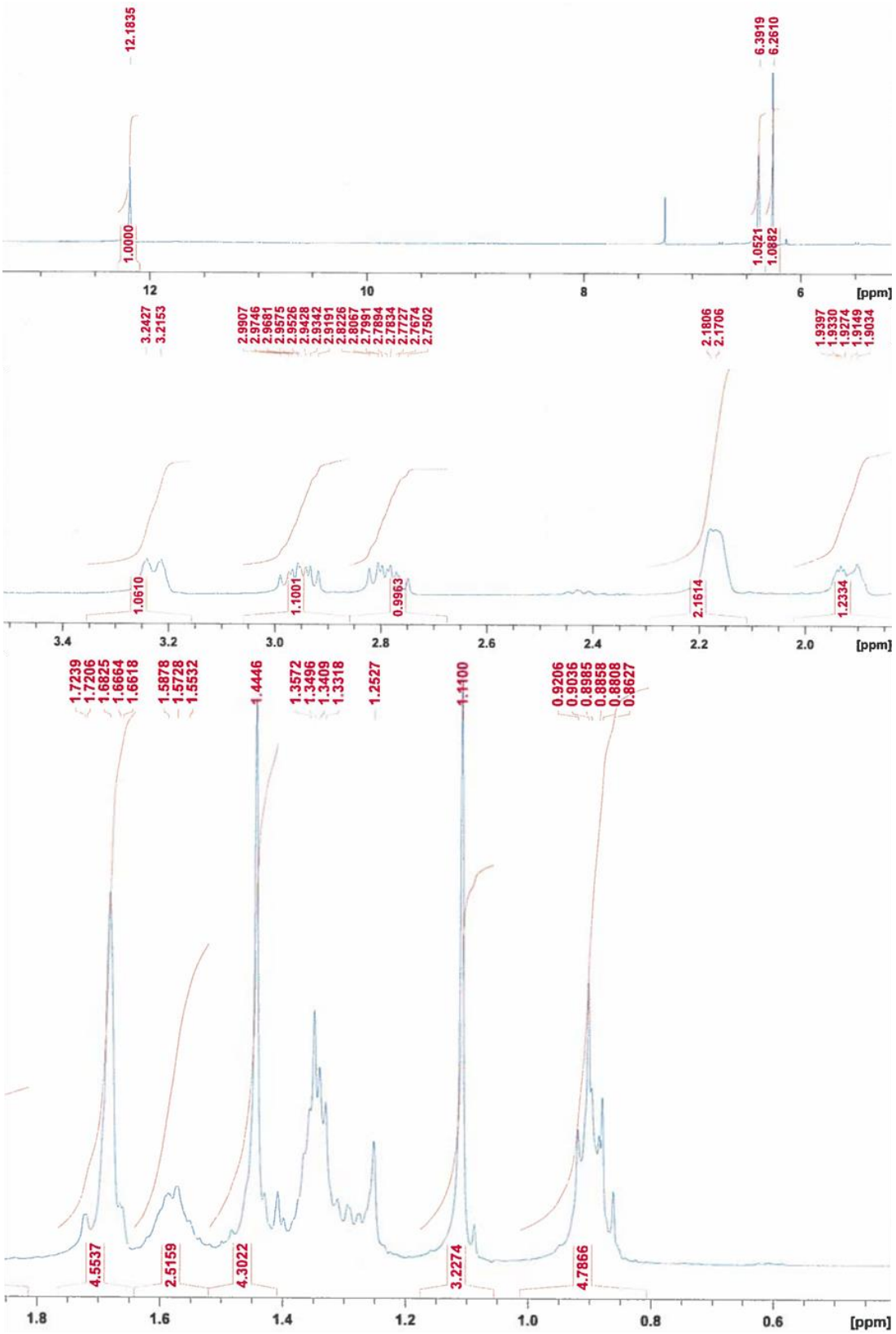

Figure 28: Integration and chemical shift of proton NMR spectra of fraction 26 (from Figure 26).

In Figure 27, a carboxylic acid proton is seen at approximately 12.21 ppm. In addition, when Figure 27 is compared to the standard Δ^9-THCA spectra by Hazekamp et al. the peaks for H-2 and H-5' at approximately 6.2 and 6.4 ppm, respectively, are present (2004). Comparing Figure 28 to the standard Δ^9-THCA spectra (Fig. 13), both the H-1'' peaks at approximately 2.78 and 2.95 as well as the H-1 doublet at approximately 3.25 are present. These observations indicated that this sample contains Δ^9-THCA.

Table 1

Comparison of Proton NMR Spectra of Fraction 26 (from Figure 26) with Proton NMR of Δ^9-THCA reported by Choi et al. (2004).

Carbon Position in Δ^9-THCA	Chemical Shift in Choi study (2004) (ppm)	Chemical Shift from Figure 28
1	3.23	3.23
2	6.39	6.39
3 – Me	1.68	1.68
4	2.17	2.18
5	1.92, 1.35	1.93, 1.25
6	1.67	1.72
8	1.44	1.44
9	1.11	1.11
5'	6.26	6.26
1''	2.94, 2.78	2.95, 2.79
2''	1.57	1.57
3''	1.35	1.35
4''	1.35	1.35
5''	0.90	0.90
COOH	12.19	12.18

The proton NMR spectrum (Figure 28) was compared to the proton NMR spectrum of Δ^9-THCA reported by Choi et al. (2004). Each of the observed peaks in both spectra have similar chemical shifts; the data from Figure 28 and the data presented by Choi et al. are compared side by side in Table 1. The largest difference between any of the chemical shifts in Figure 28 and the chemical shifts from the Choi study is 0.10 ppm

(Table 1). The numbering of the carbons used in Table 1 is the same numbering used in Figure 13. Fraction 26 from Figure 26 was also analyzed via carbon NMR and the peaks observed compared to the peaks reported by Choi et al. (2004).

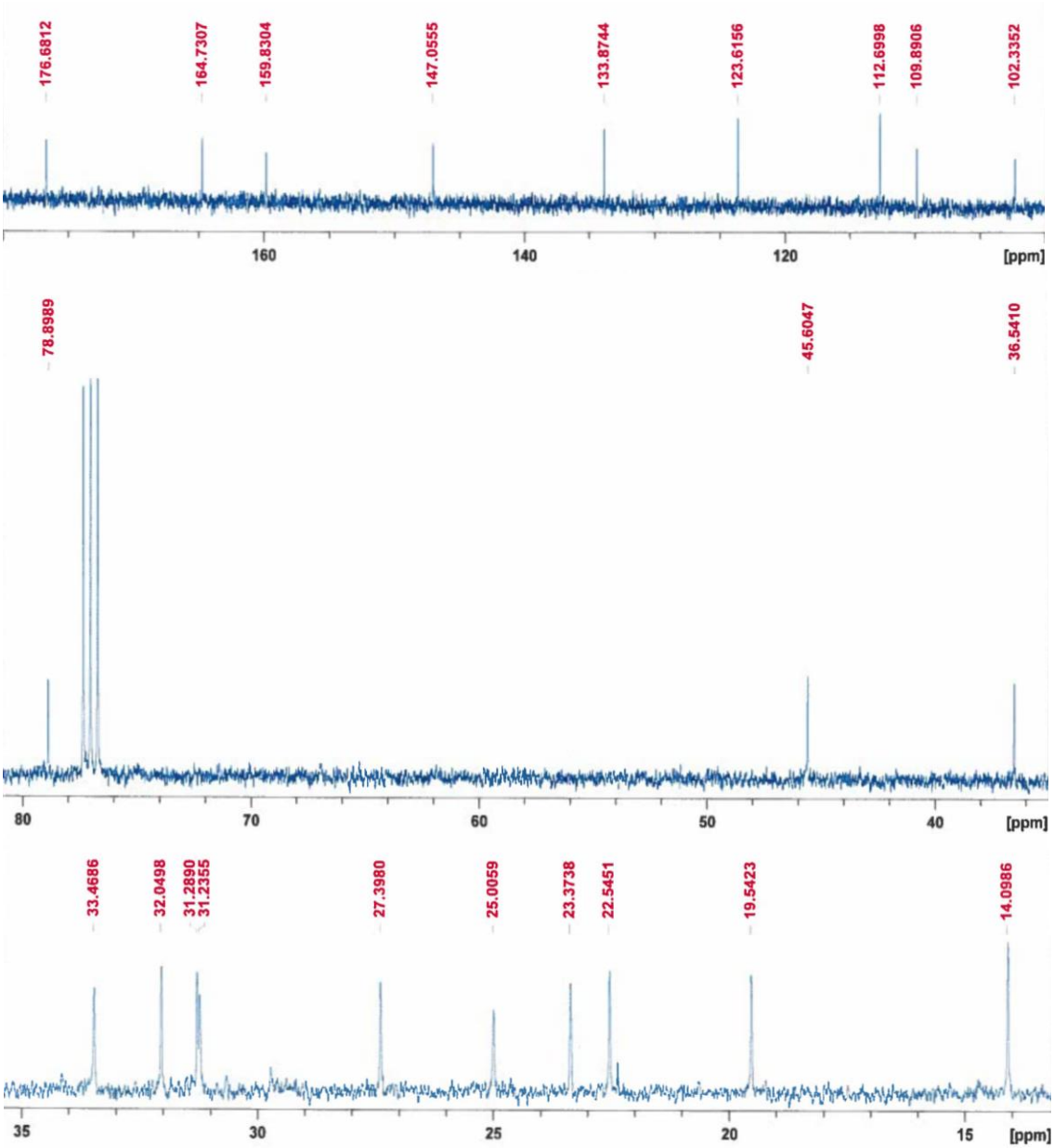

Figure 29: Carbon NMR spectra of fraction 26 (from Figure 26).

The carbon NMR spectrum (Figure 29) was compared to the carbon NMR spectrum of Δ^9-THCA reported by Choi et al. (2004). Each of the observed peaks in both

spectra have similar chemical shifts; the data from Figure 29 and the data presented by Choi et al. are compared side by side in Table 2. The largest difference between any of the chemical shifts in Figure 29 and the chemical shifts from the Choi study is 0.4812 ppm (Table 2). The numbering of the carbons used in Table 2 is the same numbering used in Figure 13.

Table 2

Comparison of Carbon NMR Spectra of Fraction 26 (from Figure 26) with Carbon NMR of Δ^9-THCA reported by Choi et al. (2004).

Carbon Position in Δ^9-THCA	Chemical Shift in Choi study (2004) (ppm)	Chemical Shift from Figure 29
1	33.5	33.5
2	123.6	123.6
3	133.8	133.9
3 – Me	23.3	23.4
4	31.2	31.2
5	25.0	25.0
6	45.6	45.7
7	78.8	78.9
8	27.4	27.4
9	19.6	19.5
1’	109.9	109.9
2’	164.7	164.7
3’	102.3	102.3
4’	146.9	147.1
5’	112.6	112.7
6’	159.8	159.8
1’’	36.5	36.5
2’’	31.3	31.3
3’’	32.0	32.1
4’’	22.5	22.6
5’’	14.1	14.1
COOH	176.2	176.7

After NMR analysis, the deuterated chloroform was evaporated from the sample collected in fraction 25 (from Figure 26) by running N_2 gas over it. A 4.0 mg/mL solution of the remaining residue was made by adding 1.425 mL of absolute ethanol. A serial

dilution of this solution was made to construct a calibration curve of the Δ^9-THCA solution using the analytical HPLC method. The 4.0 mg/mL solution from fraction 26 (from Figure 26) was also injected into the analytical HPLC to compare it to analytical HPLC analysis of the mixture of standard cannabinoids to determine the elution time of Δ^9-THCA and its purity.

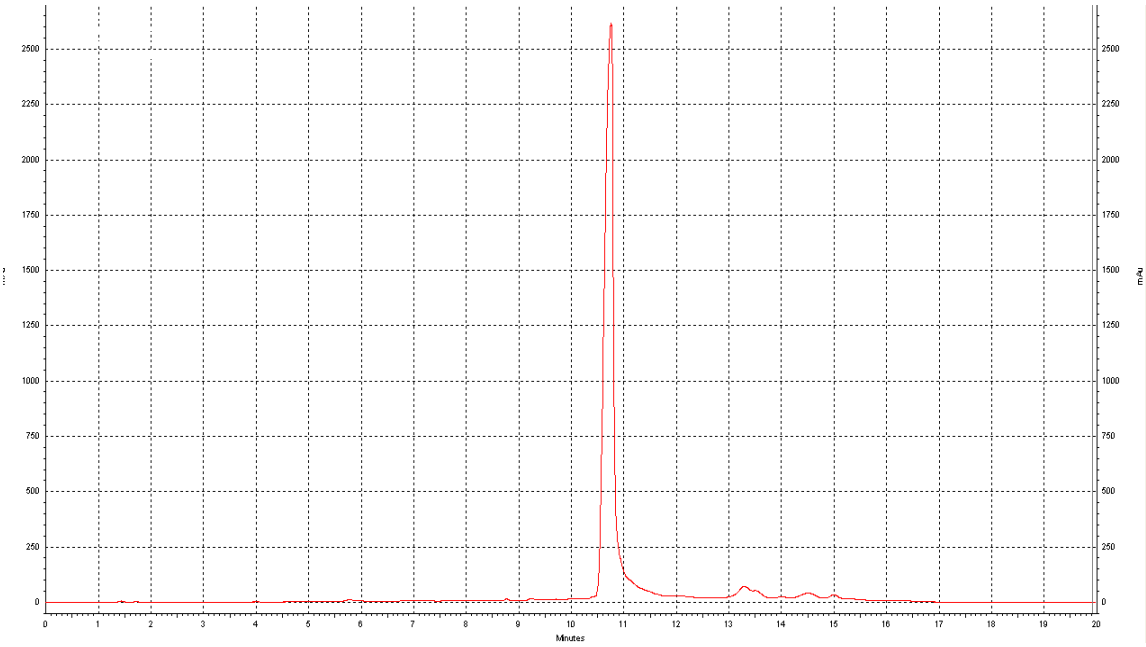

Figure 30: Analytical HPLC analysis of 4.0 mg/mL solution of fraction 26 (from Figure 26).

The most significant peak in Figure 31 has an elution time of approximately 10.75 minutes. This was the only peak in the solution detected at an intensity above 100 mAu. Comparing this peak to the mix of standard cannabinoids chromatogram (Fig. 16), along with examining the proton NMR spectra of this compound, the peak in Figure 31 can be identified as Δ^9-THCA and its elution time is approximately 10.75 minutes. Additionally, a 1 mg sample of the Δ^9-THCA collected from fraction 26 (Fig. 26) was analyzed via IR.

Figure 31: IR analysis of 4 mg/mL solution of fraction 26 (from Figure 26).

The IR spectrum in Figure 31 has a very broad peak starting at approximately 2400 cm^{-1} and ending at approximately 3600 cm^{-1}. This type of peak is indicative of a carboxylic acid. Additionally, there is a sharp peak at 1617.30 cm^{-1} and a sharp peak at 1257. 32 cm^{-1}. These are indicative of a C=O stretch and a C−O stretch, respectively. Comparing this spectrum to the IR spectrum by Smith, Lewis, and Mendez (2016), both have a broad carboxylic acid peak, along with sharp peaks at approximately 1250 cm^{-1}. Additionally, the C=O stretch peak in the Smith, Lewis, and Mendez paper is as 1614.42 cm^{-1} which corresponds to the C=O stretch in Figure 31 at 1617.30 cm^{-1}. Further, both spectra have similar sp^3 carbon stretches at approximately 2800 cm^{-1}. This provided

further confirmation that the contents of fraction 26 collected via preparative HPLC (Figure 26) contain Δ^9-THCA.

Comparison of Δ^9-Tetrahydrocannabinolic Acid Yield Between Preparative High-Performance Liquid Chromatography Method and Yamazen Method

A Soxhlet extraction of 5.01 g of 13.5% Δ^9-THCA marijuana plant was completed using 100 mL of pentane. The 250 mL round-bottom flask used for this extraction was weighed before and after it contained the dried crude cannabinoid extract. The mass of this extract was 1.0451 g. This residue was dissolved in 6.0 mL of ethanol and transferred to a test tube. Aliquots of this 0.1741 g/mL crude cannabinoid solution was then injected into both the preparative HPLC (0.25 mL aliquot) and the Yamazen Smart Flash (0.50 mL aliquot). The data used to determine the percent yield of each method are presented in Table 3.

These results indicate that the preparative HPLC method was able to isolate 99.3% of the Δ^9-THCA in the marijuana plant received by the National Institute on Drug Abuse, whereas the Yamazen Smart Flash was able to isolate 27.1% of the Δ^9-THCA in the marijuana plant.

Table 3

Comparison of Δ9-THCA Yield Between Preparative HPLC Method and Yamazen Method

Fraction	Preparative HPLC	Yamazen Smart Flash
Volume of crude cannabinoid extract injected (mL)	0.25	0.50
Equivalent mass of crude cannabinoid extract injected (mg)	44	87
Equivalent mass of marijuana plant injected (mg)	210	420
Mass of residue presumed to contain Δ^9-THCA collected from instrument (mg)	36	20
Analytical HPLC percent area under the curve of Δ^9-THCA peak	77.7	76.7
Mass of Δ^9-THCA in residue collected from instrument (mg)	28	15
% Δ^9-THCA collected from original mass of plant material injected	13.4	3.66
% Yield of Δ^9-THCA based on percent Δ^9-THCA in the marijuana plant reported by the National Institute on Drug Abuse (13.5%)	99.3	27.1

Calibration Curve for Δ^9-Tetrahydrocannabinolic Acid

The 4 mg/mL solution of Δ^9-THCA which was isolated via preparative HPLC (Fig. 30) was used to make triplicates of different concentrations of Δ^9-THCA to be analyzed via analytical HPLC. The concentration of the solutions made in triplicate were 4 mg/mL, 2 mg/mL, 1 mg/mL, 0.5 mg/mL, and 0.25 mg/mL. The area under each peak was determined using the CLASS-VP 7.2.1 SP1 software program. The data are presented in Table 4.

Table 4

Calibration Curve Data for Δ^9-THCA Using the Analytical HPLC Method

Concentration (mg/mL)	Area under the curve for each triplicate (area units)	Average area under the curve (area units)
4	51311413 53793629 48684559	51263200
2	31260848 34462434 33824056	33182446
1	24010586 22920013 25278396	24069665
0.5	15092733 13417926 16755497	15088719
0.25	6729947 7936614 7648819	7438460
0.125	2042008 4089147 7108877	4413344
0.0625	4399080 3404844 4439564	4081163

Each injection resulted in a chromatogram similar to that in Figure 31, that is, there was only one major peak which eluted at 10.75 minutes. A standard curve was generated and is presented in Figure 32. When analyzing the samples from the cell line assays via analytical HPLC, the equation from Figure 32, y = 1E+07x + 6E+06, can be used to determine the concentration of Δ^9-THCA in each sample.

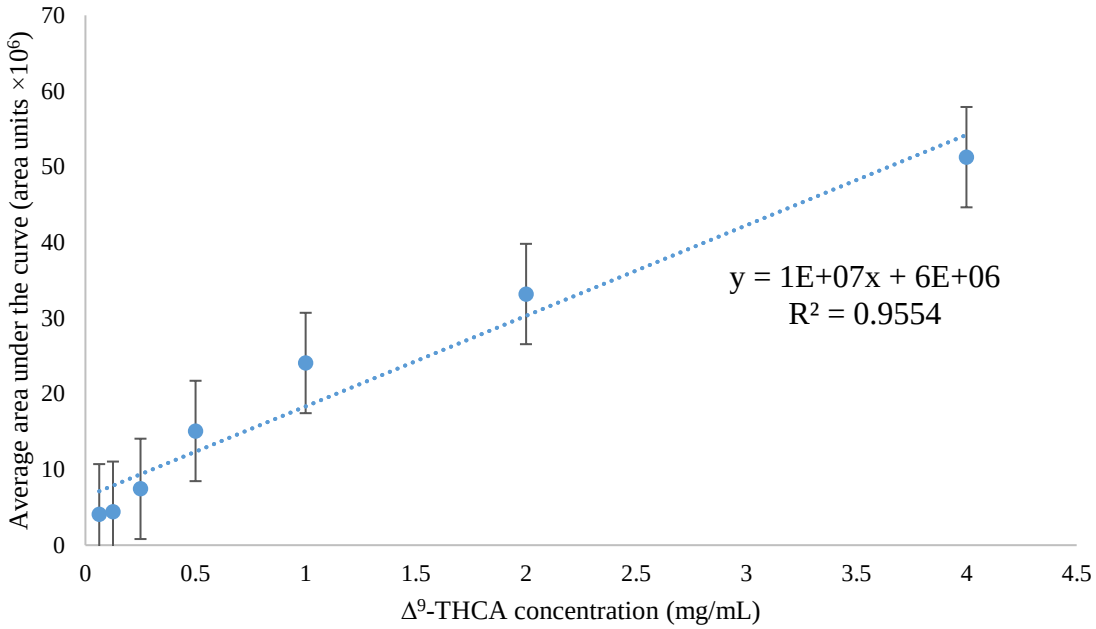

Figure 32: Calibration curve for Δ^9-THCA using the analytical HPLC method. (Detector at 254 nm)

Calibration Curve for Δ^9-Tetrahydrocannabinol

A 5 mg/mL solution of Δ^9-THC in absolute ethanol was made from the Δ^9-THC standard. This was used to make triplicates of different concentrations of Δ^9-THC to be analyzed via analytical HPLC. First, three 4 mg/mL solutions were made by taking 0.16 mL of the 5 mg/mL solution and adding 0.04 mL of absolute ethanol. Then a serial dilution occurred using each of the 4 mg/mL solutions. The concentration of the additional solutions made in triplicate were 2 mg/mL, 1 mg/mL, 0.5 mg/mL, and 0.25 mg/mL. Each injection resulted in a chromatogram similar to that in Figure 15, that is, there was only one major peak which eluted at 10.0 minutes. The area under each peak was determined using the CLASS-VP 7.2.1 SP1 software program. The data are presented in Table 5.

Table 5

Calibration Curve Data for Δ^9-THC Using the Analytical HPLC Method

Concentration (mg/mL)	Area under the curve for each triplicate (area units)	Average area under the curve (area units)
4	26024291 29802271 28361482	28062681
2	21636759 22961743 22175662	22258055
1	18434083 19054194 18254328	18580868
0.5	16044129 16906442 15362906	16104492
0.25	15155494 14208841 13314282	14226206

A standard curve was generated and presented in Figure 33. When analyzing the samples from the cell line assays via analytical HPLC, the equation from Figure 33, y = 4E+06x + 1E+07, can be used to determine the concentration of Δ^9-THC in each sample.

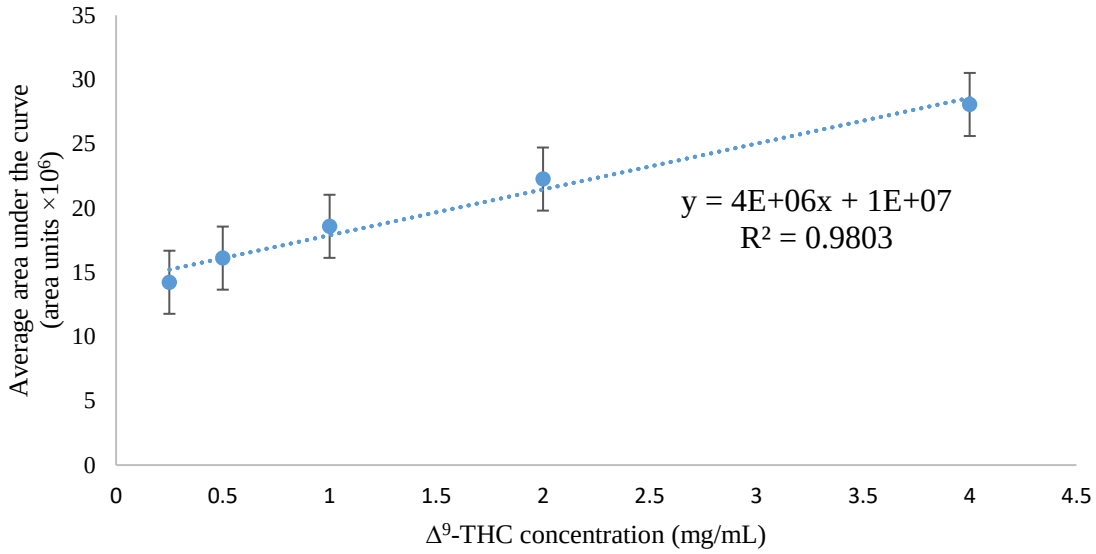

Figure 33: Calibration curve for Δ^9-THC using the analytical HPLC method. (Detector at 254 nm)

Assessment of Δ^9-Tetrahydrocannabinolic Acid Decarboxylation in Different Cell Lines

Five assays of *Pseudomonas putida* were conducted to determine the ability of the microbial cells to decarboxylate Δ^9-THCA. The data from these assays suggest that *Pseudomonas putida* is unable to decarboxylate Δ^9-THCA. The chromatogram for each aliquot taken in each assay, along with the specific volume and concentration of cells used in each assay, and concentration of Δ^9-THCA used are found in Appendices D – H.

First *P. putida* Assay

All the chromatograms of aliquots taken in this assay are found in Appendix D. Initially, this assay appears to show some decarboxylation activity since a peak at approximately 10.7 minutes, which was not present in the time = 0 hr aliquot, appears in the time = 1 hr, time = 5 hr, and time = 6 hr chromatograms (Fig. D4, D12, & D13). This peak elutes at approximately the same time as the Δ^9-THC standard peak which was analyzed before the assay aliquots (Fig. D2). However, this peak does not appear in the

time = 2 hr, time = 3 hr, and time = 4 hr aliquots (Fig. D8, D10, & D11). Additionally, when some of these aliquot samples were reanalyzed via analytical HPLC, there were major inconsistences between the peaks seen in samples when comparing the first and subsequent analyses of the same sample. The time = 1 hr chromatograms (Fig. D4, D5, D6, & D7) vary significantly, with only the first chromatogram (Fig. D4) displaying either the Δ^9-THC or the Δ^9-THCA peaks. The repeats of the time = 2 hr aliquot analyses (Fig. D8 & D9) also show major inconsistences with only Figure D9 showing a Δ^9-THCA peak. Finally, since there was no control assay run alongside this one, the peaks which appear to elute at the same time as Δ^9-THC (Fig. D4, D12, & D13) could be from compounds extracted from the microbial growth media. Thus, all assays after this had control assays to more easily identify a Δ^9-THC peak, if one is present, and allow for the identification of peaks resulting from the extraction of compounds in the growth media.

Second *P. putida* Assay

All the chromatograms of aliquots taken in this assay are in Appendix E. The Δ^9-THC standard was analyzed before the microbial aliquot samples and revealed that the Δ^9-THC peak eluted at 11.9 minutes. There was only one major peak for the time = 0 hr aliquot and the time = 0 hr control aliquot, which was at time 12.7 (Fig. E2 & E15) This peak is the Δ^9-THCA peak which was originally added to the bacteria medium and when compared to Figure 22, the elution time is at approximately the same time as the major peak in Figure 22. As the incubation time progressed, this peak corresponding to Δ^9-THCA decreased in size and its elution time shifts to 14.5 minutes (aliquot for time = 3 hr) (Fig. E6).

As the original large Δ^9-THCA peak decreased in size, simultaneously a peak with a shorter elution time increased in size. This peak is first visible in the time one-hour aliquot at approximately 9.3 minutes. This peak increased from aliquot to aliquot until it is clearly visible at 8.3 minutes in the six-hour aliquot (Fig. E13 & E14). The Δ^9-THCA peak decreasing in size and the Δ^9-THC peak increasing in size would indicate that over time in this setup, Δ^9-THCA is being converted to Δ^9-THC. However, this peak does not elute at the time which the Δ^9-THC does in the Δ^9-THC standard (Fig. E1). Additionally, this peak appears in the control assay in the time = 1 hr, time = 3 hr, time = 4 hr, and time = 6 hr aliquots (Fig. E16, E18, E19, E20, E22, & E23). This indicates that this peak could be a component of the cell media which is being extracted along with the cannabinoids.

Several of these aliquots were analyzed via analytical HPLC multiple times due to irregularities in the chromatograms. For example, the time = 2 hr aliquot was analyzed twice (Fig. E4 & E5). On the second analysis (Fig. E5), from 11.5 minutes to 14.5 minutes several peaks eluted which did not appear in the first chromatogram (Fig. E4), indicating that some component from previous injections may have been adhering to the column and eluting in later sample runs. This phenomenon was seen again when comparing the two analyses for the time = 3 hr aliquot (Fig. E6 & E7), the three analyses for the time = 4 hr aliquot (Fig. E8 – E10), the two analyses for the time = 5 aliquot (Fig. E11 & E12), and the two analyses for the time = 6 hr aliquot (Fig. E13 & E14). This brings all of the peaks observed in this assay into question, since this allows for the possibility of some component adhering to the column and eluting at any time during any sample.

After all the aliquots were analyzed via analytical HPLC, two cleaning methods were developed for the analytical HPLC which were run in hopes of removing all the compounds adhering to the column. The first cleaning method was five hours long; line A was HPLC-grade acetonitrile and line B was HPLC-grade water. The run began with 60% A and increased to 95% A over 10 minutes. It was held at this concentration for 280 minutes, and in the last ten minutes decreased to 60% A. The second cleaning method was five hours long; line A was HPLC-grade methanol and line B was HPLC-grade water. The run began with 60% A and increased to 95% A over 10 minutes. It was held at this concentration for 280 minutes, and in the last ten minutes decreased to 60% A.

Third *P. putida* Assay

All the chromatograms of aliquots taken in this assay are in Appendix F. Immediately it was apparent that the flush methods developed to clean the column after the previous assay were not effective. The Δ^9-THC standard analysis showed the Δ^9-THC peak eluting at 10.8 minutes. There were several additional peaks eluting from 8 minutes to 10.2 minutes and 11.2 minutes to 16.0 minutes (Fig. F1). These peaks were visible in all the other aliquots analyzed for this assay (Fig. F2 – F15). The time = 0 hr aliquot and the time = 0 hr control aliquot have a major peak which eluted at 11.0 minutes (Fig. F2 & F9). This was the Δ^9-THCA peak. This peak was visible in all other aliquots analyzed in this assay. However, if there was any decarboxylation, the peak for the Δ^9-THC produced was buried in the multiple peaks resulting from cannabinoids adhering to the column. This made the assay uninterpretable. The final analysis conducted for this assay was that of a sample of absolute ethanol to show the peaks which were due to the accumulation of compounds adhering to the column (Fig. F16).

More intensive flush methods were developed for the analytical HPLC and were run before the next assay to avoid a repetition of this problem. The first step of the flush method was running an isocratic method of 95% HPLC-grade water, and 5% HPLC-grade acetonitrile at a flow rate of 1.0 mL/min for 35 minutes. This was followed by an isocratic method of 95% HPLC-grade acetonitrile, and 5% isopropanol at a flow rate of 1.0 mL/min for 35 minutes. This was followed by an isocratic method of 95% isopropanol, and 5% HPLC-grade hexane at a flow rate of 1.0 mL/min for 9 minutes. This was followed by an isocratic method of 95% HPLC-grade hexane, and 5% isopropanol at a flow rate of 1.0 mL/min for 35 minutes. This was followed by an isocratic method of 95% isopropanol, and 5% HPLC-grade acetonitrile at a flow rate of 1.0 mL/min for 9 minutes. The method finishes with an isocratic method of 95% HPLC-grade acetonitrile, and 5% HPLC-grade water at a flow rate of 1.0 mL/min for 35 minutes. In between each of these isocratic methods a 5-minute-long gradient method was run to slowly adjust the type of the solvent used for each isocratic run described.

Fourth *P. putida* Assay

All the chromatograms of aliquots taken in this assay are in Appendix G. There was one major peak at approximately 10.5 minutes for both the time = 0 hr aliquot and the time = 0 hr control aliquot (Fig. G2 & G9). This peak represents the Δ^9-THCA added at the start of the assay (Fig. G1). A peak eluted at approximately 7.8 minutes and another at approximately 8.2 minutes in the time = 1 hr, time = 3 hr, time = 4 hr, and time = 5 hr samples, as well as in the control time = 3 hr, and time = 5 hr samples. Since these peaks appeared in both the control samples as well as the experimental samples, they were most likely compounds extracted along with the cannabinoids originally in the

cell media. If there was any decarboxylation activity of Δ^9-THCA by the cell line, a peak for Δ^9-THC would elute at an earlier time than the observed Δ^9-THCA peak, which eluted at 10.7 minutes (Fig. G1). This Δ^9-THC peak would appear in aliquots collected towards the end of the assay. There were no peaks with a retention time of Δ^9-THC which eluted in any of the aliquots collected in this assay (Fig. G2 – G15) indicating that there was no decarboxylation activity.

Fifth *P. putida* Assay

All the chromatograms of aliquots taken in this assay are in Appendix H. There was one major peak at approximately 10.5 minutes for both the time = 0 hr aliquot and the time = 0 hr control aliquot (Fig. H4 & H11). This peak represents the Δ^9-THCA added at the start of the assay (Fig. H3). The Δ^9-THC standard was analyzed via analytical HPLC before the aliquot samples from the assay and the Δ^9-THC had an elution time of 9.8 minutes (Fig. H2). There were no peaks visible at the elution time for Δ^9-THC in any of the samples analyzed during this assay (Fig. H4 – H17).

To ensure that the Δ^9-THC and the Δ^9-THCA peaks were not buried within each other on the chromatogram, and additional 0.1 mg of Δ^9-THCA was added to the sample from time = 1 hr and to the sample from time = 3 hr and each were analyzed via analytical HPLC again (Fig. H18 & H19). Additionally, 0.12 mg of Δ^9-THC standard was added to a 0.1 mL aliquot of the sample from time = 1 hr and analyzed via analytical HPLC (Fig. H20). Both samples which had additional Δ^9-THCA added to them had a peak which eluted at approximately 10.2 minutes (Fig. H18 & H19). Compared to the chromatograms of these samples before they had the added Δ^9-THCA (Fig. H7 & H5, respectively), all four samples had a major peak which eluted between 10.0 and 10.7

minutes. The samples depicted in Figures H18 and H19 had larger peaks at this elution time than the samples with similar peaks in Figures H7 and H5. The sample from time = 1 hr which had an added 0.12 mg of Δ^9-THC standard had one peak which eluted at 9.8 minutes and a second which eluted at 10.2 minutes (Fig. H20). The peak which eluted at 9.8 minutes was the Δ^9-THC standard, and the peak which eluted at 10.2 minutes was the Δ^9-THCA added to the microbial solution at the start of the assay (Fig. H2, H3, & H20). This demonstrated that if there was a decarboxylation of the Δ^9-THCA during this assay, the Δ^9-THC produced would elute as a separate peak from the Δ^9-THCA. Since there was not a peak visible at the elution time of 9.8 minutes in any of the samples, and the additional analyses of aliquots with added Δ^9-THCA and Δ^9-THC which show that they would elute at different time, it was determined that there was no Δ^9-THCA decarboxylation activity in this assay (Fig. H4 – H20).

Analysis of Fifth *P. putida* Assay Using the Δ^9-Tetrahydrocannabinolic Acid Calibration Curve

The fifth *P. putida* assay was conducted using 16.0 mL of a 68.7 mg/mL microbial solution which was incubated with 0.1 mL of 4 mg/mL Δ^9-THCA isolated using the preparative HPLC method (Fig. 30). This was assessed alongside a control autoclaved microbial cell assay which consisted of 16.0 mL of a 60.60 mg/mL microbial solution which was also incubated with 0.1 mL of 4 mg/mL Δ^9-THCA isolated using the preparative HPLC method (Fig. 30). Each 2-mL aliquot therefore should contain approximately 0.025 mg/mL of Δ^9-THCA. The area under the curve of the Δ^9-THCA peak in each of the aliquots can be determined using the CLASS-VP 7.2.1 SP1 software program, and then using the equation from Figure 32, y = 1E+07x + 6E+06, the

concentration of Δ^9-THCA in each sample can be determined. These data are displayed in Table 6.

Table 6

Calculation of the Concentration of Δ^9-THCA in Each of the Aliquots Collected During the Fifth P. putida Assay Using the Δ^9-THCA Calibration Curve.

Aliquot	Area under the curve (AU)	Concentration of Δ9-THCA (mg/mL)*
Time = 0 hr	175840	-0.582416
Time = 1 hr	329167	-0.5670833
Time = 2 hr	443777	-0.5556223
Time = 3 hr	706271	-0.5293729
Time = 4 hr	343161	-0.5656839
Time = 5 hr	263011	-0.5736989
Time = 6 hr	592775	-0.5407225
Time = 0 hr control	711068	-0.5288932
Time = 1 hr control	712563	-0.5287437
Time = 2 hr control	653856	-0.5346144
Time = 3 hr control	641541	-0.5358459
Time = 4 hr control	542118	-0.5457882
Time = 5 hr control	769166	-0.5230834
Time = 6 hr control	604389	-0.5395611

* calculated using the equation from Figure 32

All the calculated values for the concentration of Δ^9-THCA in the samples from the fifth assay were negative. It was previously calculated that each 2-mL aliquot should contain approximately 0.025 mg/mL of Δ^9-THCA. This value is smaller than the smallest concentration in the calibration curve, so it is expected that these calculations could not be completely accurate. However, they do show that each aliquot contains approximately the same amount of Δ^9-THCA.

CHAPTER V

CONCLUSIONS AND FUTURE WORK

There were two purposes of this study. First, was to produce a method of isolating Δ^9-THCA from marijuana plant material. The second was to attempt to determine a cell line containing an enzyme capable of decarboxylating Δ^9-THCA, converting it to Δ^9-THC. This has significance to a future chemotherapy drug delivery system using Cell-in-a-Box® technology. *Pseudomonas putida* was assayed to determine if it had any decarboxylation activity for the Δ^9-THCA. The Δ^9-THCA used to assay the cell lines was isolated from marijuana plant material in-house. Two methods for producing a crude extract of cannabinoids from the plant material were developed, as well as two methods for isolating the Δ^9-THCA from these crude extracts.

Isolation of Δ^9-Tetrahydrocannabinolic Acid

The Soxhlet extraction method for producing crude cannabinoid extract required much less physical work compared to the sonication extraction method. The crude extracts were further purified via either preparative HPLC or Yamazen Smart Flash chromatography. Both methods were effective for the purification of Δ^9-THCA from the crude extract but to different degrees of purity. The Δ^9-THCA isolate obtained from both the HPLC and the Yamazen methods were analyzed via proton NMR and analytical HPLC to compare their relative purity. Comparing the analytical HPLC analysis of the Δ^9-THCA isolates from both the preparative HPLC method (Fig.38) and the Yamazen method (Fig.24), using the preparative HPLC method was able to isolate Δ^9-THCA

almost entirely, whereas the sample containing Δ^9-THCA obtained using Yamazen Smart Flash method contained a mixture of other compounds. Additionally, when assessing the percent yield of Δ^9-THCA from 13.5% Δ^9-THCA marijuana using each of the isolation methods, the preparative HPLC method has a much higher percent yield than the Yamazen method (99.3% and 27.1%, respectively).

The method of isolating Δ^9-THCA from a crude extract of cannabinoids using the Yamazen Smart Flash could be improved through further experimentation with reverse phase TLC plates. The Yamazen uses a TLC plate when making its solvent system, and the better resolved the compound is on the TLC plate, the better it will be isolated when employing the Yamazen. The TLC plate were developed in 80% acetonitrile, 10% methanol, and 10% 20 mM ammonium formate, pH 3.20**.** This did result in the Δ^9-THCA having an R_f of approximately 0.2, but there was some streaking on the plate, meaning the Δ^9-THCA spot was not totally pure. Further tweaking of the solvent system could result in a TLC plate with less streaking which would lead to better separation when using the instrument.

Another option is reinjecting the Δ^9-THCA isolate initially collected from the Yamazen Smart Flash (fraction 4 from Fig. 20) into the Yamazen for a second time to further isolate the Δ^9-THCA. This could be done using the same solvent system and TLC plate as the first injection. However, better separation could be possible if further TLC experimentation was conducted with the initial Δ^9-THCA isolate collected from the Yamazen. This Δ^9-THCA isolated could be spotted on a TLC plate along with the Δ^9-THCA isolate collected via preparative HPLC (fraction 26 from Fig. 26), the Δ^9-THC standard, and the mixture of cannabinoids obtained from Cayman Chemical Company.

Then a variety of solvent systems could be tested to develop TLC plates with these spots to determine a solvent system able to isolate the Δ^9-THCA from the other compounds collected in the initial Yamazen isolate. The Δ^9-THCA isolate collected from the preparative HPLC, the Δ^9-THC standard, and the mixture of cannabinoids will allow for identification of the spots in the Δ^9-THCA isolate mixture obtained from the Yamazen. Once a TLC solvent system which can separate the Δ^9-THCA from the other compounds in the Yamazen sample, it can be reinjected into the Yamazen Smart Flash using this solvent system and TLC plate to develop the method.

Additionally, when comparing the preparative HPLC method and the Yamazen Smart Flash method it can be noted that the preparative HPLC method uses 750 mL of mobile phase, and the Yamazen method uses 800 mL of mobile phase, along with 80 mL of HPLC-grade water (see Methods). This is not a significant difference in volume when considering sustainability; however, there is a major sustainability difference between the methods when taking the columns that each use into consideration. The preparative HPLC column used in this study which was sold by Phenomenex with the intention that it will be used many times. Both the Yamazen inject column, and the universal column used in this study were single use columns. Comparing both these methods of the isolation of Δ^9-THCA in a long-term time frame, the fact that the Yamazen columns need to be replaced more often, and that the method uses more solvent, the Yamazen method would be more expensive than the preparative HPLC method, and less sustainable.

Assessment of Δ^9-Tetrahydrocannabinolic Acid Decarboxylation in Different Cell Lines

Since the multiple *Pseudomonas putida* assays indicated that this cell line most likely does not have an enzyme which efficiently decarboxylates Δ^9-THCA to Δ^9-THC,

more cell lines need to be assayed. Other options of bacteria or fungi cell lines are those which were discussed in the literature review, including *Aspergillus clavatus, Aspergillus giganteus, Aspergillus longivesica, Byssochlamys nivea, Penicillium expansum*, *Trichosporon moniliiforme, Aspergillus oryzae, Aspergillus niger, Acinetobacter calcoaceticus, Alcaligenes eutrophus,* and *Pseudomonas cepacia.* Once a cell line able to convert Δ^9-THCA to Δ^9-THC is identified, the specific gene and enzyme responsible for this conversion needs to be identified. Then, through genetic engineering, this gene can be inserted into a human embryonic kidney cell. This embryonic kidney cell line is what Austranova would encapsulate using their novel cellulose-based polymer (Cell-in-a-Box®). Finally, these cells can be explored as a possible novel chemotherapy treatment, using Δ^9-THCA as a pro-drug which would be converted to Δ^9-THC at the location of the tumor where the encapsulated cells are injected into the patient.

REFERENCE LIST

Battista, N., Di Tommaso, M., Bari, M., & Maccarrone, M. (2012). The endocannabinoid system: an overview. *Frontiers in Behavioral Neuroscience. 6*(9), 1-7.

Cannabinoids on Luna Omega Polar C18 100x2.1mm. (n.d.). Retrieved from http://www.phenomenex.com/Application/Detail/23580

Carchman, R. A., Harris, L.S., & Munson, A.E. (1976). The inhibition of DNA synthesis by cannabinoids. *American Association for Cancer Research. 36*, 95-100.

Choi, Y., Hazekamp, A., Peltenburg-Looman, A., Frédérich, M., Erkelens, C., Lefeber, A., & Verpoorte, R. (2004). NMR assignments of the major cannabinoids and cannabiflavonoids isolated from flowers of *Cannabis sativa*. *Phytochemical Analysis. 15*, 345-354. doi:10.1002.pca.787

Cribbs, J. P. (2016). *Enzymatic conversion of model compounds that represent pharmacologically active pro-drugs* (Unpublished master's thesis). University of Northern Colorado, Greeley, Colorado.

Fernández-Ruiz, J., Romero, J., Velasco, G., Tolón, R., Ramos, J., & Guzmán, M. (2007). Cannabinoid CB2 receptor: a new target for controlling neural cell survival? *TRENDS in Pharmacological Sciences. 28*(1), 39-45. doi:10.1016/j.tips.2006.11.001

Gaffal, E., Cron, M., Glodde, N., & Tüting, T. (2013). Anti-inflammatory activity of topical THC in DNFB-mediated mouse allergic contact dermatitis independent of CB1 and CB2 receptors. *Allergy. 68*, 994-1000.

Gaoni, Y., & Mechoulam, R. (1964). Isolation, structure, and partial synthesis of an active constituent of hashish. *Journal of the American Chemical Society. 86*(8), 1646-1647. doi:10.1021/ja01062a046

Glodde, N., Jakobs, M., Bald, T., Tüting, T., & Gaffal, E. (2015). Differential role of cannabinoids in the pathogenesis of skin cancer. *Life Sciences. 138*, 35-40. doi:10.1016/j.lfs.2015.04.003

Grotenhermen, F., & Müller-Vahl, K. (2012). The therapeutic potential of cannabis and cannabinoids. *Dtsch Arztebl International. 109*(29-30), 495-501. doi:10.3238/arztebl.2012.0495

Hazekamp, A., Choi, Y., & Verpoorte, R. (2004). Quantitative analysis of cannabinoids from *Cannabis sativa* using ^{1}H-NMR. *Chemical & Pharmaceutical Bulletin. 52*(6), 718-721.

Iding, H., Dünnwald, T., Greiner, L., Liese, A., Müller, M., Siegert, P., … & Pohl, M. (2000). Benzoylformate decarboxylase from *Pseudomonas putida* as stable catalyst for the synthesis of chiral 2-hydroxy ketones. *Chemistry: A European Journal. 6*(No.8), 1483-1495.

Izzo, A., Borrelli, F., Capasso, R., Di Marzo, V., & Machoulam, R. (2009). Non-psychotropic plant cannabinoids: new therapeutic opportunities from an ancient herb. *Trends in Pharmacological Science. 30*(10), 515-527.

Kirimura, K., Gunji, H., Wakayama, R., Hattori, T., & Ishii, Y. (2010). Enzymatic Kolbe-Schmitt reaction to form salicylic acid from phenol: Enzymatic characterization and gene identification of a novel enzyme, *Trichosporon moniliiforme* salicylic

acid decarboxylase. *Biochemical and Biophysical Research Communications. 394*, 279-284. doi:10.1016/j.bbrc.2010.02.154

Live Cell Encapsulation Technology. (2017) Retrieved from http://pharmacyte.com/live-cell-encapsulation/

Löhr, M., Hoffmeyer, A., Kröger, J., Freund, M., Hain, J., Holle, A., … & Salmons, B. (2001). Microencapsulated cell-mediated treatment of inoperable pancreatic carcinoma. *The Lancet. 357*, 1591-1592.

Massi, P., Solinas, M., Cinquina, V., & Parolaro, D. (2012). Cannabidiol as potential anticancer drug. *British Journal of Clinical Pharmacology. 72*(2), 303-312. doi:10.1111/j.1365-2125.2012.04298.x

McKallip, R., Lombard, C., Fisher, M., Martin, B., Ryu, S., Grant, S., … & Nagarkatti, M. (2002). Targeting CB2 cannabinoid receptors as a novel therapy to treat malignant lymphoblastic disease. *Blood. 100*, 627-634. doi:10.1182/blood-2002-01-0098

Pacher, P., Batkai, S., & Kunos, G. (2006). The endocannabinoid system as an emerging target of pharmacotherapy. *Pharmacological Reviews. 58*(3), 389-462. doi:10.1124/pr.58.3.2

PharmaCyte Biotech. PharmaCyte Biotech discusses upcoming clinical trial in pancreatic cancer with first principal investigator. (2016, Dec 7). Retrieved from http://pharmacyte.com/pharmacyte-biotech-discusses-upcoming-clinical-trial-in-pancreatic-cancer-with-first-principal-investigator/

Plotnikov, A., Zehorai, E., Procaccia, S., & Seger, R. (2011). The MAPK cascades: signaling components, nuclear roles and mechanisms of nuclear translocation. *Biochimica et Biophysica Acta. 1813*(9), 1619-1633.

Preet, A., Ganju, R. K., & Groopman, J.E. (2008). Δ^9–Tetrahydrocannabinol inhibits epithelial growth factor-induced lung cancer cell migration *in vitro* as well as its growth and metastasis *in vivo*. *Oncogene. 27*, 339-346. doi:10.1038/sj.onc.1210641

Reiner, A. (1971). Metabolism of benzoic acid by bacteria: 3,5-cyclohexadiene-1,2-diol-1-carboxylic acid is an intermediate in the formation of catechol. *Journal of Bacteriology. 108,* 89-94.

Russo, E., & Guy, G. (2005). A tale of two cannabinoids: The therapeutic rationale for combining tetrahydocannabinol and cannabidiol. *Medical Hypotheses. 66,* 234-246. doi:10.1016/j.mehy.2005.08.026

Sánchez, C., Galve-Roperh, I., Canova, C., Brachet, P., & Guzmán, M. (1998). Δ^9–Tetrahydrocannabinol induces apoptosis in C6 glioma cells. *Federation of European Biochemical Societies*. *436*, 6-10.

Santha, R., Rao, N., & Vaidyanathan, C. (1996). Identification of the active-site peptide of 2,3- dihydroxybenzoid acid decarboxylase from *Aspergillus oryzae. Biochimica et Biophysica Acta. 1293*, 191-200.

Smith, B., Lewis, M., & Mendez, J. (2016). Optimization of cannabis grows using fourier transform midinfrared spectroscopy. *PerkinElmer.*

Snini, S., Tadrist, S., Laffitte, J., Jamin, E., Oswald, I., & Puel, O. (2013). The gene *PatG* involved in the biosynthesis pathway of patulin, a food-borne mycotoxin,

encodes a 6-methylsalicylic acid decarboxylase. *International Journal of Food Microbiology*. *171*, 77-83.

Turu, G., & Hunyady, L. (2010). Signal transduction of the CB_1 cannabinoid receptor. *Journal of Molecular Endocrinology*. *44*, 75-85. doi:10.1677/JME-08-0190

Wang, M., Wang, Y., Avula, B., Radwan, M., Wanas, A., van Antwerp, J., … & Khan, I. (2016). Decarboxylation study of acidic cannabinoids: a novel approach using ultra-high-performance supercritical fluid chromatography/photodiode array-mass spectrometry. *Cannabis and Cannabinoid Research. 1.1*, 262-271. doi:10.1089/can.2016.0020

APPENDIX A

Phenomenex Mixture of Cannabinoids Chromatogram

Phenomenex's chromatogram of a mixture of cannabinoids containing CBDV, CBD, CBG, CBDA, CBGA, CBN, Δ^9-THCA, Δ^9-THC, Δ^8-THC, and CBC, chromatographed on a Luna Omega 1.6 μm polar C18 100Å column with a fifteen-minute-long method. Line A was 20 mM 3.20 pH ammonium formate, and line B was acetonitrile. The method began at 60% B, which was raise to 95% B over 12 minutes, held at 95% B for one minute, and then at 13.01 minutes reduced to 60% B and held there until the end of the run.

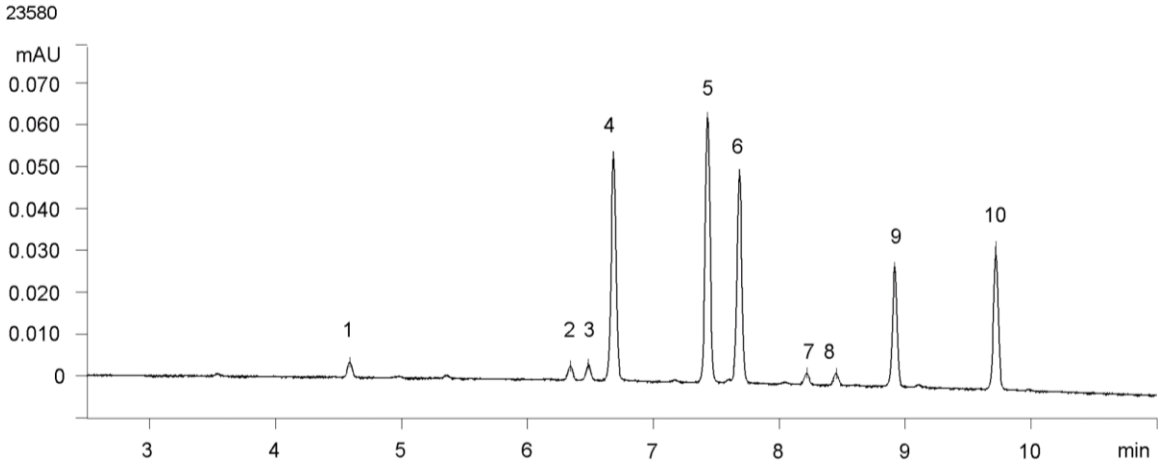

Figure A1: Chromatograph of mixture of cannabinoids containing CBDV (1), CBD (2), CBG (3), CBDA (4), CBGA (5), CBN (6), Δ^9-THC (7), Δ^8-THC (8), CBC (9), and Δ^9-THCA (10) (from "Cannabinoids on Luna Omega Polar C18 100x2.1mm", n.d.).

APPENDIX B

Nuclear Magnetic Resonance Spectra of Peaks Collected via Yamazen Chromatography

The following are the NMR spectra for the peaks collected via Yamazen chromatography which did not appear to contain any Δ^9-THCA.

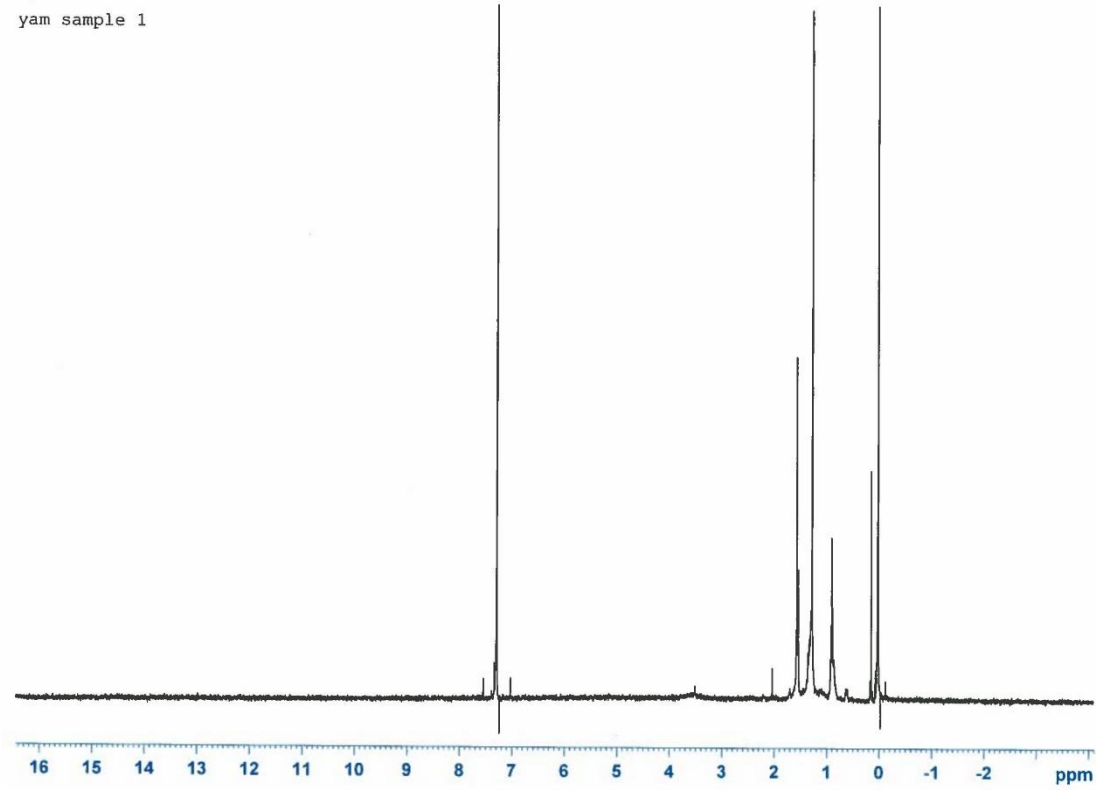

Figure B1: Proton NMR chromatogram of fraction 1 (from Figure 20).

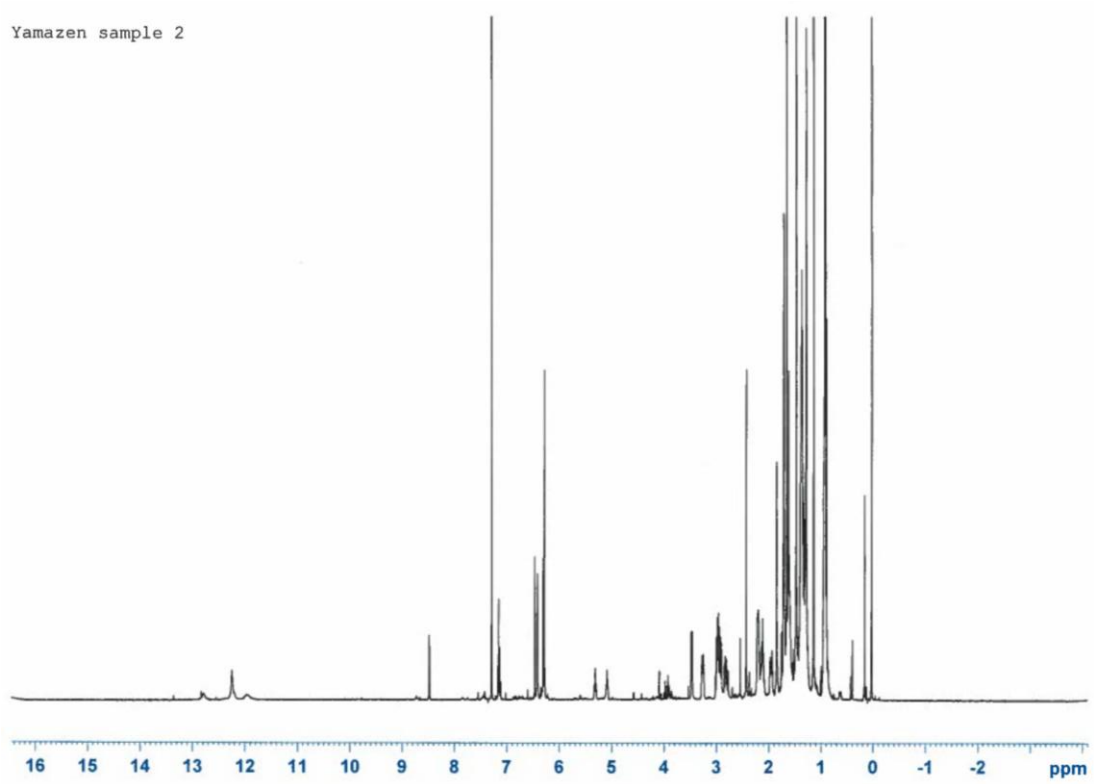

Figure B2: Proton NMR chromatogram of fraction 2 (from Figure 20).

APPENDIX C

Nuclear Magnetic Resonance Spectra of Peaks Collected via Preparative High-Performance Liquid Chromatography

The following are the NMR spectra for the peaks collected via preparative HPLC which did not appear to contain any Δ^9-THCA.

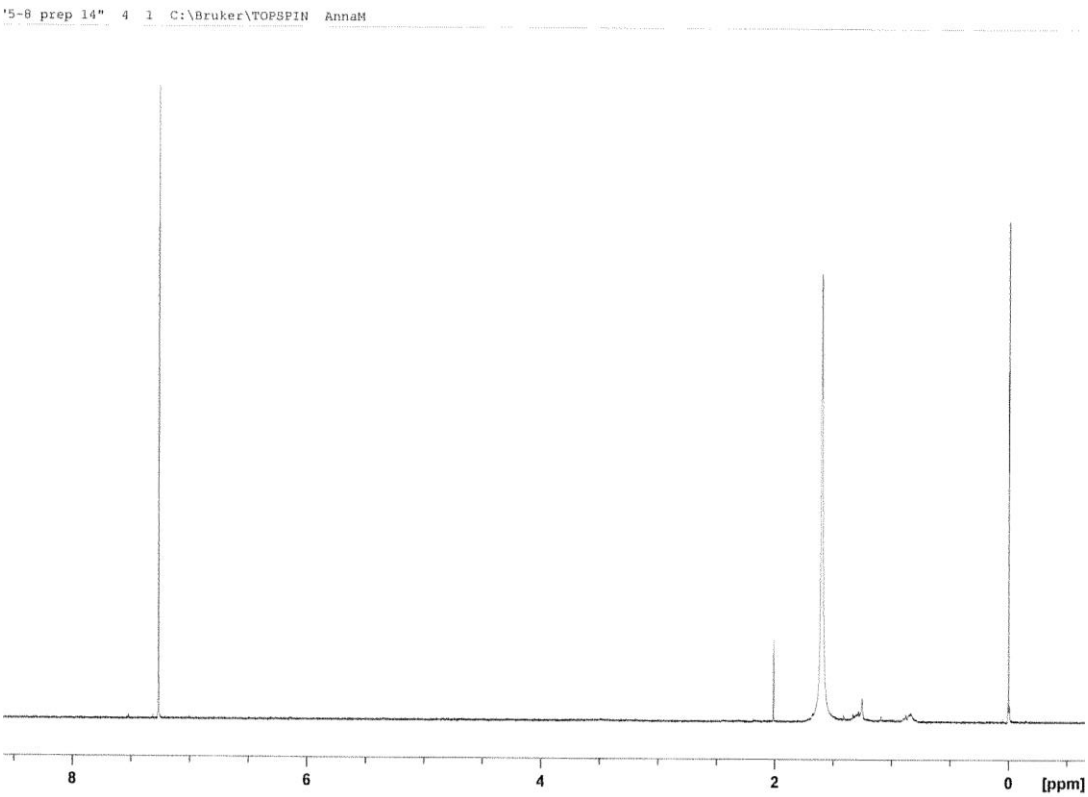

Figure C1: Proton NMR spectra of fraction 14 (from Figure 26).

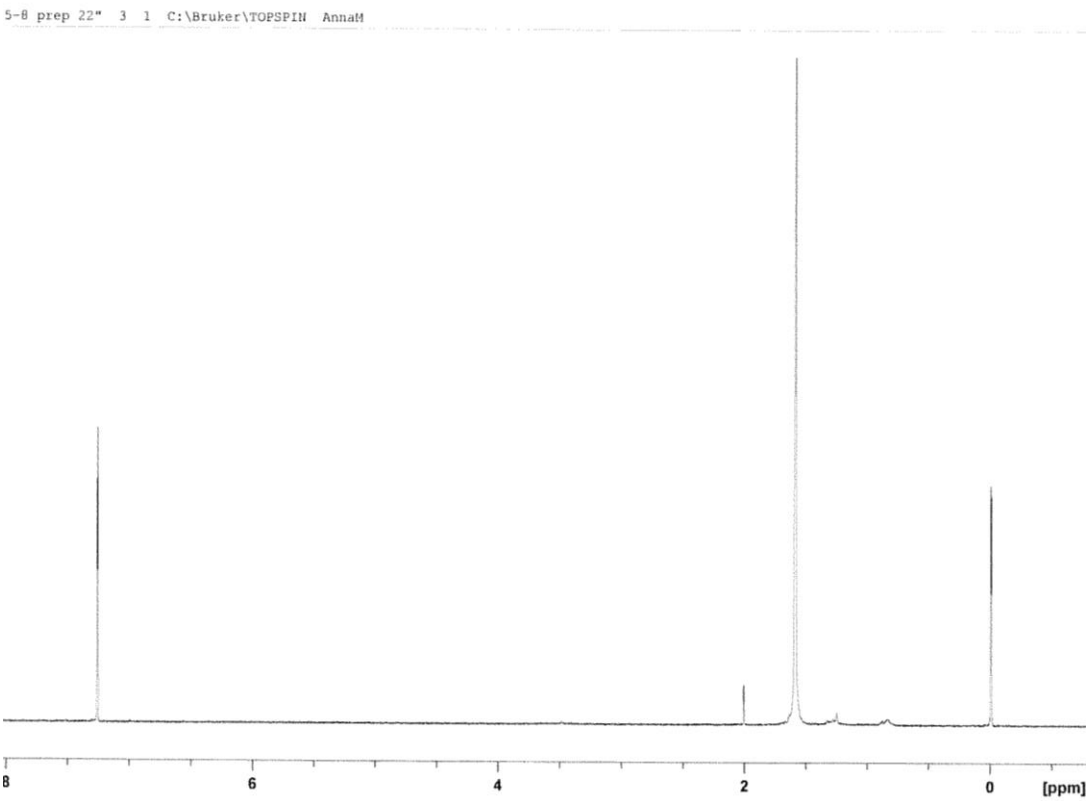

Figure C2: Proton NMR spectra of fraction 22 (from Figure 26).

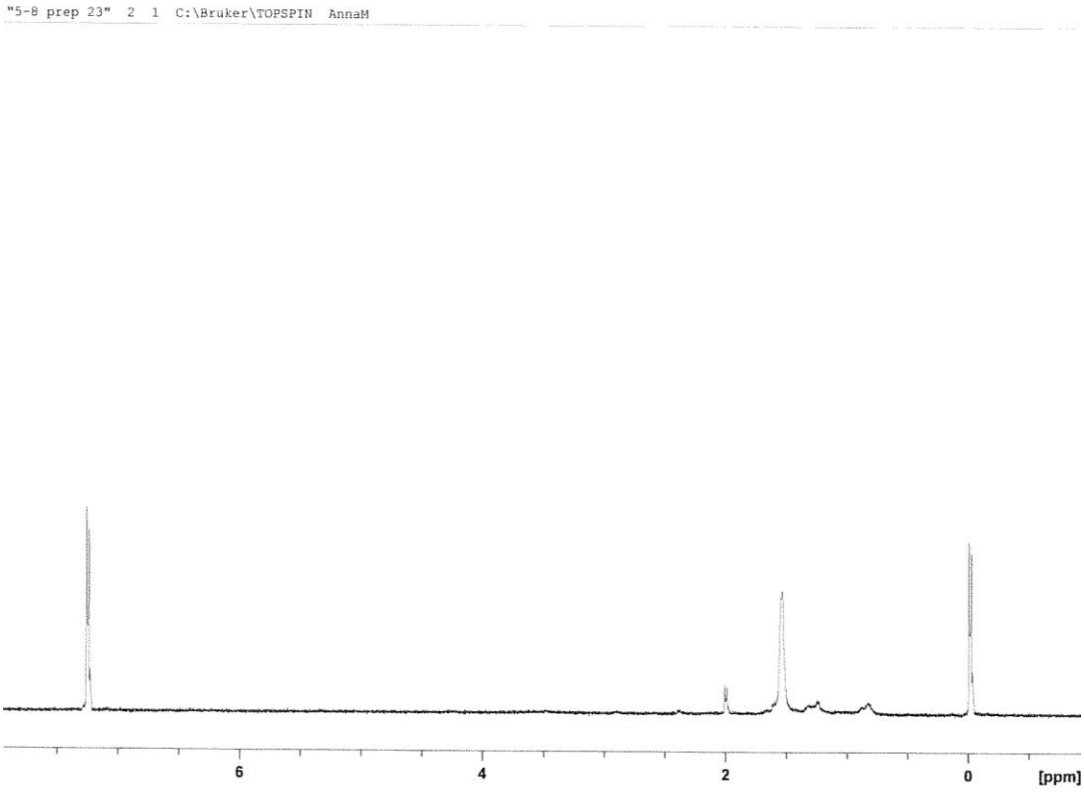

Figure C3: Proton NMR spectra of fraction 23 (from Figure 26).

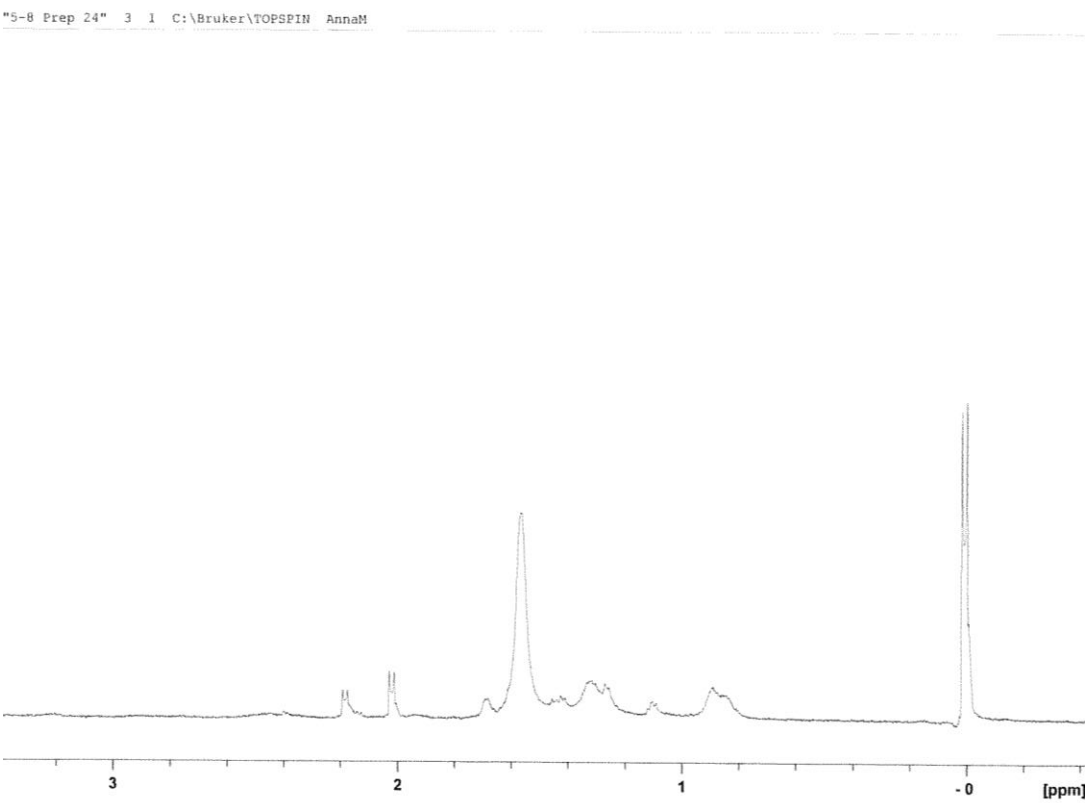

Figure C4: Proton NMR spectra of fraction 24 (from Figure 26).

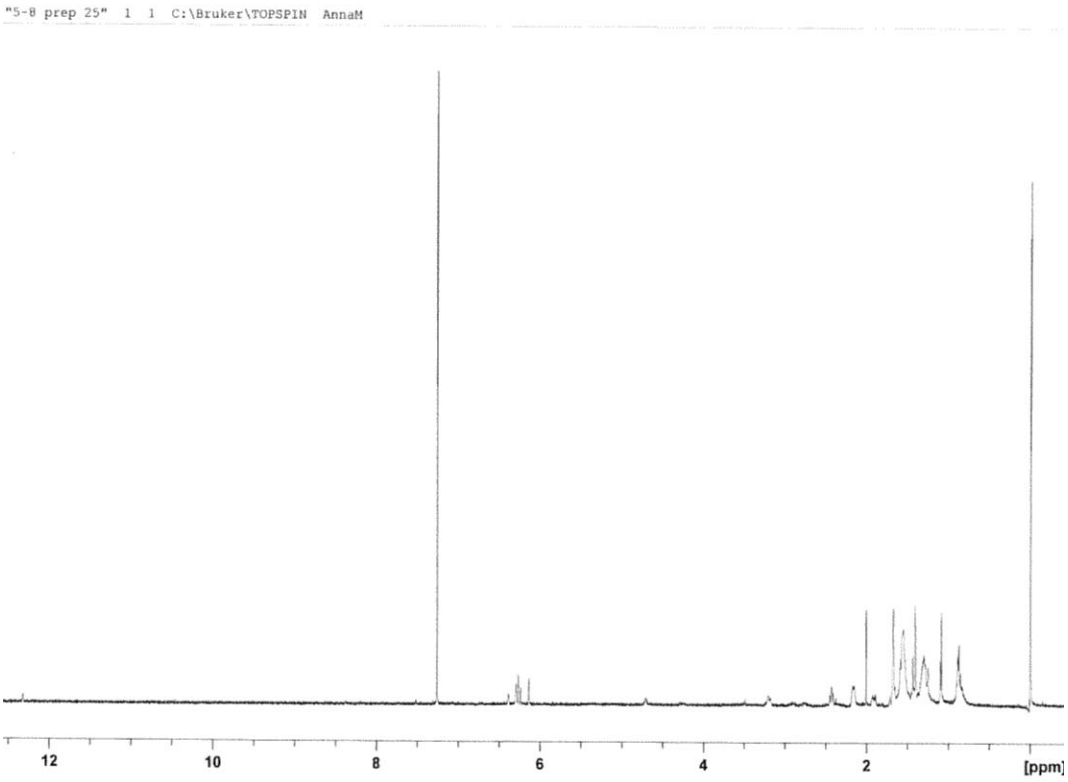

Figure C5: Proton NMR spectra of fraction 25 (from Figure 26).

APPENDIX D

First *P. putida* Assay

The first *Pseudomonas putida* assay was conducted using 16.0 mL of a 24.4 mg/mL microbial solution. The microbial cells were incubated with 0.1 mL of approximately 85 mg/mL Δ^9-THCA isolated using the Yamazen method (Fig. 22). This is the only assay which was not run along side a control autoclaved microbial cell assay. The Δ^9-THC standard and the mix of cannabinoid standards were analyzed via analytical HPLC before the aliquots for this assay to identify the peaks in the aliquot samples.

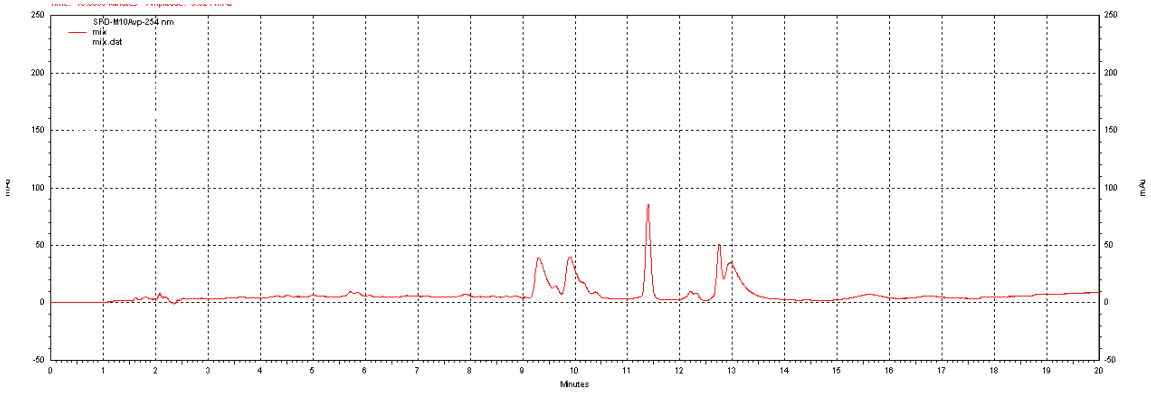

Figure D1: Analytical HPLC method chromatogram of cannabinoid mixture standard containing CBDA, CBGA, CBG, CBD, THCV, CBN, Δ^9-THCA, Δ^9-THC, Δ^8-THC, and CBC (100 µg/mL each in acetonitrile).

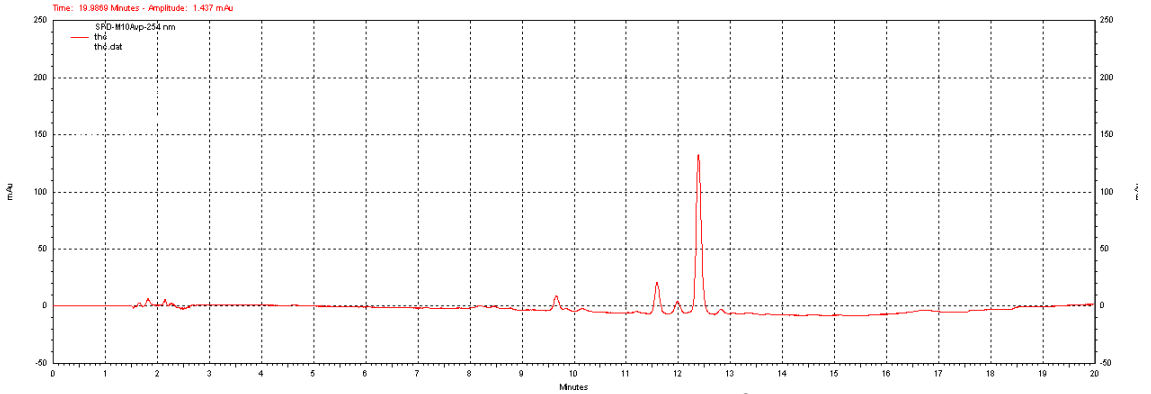

Figure D2: Analytical HPLC method chromatogram of Δ^9-THC standard (1.2 mg/mL in ethanol).

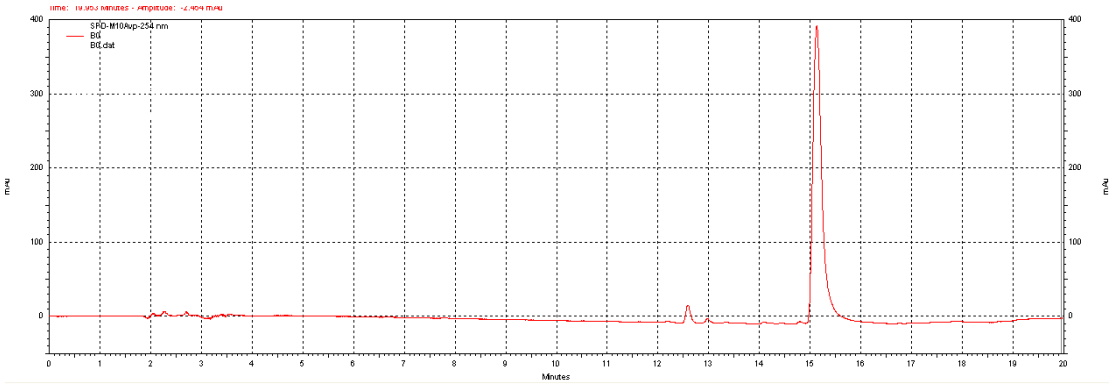

Figure D3: Chromatogram of time = 0 hr aliquot of incubation of Δ^9-THCA with *P. putida.*

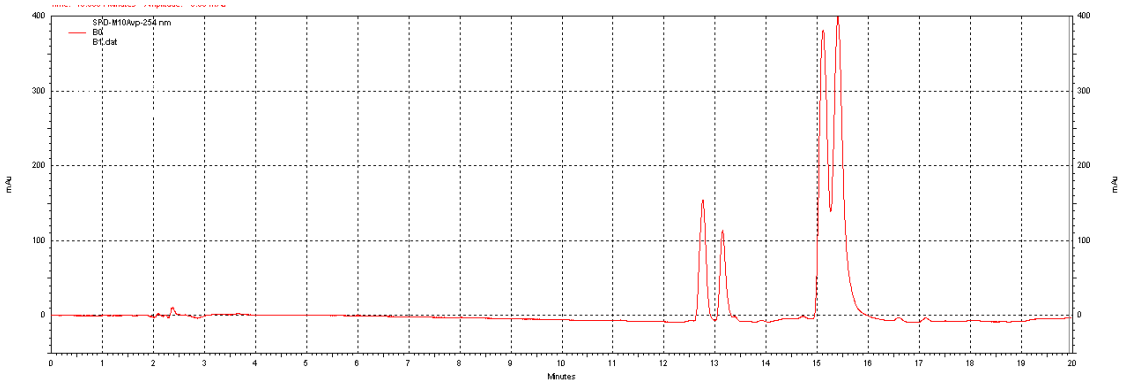

Figure D4: Chromatogram of time = 1 hr aliquot of incubation of Δ^9-THCA with *P. putida.*

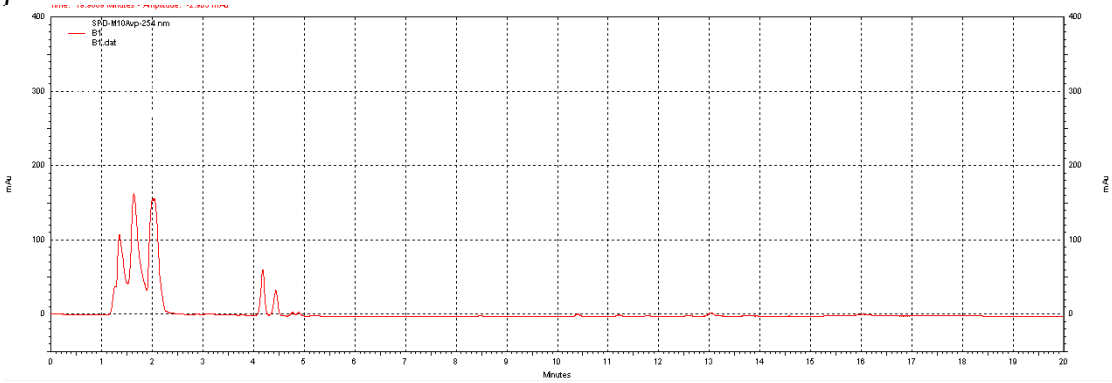

Figure D5: Repeat of chromatogram of time = 1 hr aliquot of incubation of Δ^9-THCA with *P. putida.*

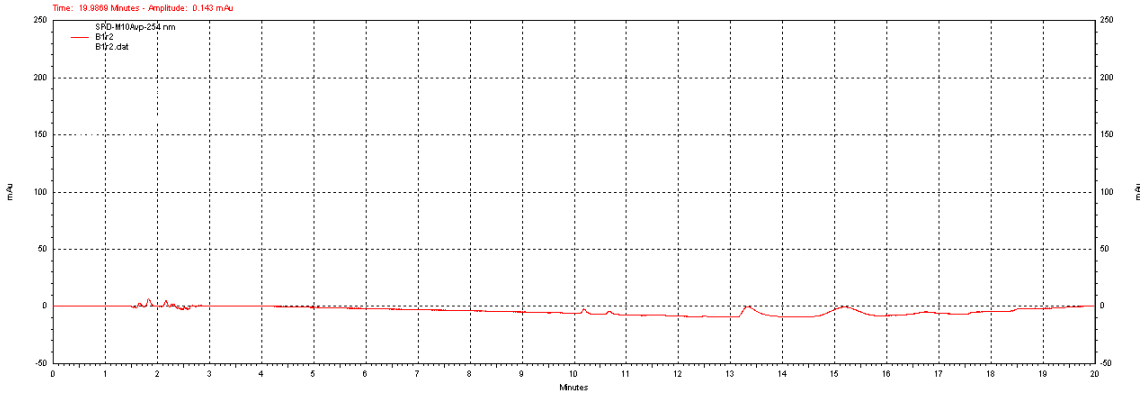

Figure D6: Second repeat of chromatogram of time = 1 hr aliquot of incubation of Δ^9-THCA with *P. putida.*

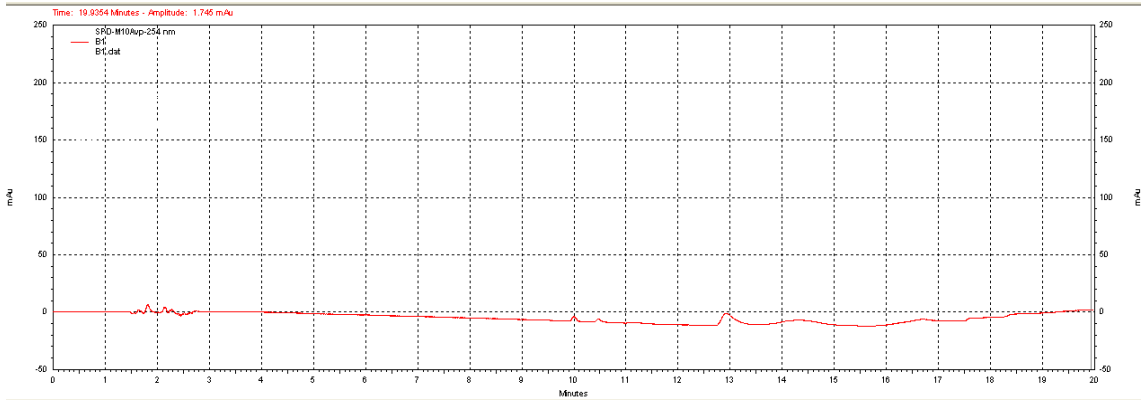

Figure D7: Third repeat of chromatogram of time = 1 hr aliquot of incubation of Δ^9-THCA with *P. putida.*

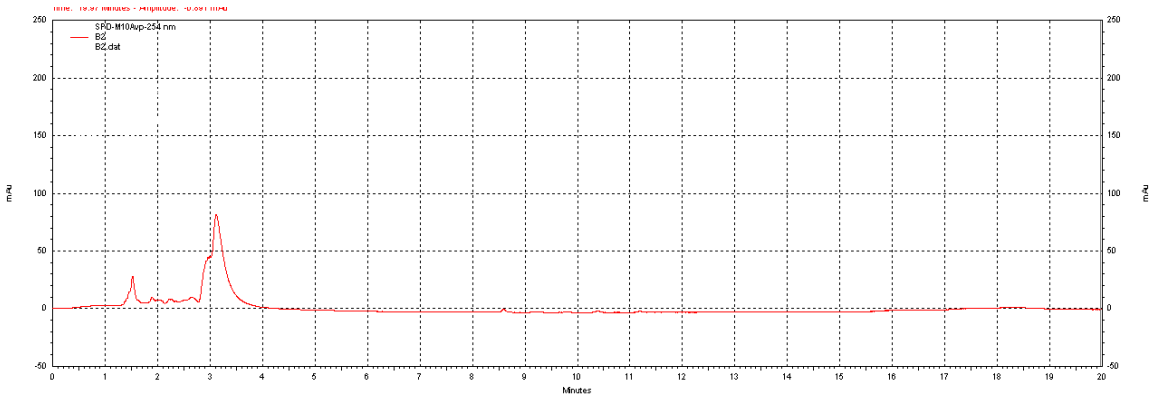

Figure D8: Chromatogram of time = 2 hr aliquot of incubation of Δ^9-THCA with *P. putida.*

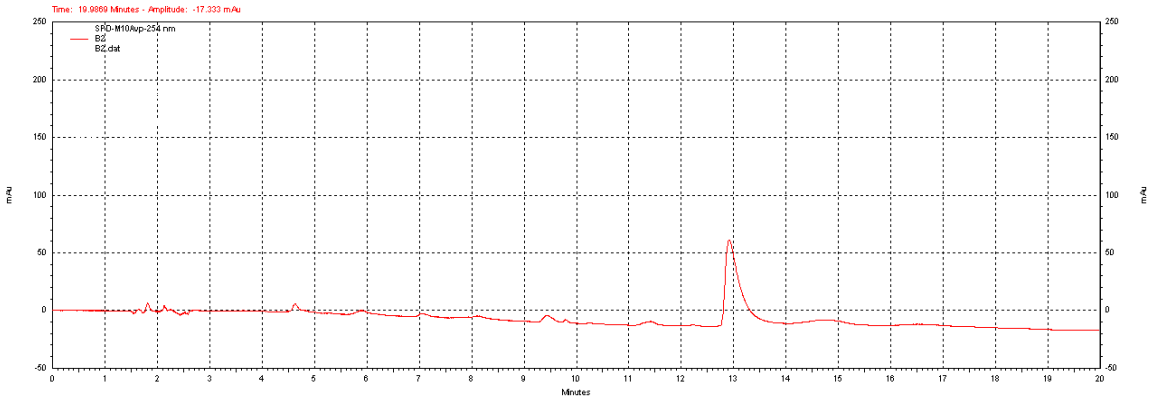

Figure D9: Repeat of chromatogram of time = 2 hr aliquot of incubation of Δ^9-THCA with *P. putida.*

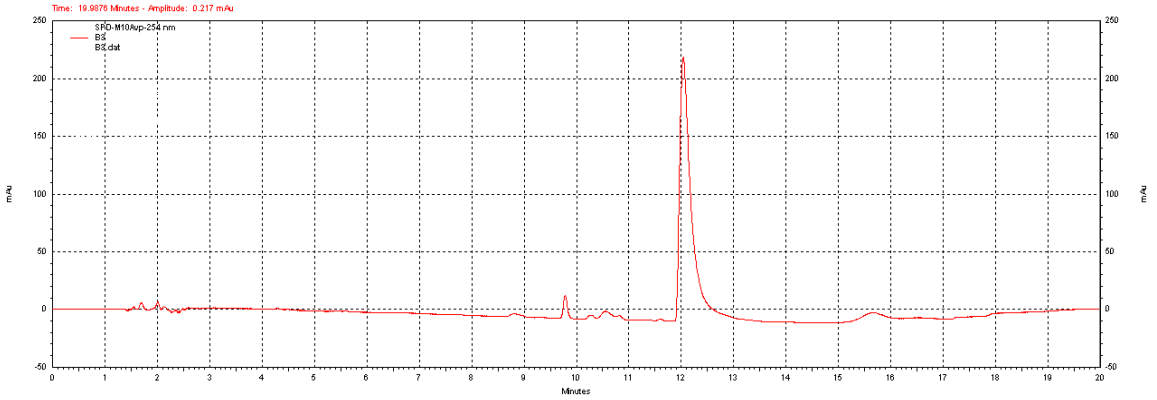

Figure D10: Chromatogram of time = 3 hr aliquot of incubation of Δ^9-THCA with *P. putida.*

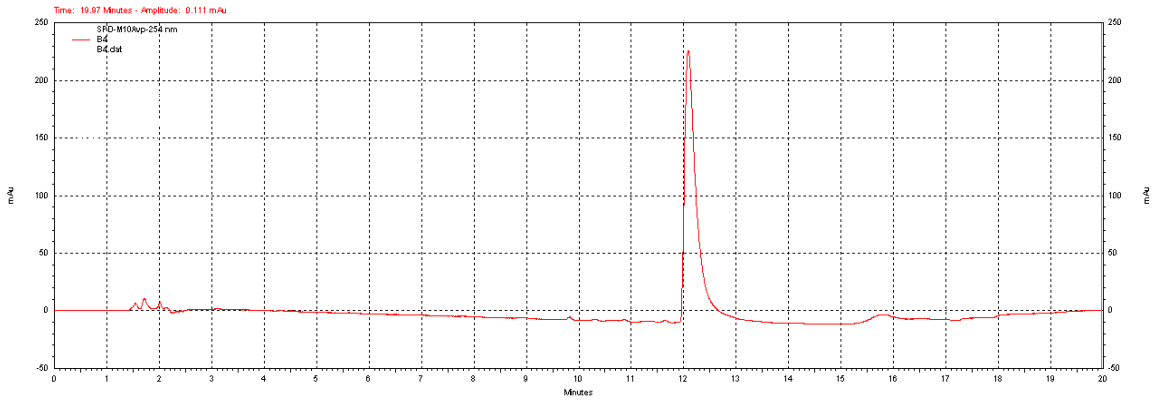

Figure D11: Chromatogram of time = 4 hr aliquot of incubation of Δ^9-THCA with *P. putida.*

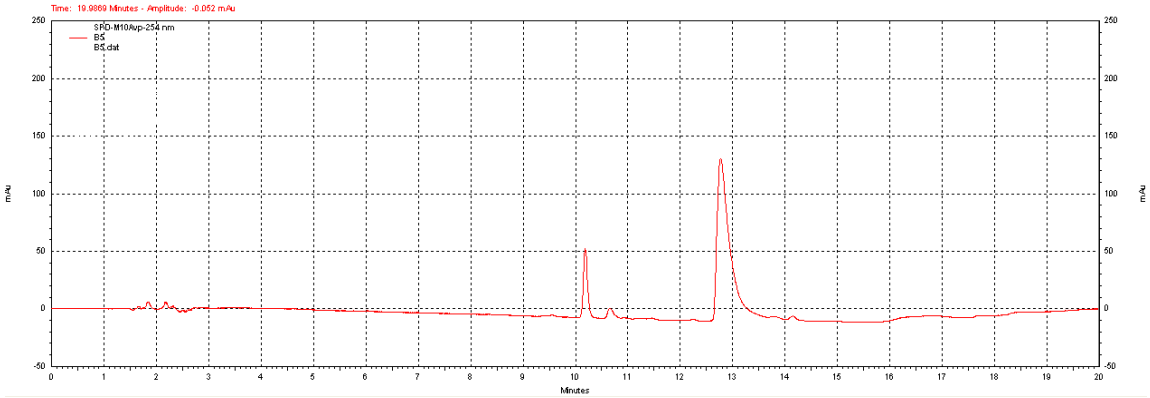

Figure D12: Chromatogram of time = 5 hr aliquot of incubation of Δ^9-THCA with *P. putida.*

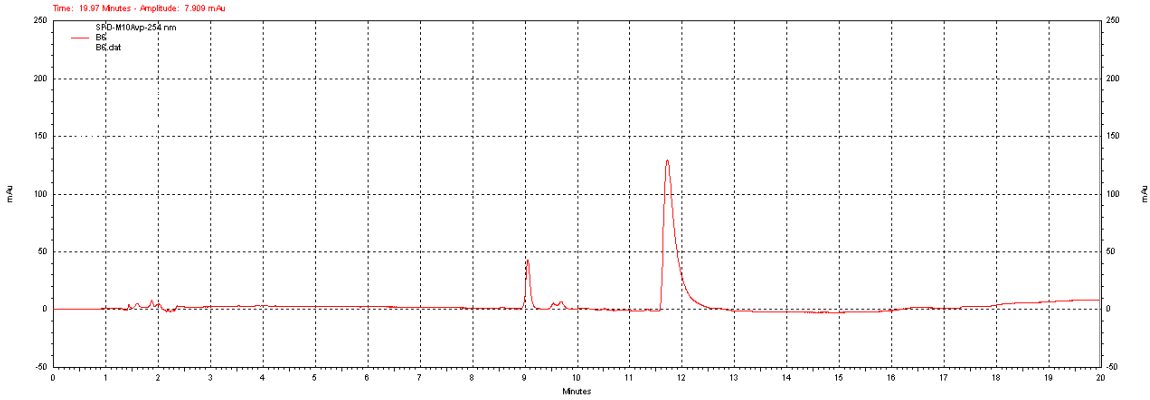

Figure D13: Chromatogram of time = 6 hr aliquot of incubation of Δ^9-THCA with *P. putida.*

APPENDIX E

Second *P. putida* Assay

The second *Pseudomonas putida* assay was conducted using 16.0 mL of a 22.3 mg/mL microbial solution. The microbial cells were incubated with 0.1 mL of approximately 85 mg/mL Δ^9-THCA isolated using the Yamazen method (Fig. 22). This was run alongside a control autoclaved microbial cell assay which consisted of 16.0 mL of a 25.5 mg/mL microbial solution which was incubated with 0.1 mL of approximately 85 mg/mL Δ^9-THCA isolated using the Yamazen method (Fig. 22). The Δ^9-THC standard was analyzed via analytical HPLC before the aliquots for this assay to identify the peaks in the aliquot samples.

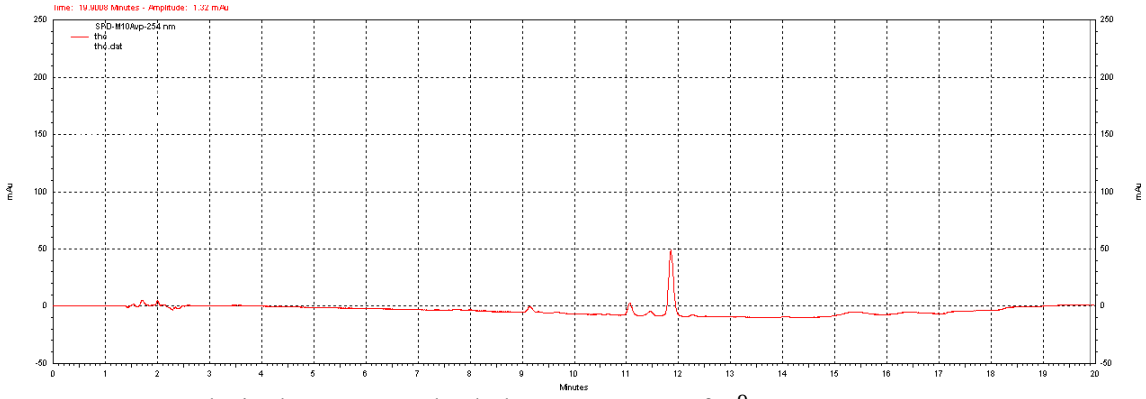

Figure E1: Analytical HPLC method chromatogram of Δ^9-THC standard (1.2 mg/mL in ethanol).

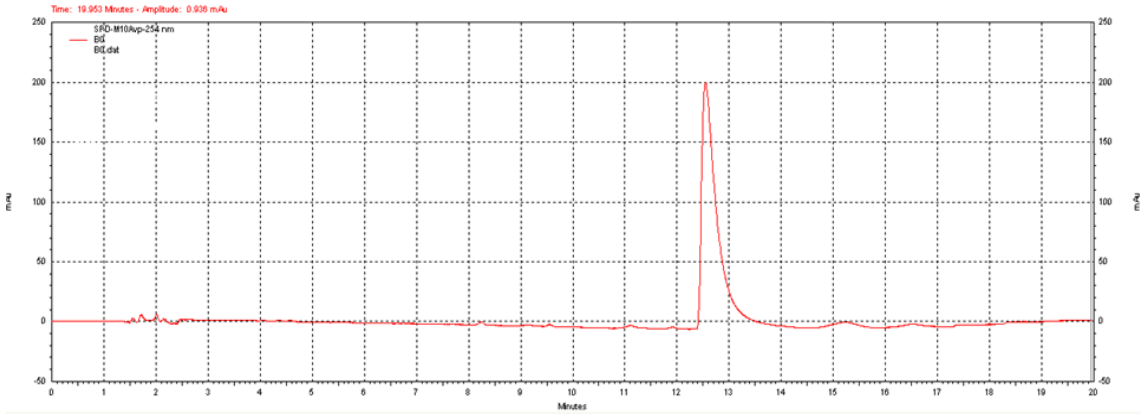

Figure E2: Chromatogram of time = 0 hr aliquot of incubation of Δ^9-THCA with *P. putida.*

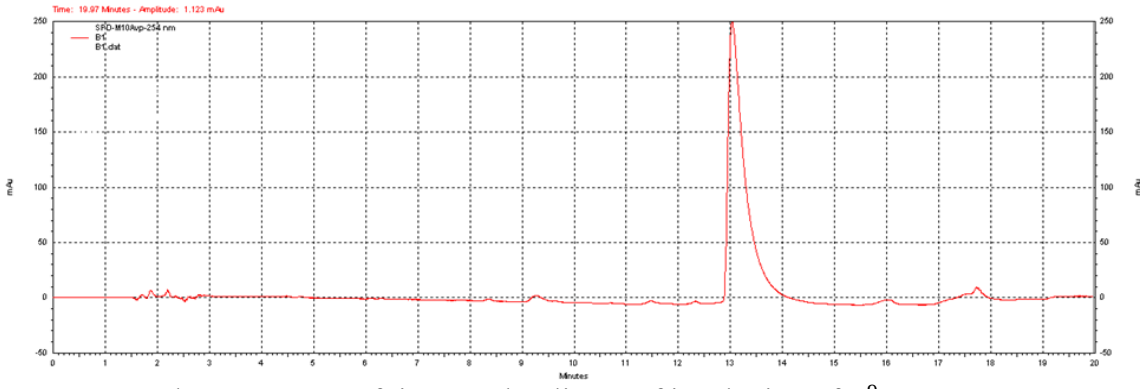

Figure E3: Chromatogram of time = 1 hr aliquot of incubation of Δ^9-THCA with *P. putida.*

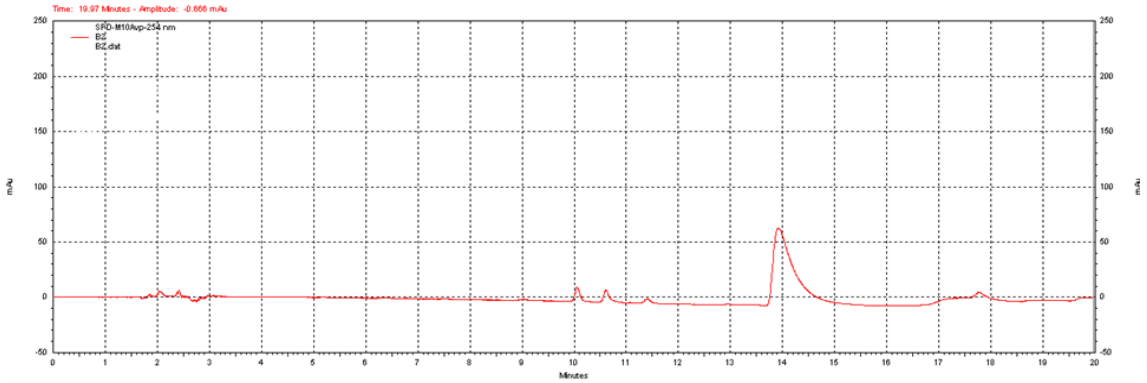

Figure E4: Chromatogram of time = 2 hr aliquot of incubation of Δ^9-THCA with *P. putida.*

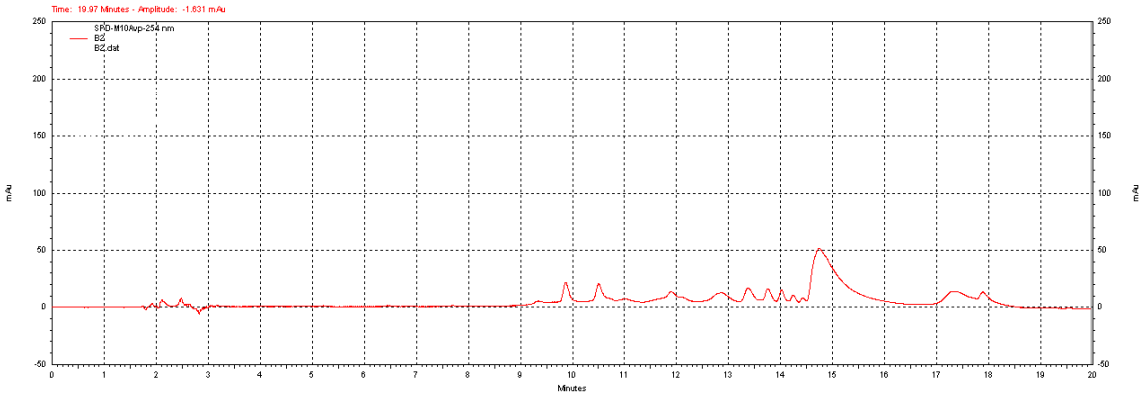

Figure E5: Repeat of chromatogram of time = 2 hr aliquot of incubation of Δ^9-THCA with *P. putida.*

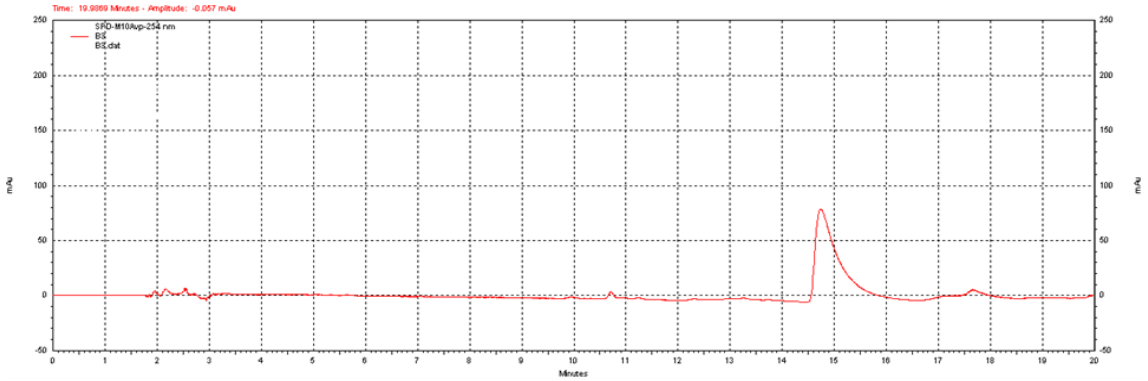

Figure E6: Chromatogram of time = 3 hr aliquot of incubation of Δ^9-THCA with *P. putida.*

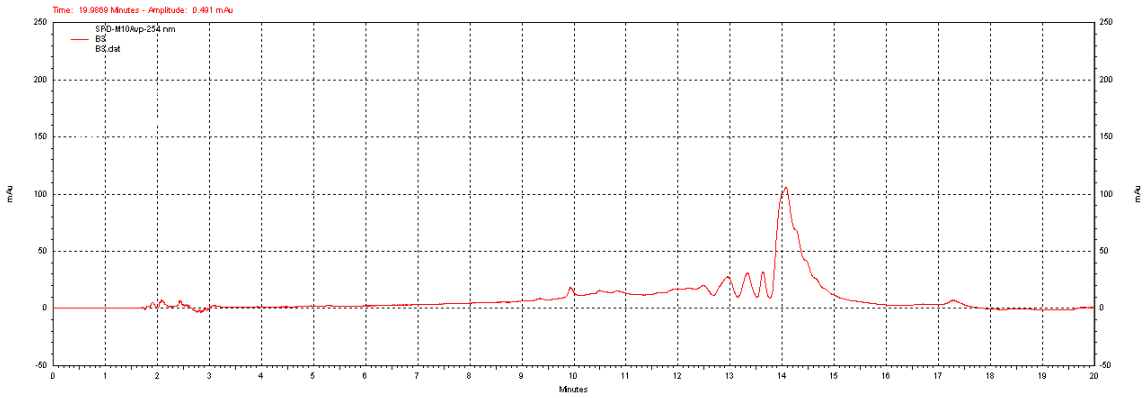

Figure E7: Repeat of chromatogram of time = 3 hr aliquot of incubation of Δ^9-THCA with *P. putida.*

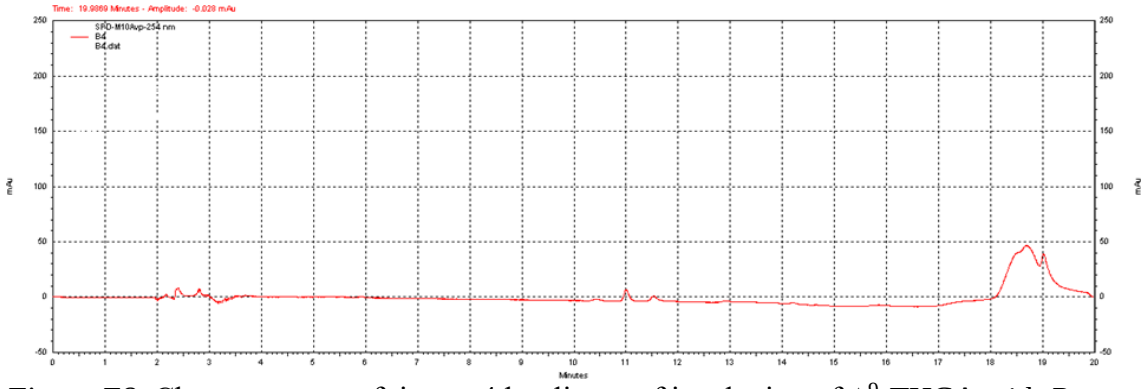

Figure E8: Chromatogram of time = 4 hr aliquot of incubation of Δ^9-THCA with *P. putida.*

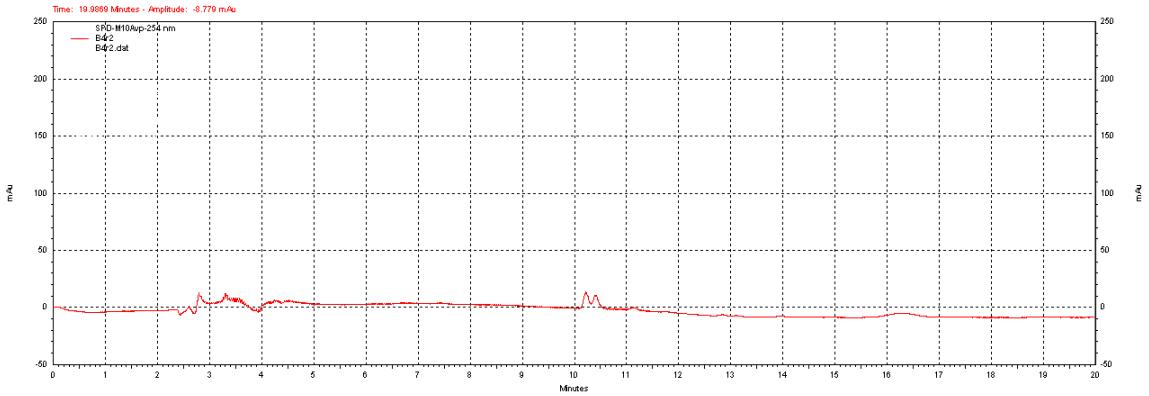

Figure E9: Repeat of chromatogram of time = 4 hr aliquot of incubation of Δ^9-THCA with *P. putida.*

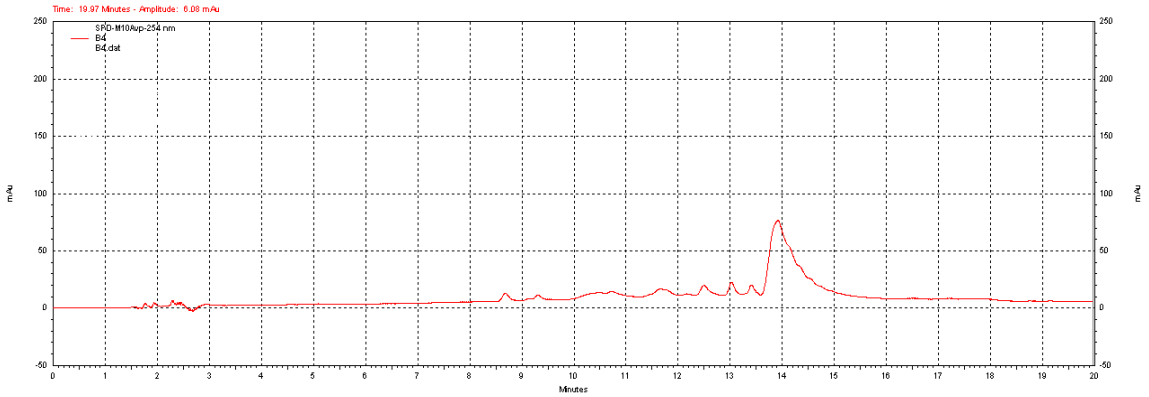

Figure E10: Second repeat of chromatogram of time = 4 hr aliquot of incubation of Δ^9-THCA with *P. putida.*

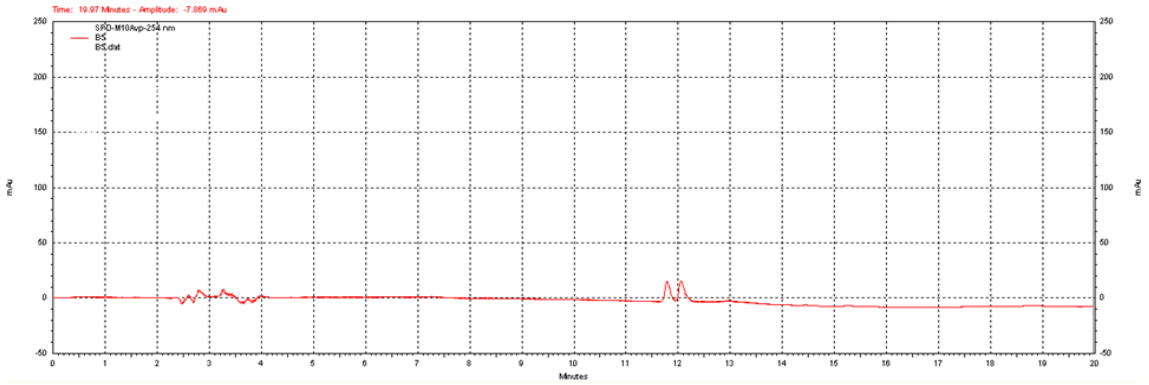

Figure E11: Chromatogram of time = 5 hr aliquot of incubation of Δ^9-THCA with *P. putida.*

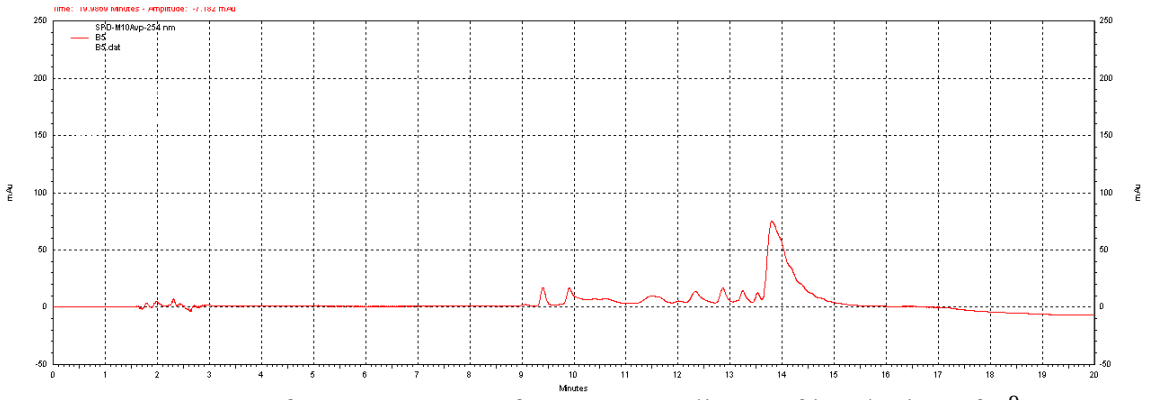

Figure E12: Repeat of chromatogram of time = 5 hr aliquot of incubation of Δ^9-THCA with *P. putida.*

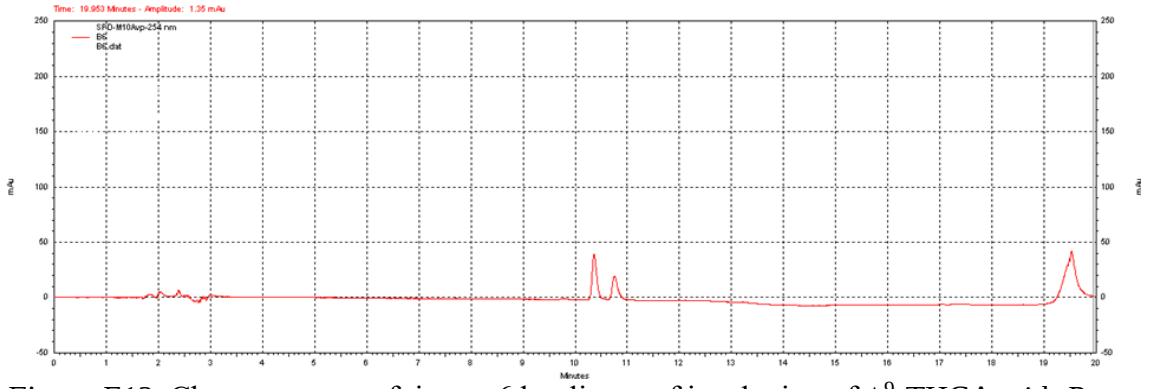

Figure E13: Chromatogram of time = 6 hr aliquot of incubation of Δ^9-THCA with *P. putida.*

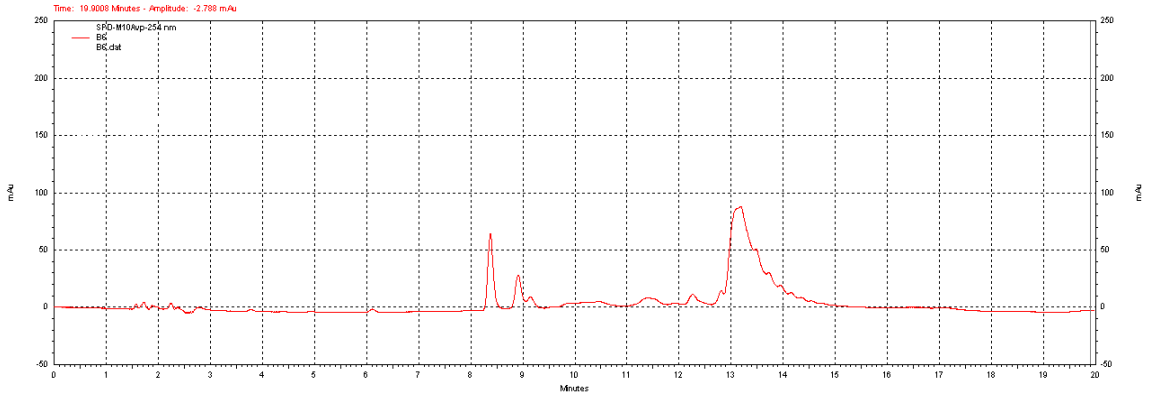

Figure E14: Repeat of chromatogram of time = 6 hr aliquot of incubation of Δ^9-THCA with *P. putida.*

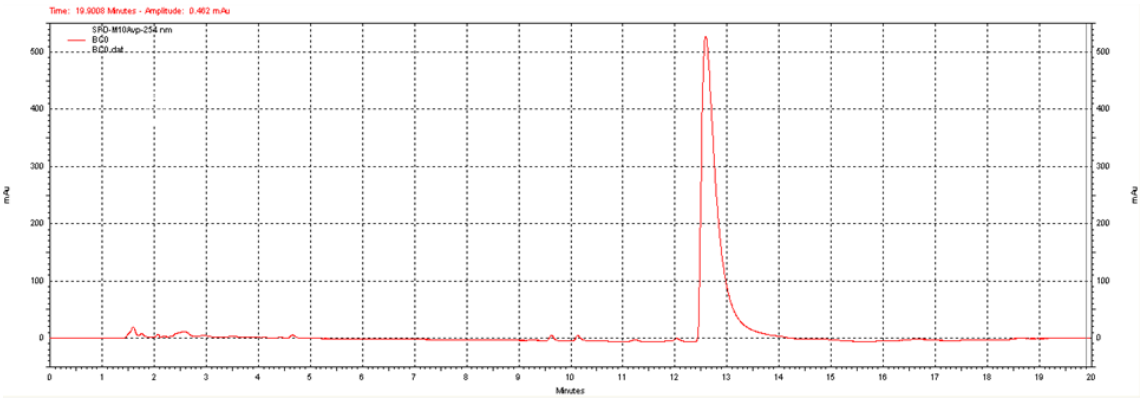

Figure E15: Chromatogram of time = 0 hr control aliquot of incubation of Δ^9-THCA with *P. putida.*

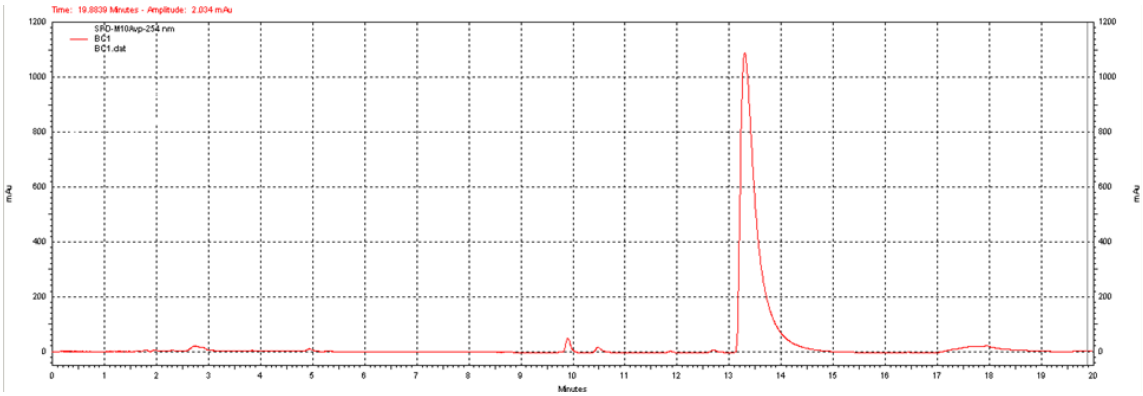

Figure E16: Chromatogram of time = 1 hr control aliquot of incubation of Δ^9-THCA with *P. putida.*

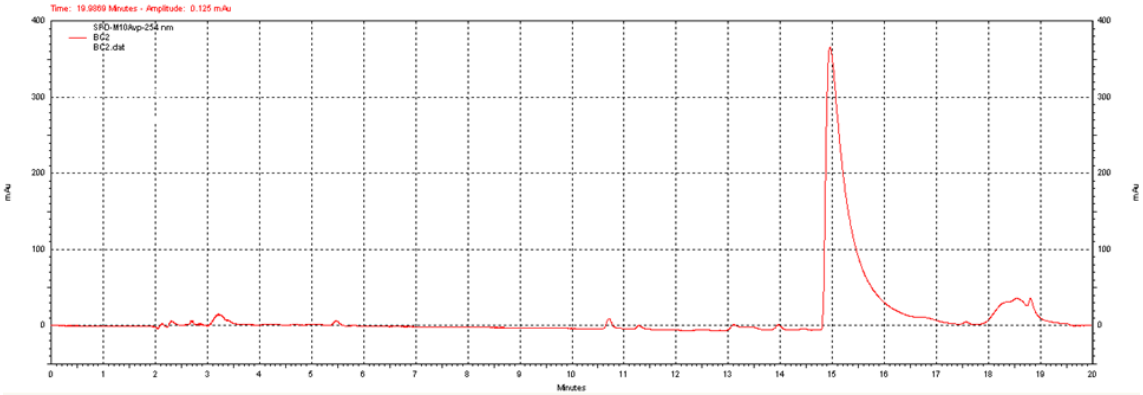

Figure E17: Chromatogram of time = 2 hr control aliquot of incubation of Δ^9-THCA with *P. putida.*

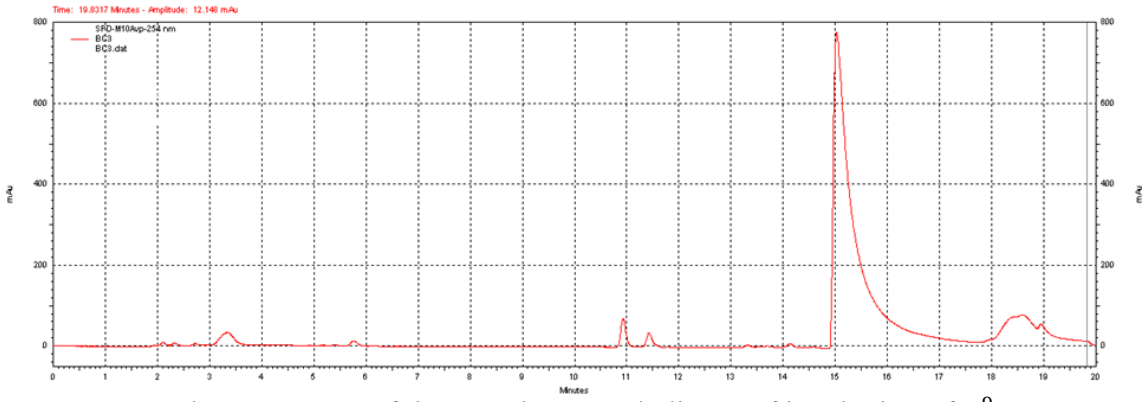

Figure E18: Chromatogram of time = 3 hr control aliquot of incubation of Δ^9-THCA with *P. putida.*

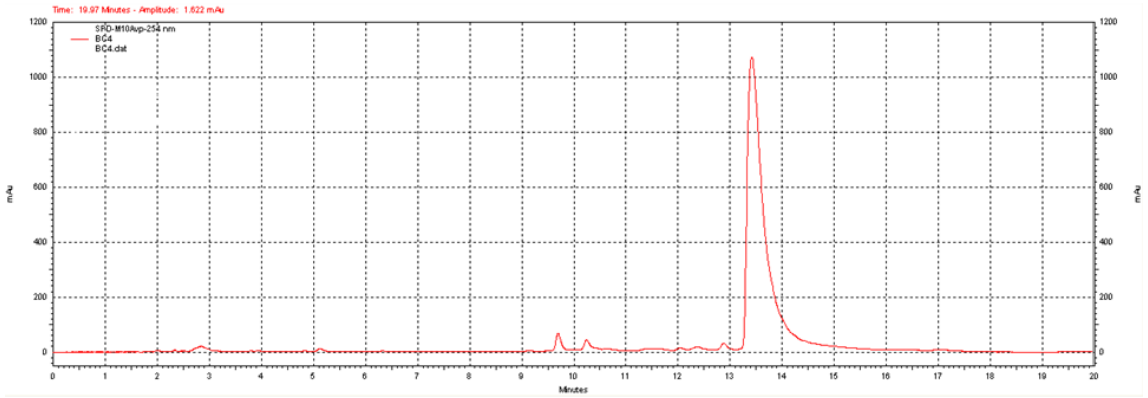

Figure E19: Chromatogram of time = 4 hr control aliquot of incubation of Δ^9-THCA with *P. putida.*

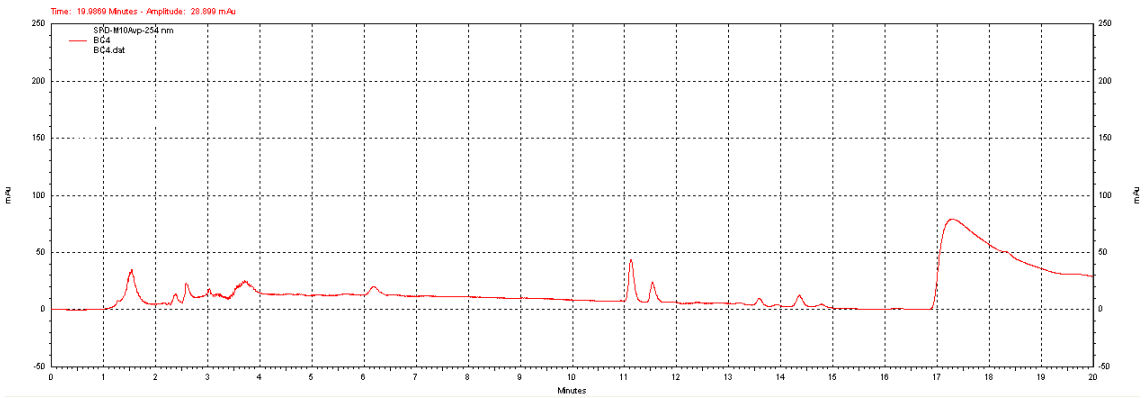

Figure E20: Repeat of chromatogram of time = 4 hr control aliquot of incubation of Δ^9-THCA with *P. putida.*

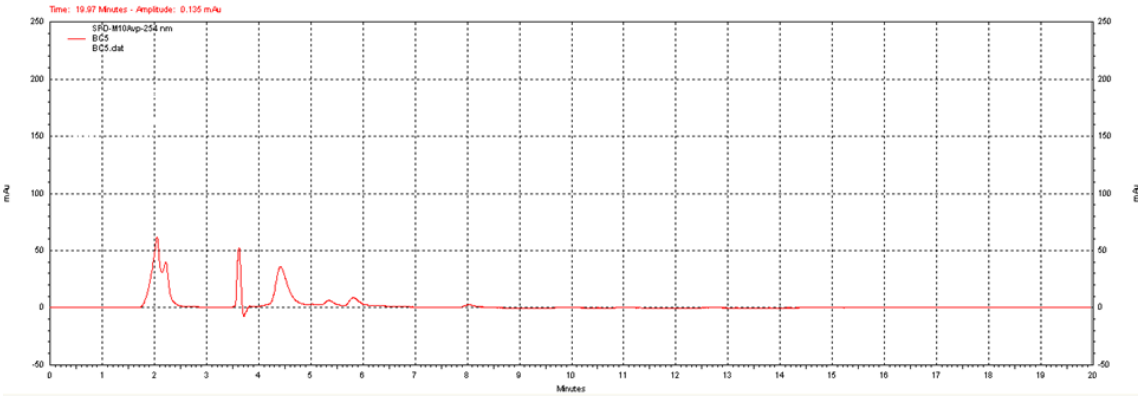

Figure E21: Chromatogram of time = 5 hr control aliquot of incubation of Δ^9-THCA with *P. putida.*

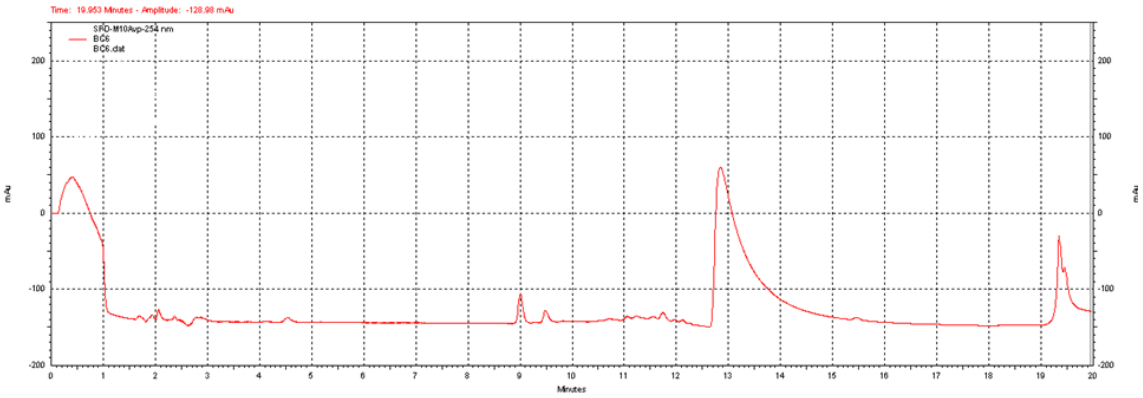

Figure E22: Chromatogram of time = 6 hr control aliquot of incubation of Δ^9-THCA with *P. putida.*

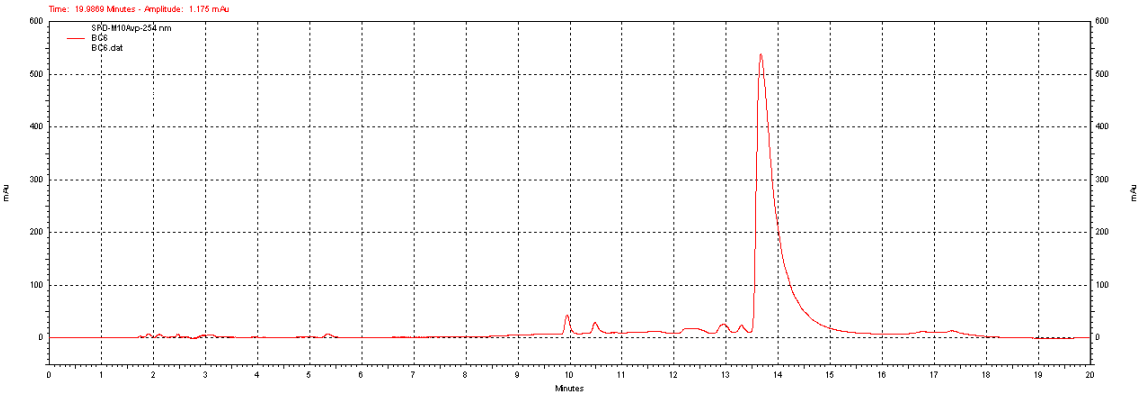

Figure E23: Repeat of chromatogram of time = 6 hr control aliquot of incubation of Δ^9-THCA with *P. putida.*

APPENDIX F

Third *P. putida* Assay

The third *Pseudomonas putida* assay was conducted using 16.0 mL of a 55.5 mg/mL microbial solution. The microbial cells were incubated with 0.1 mL of approximately 85 mg/mL Δ^9-THCA isolated using the Yamazen method (Fig. 22). This was run alongside a control autoclaved microbial cell assay which consisted of 16.0 mL of a 20.0 mg/mL microbial solution which was incubated with 0.1 mL of approximately 85 mg/mL Δ^9-THCA isolated using the Yamazen method (Fig. 22). The Δ^9-THC standard was analyzed via analytical HPLC before the aliquots for this assay to identify the peaks in the aliquot samples. After the aliquot samples were analyzed a sample of absolute ethanol was analyzed to see the amount of contamination stuck to the column.

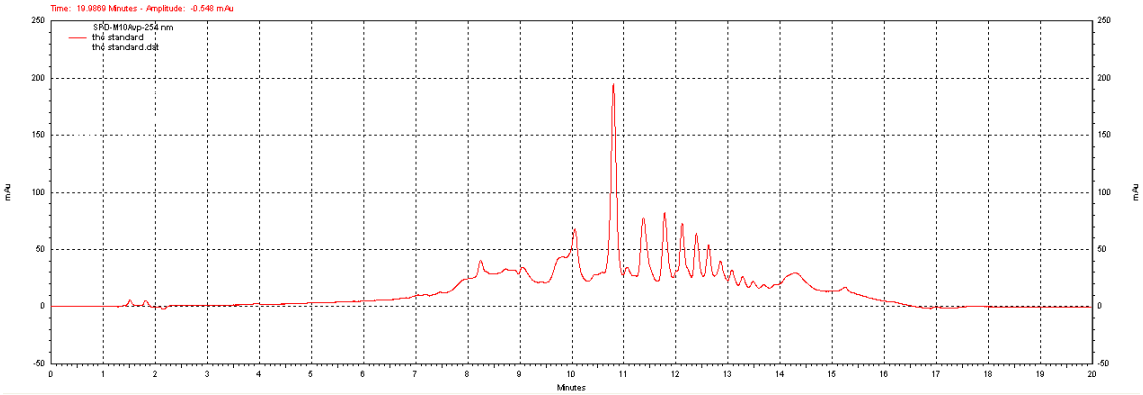

Figure F1: Analytical HPLC method chromatogram of Δ^9-THC standard (1.2 mg/mL in ethanol).

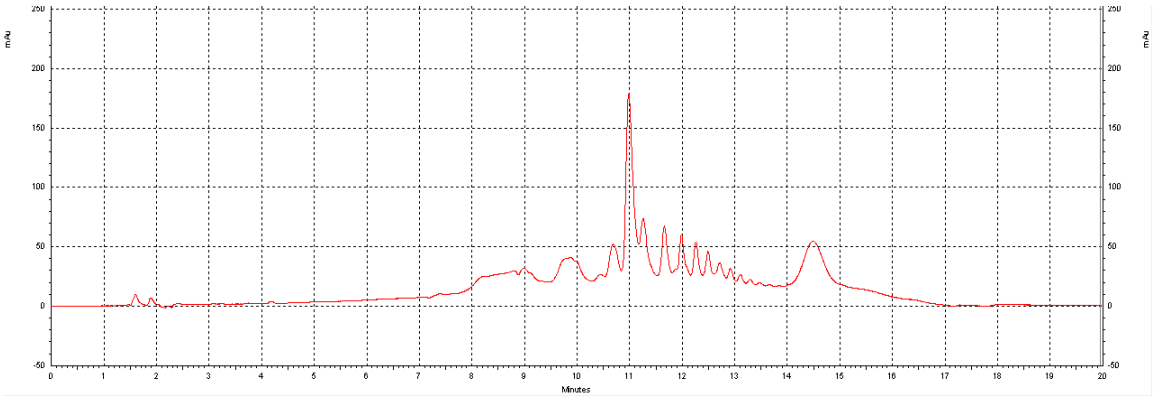

Figure F2: Chromatogram of time = 0 hr aliquot of incubation of Δ^9-THCA with *P. putida.*

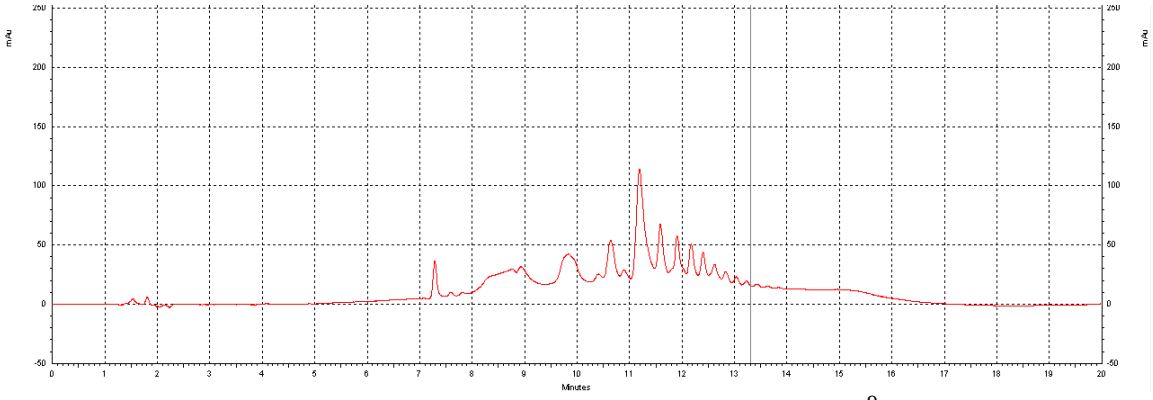

Figure F3: Chromatogram of time = 1 hr aliquot of incubation of Δ^9-THCA with *P. putida.*

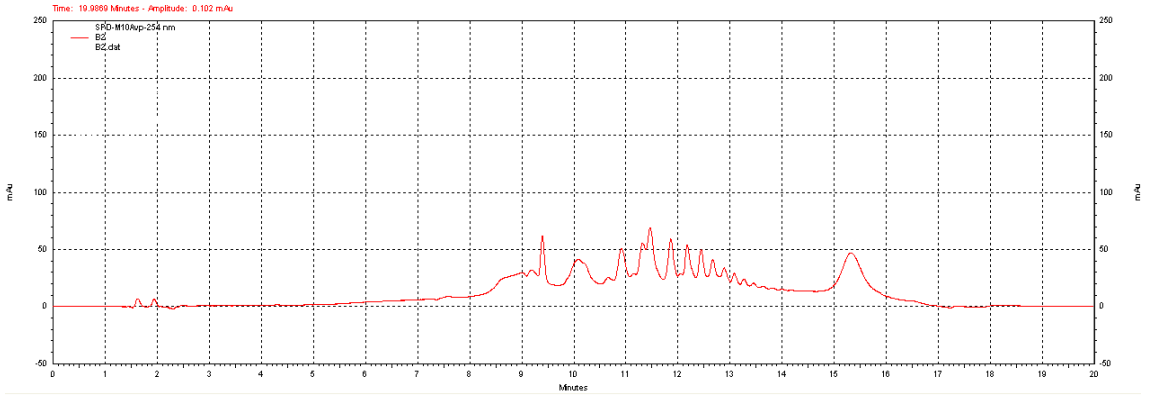

Figure F4: Chromatogram of time = 2 hr aliquot of incubation of Δ^9-THCA with *P. putida.*

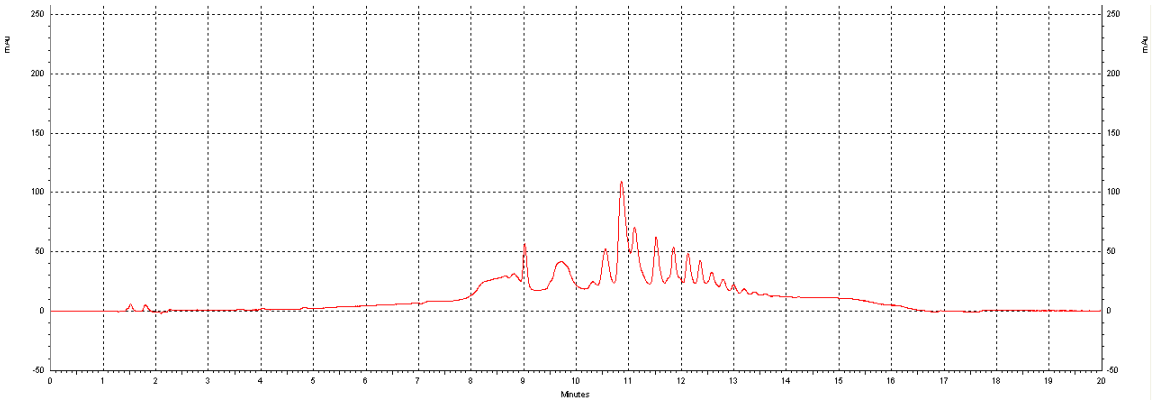

Figure F5: Chromatogram of time = 3 hr aliquot of incubation of Δ^9-THCA with *P. putida.*

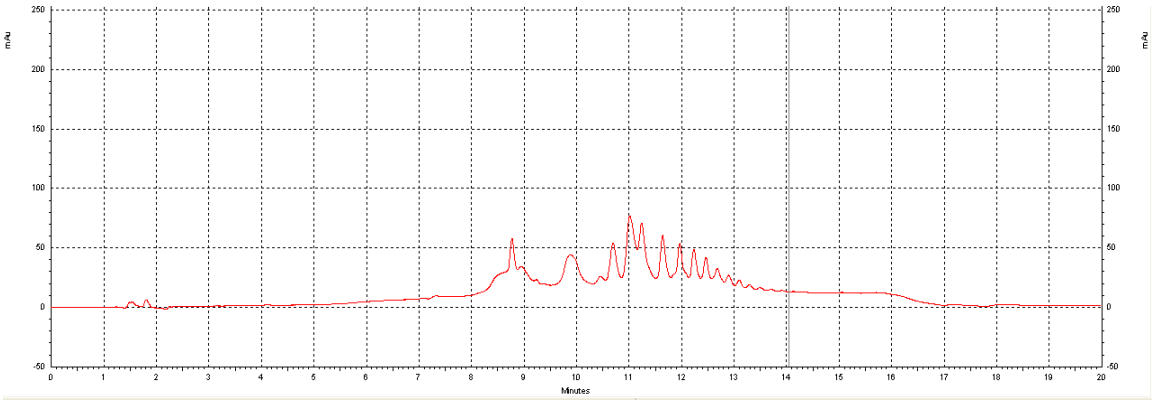

Figure F6: Chromatogram of time = 4 hr aliquot of incubation of Δ^9-THCA with *P. putida.*

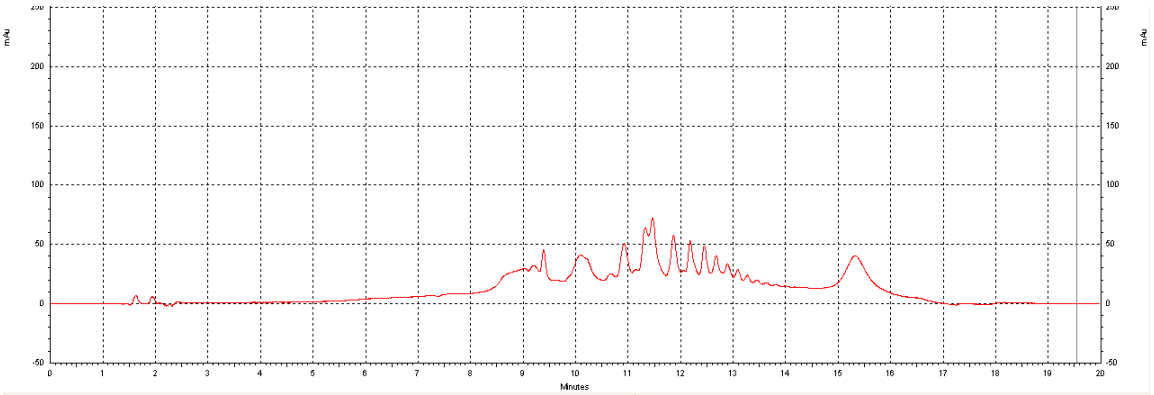

Figure F7: Chromatogram of time = 5 hr aliquot of incubation of Δ^9-THCA with *P. putida.*

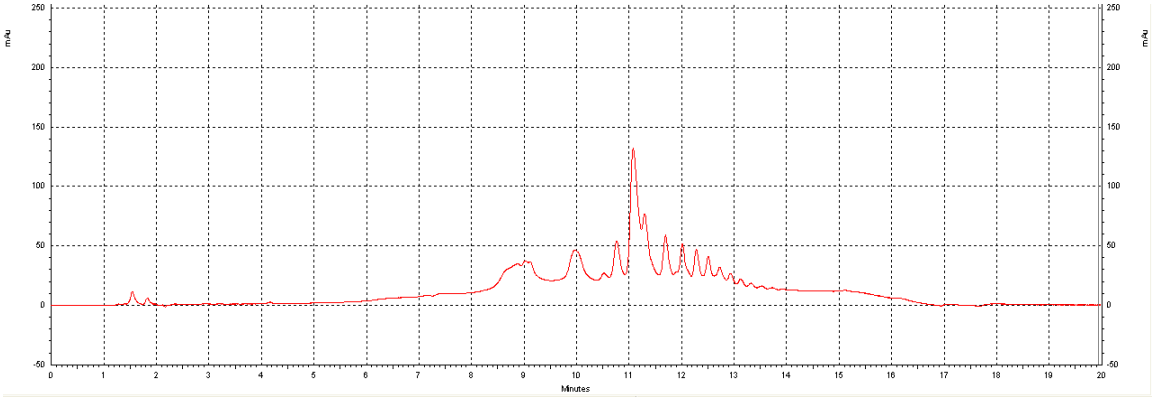

Figure F8: Chromatogram of time = 6 hr aliquot of incubation of Δ^9-THCA with *P. putida.*

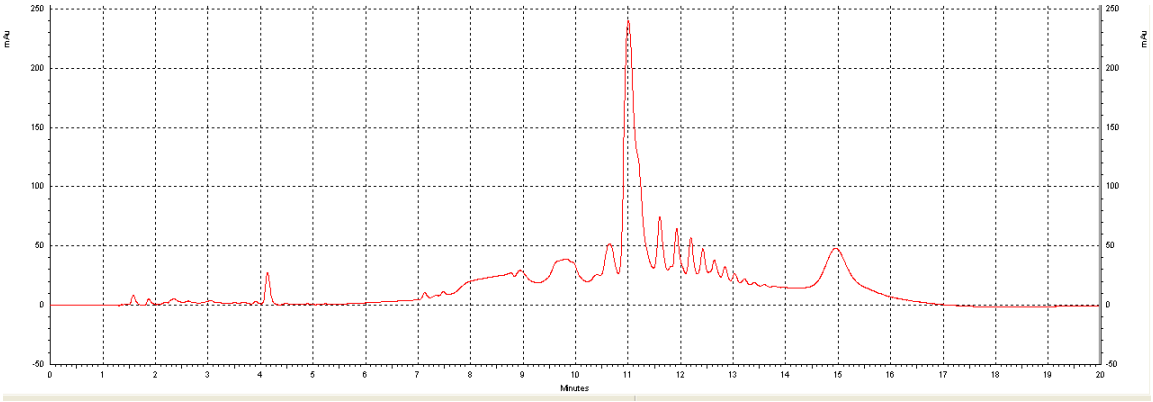

Figure F9: Chromatogram of time = 0 hr control aliquot of incubation of Δ^9-THCA with *P. putida.*

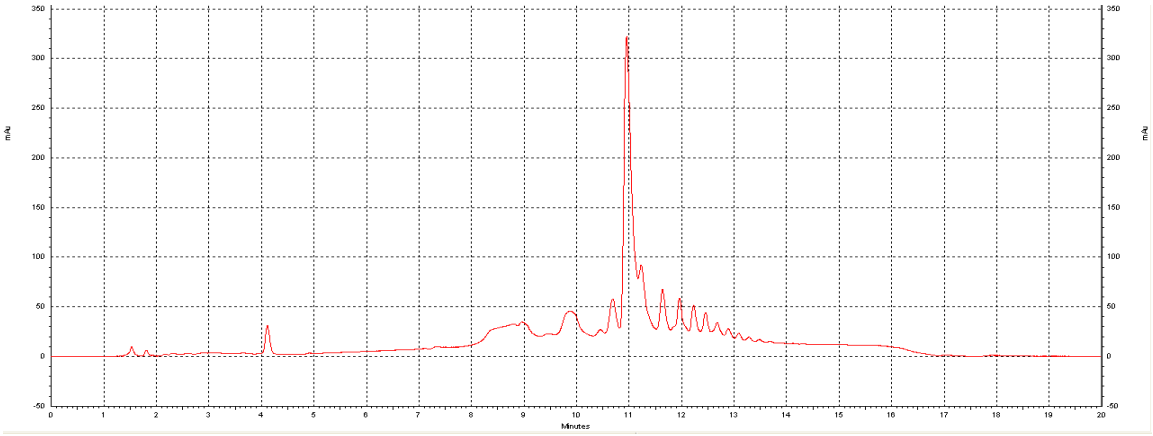

Figure F10: Chromatogram of time = 1 hr control aliquot of incubation of Δ^9-THCA with *P. putida.*

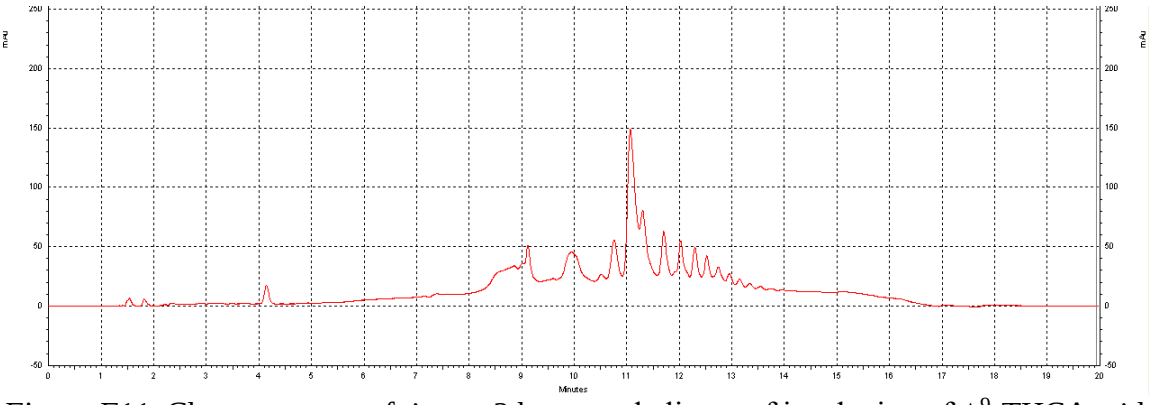

Figure F11: Chromatogram of time = 2 hr control aliquot of incubation of Δ^9-THCA with *P. putida.*

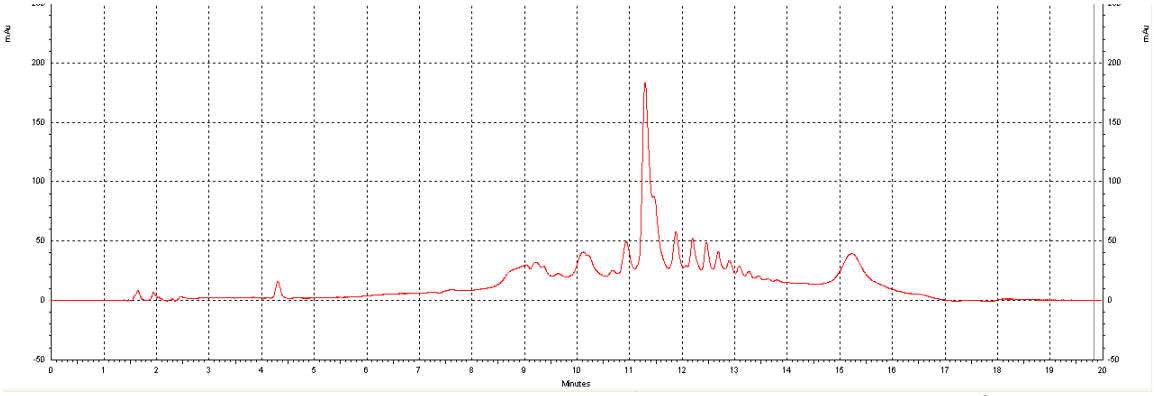

Figure F12: Chromatogram of time = 3 hr control aliquot of incubation of Δ^9-THCA with *P. putida.*

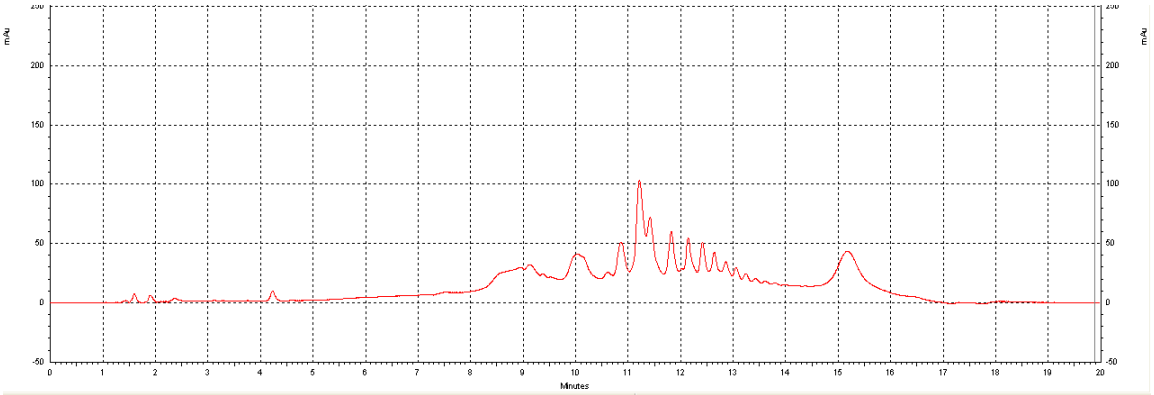

Figure F13: Chromatogram of time = 4 hr control aliquot of incubation of Δ^9-THCA with *P. putida.*

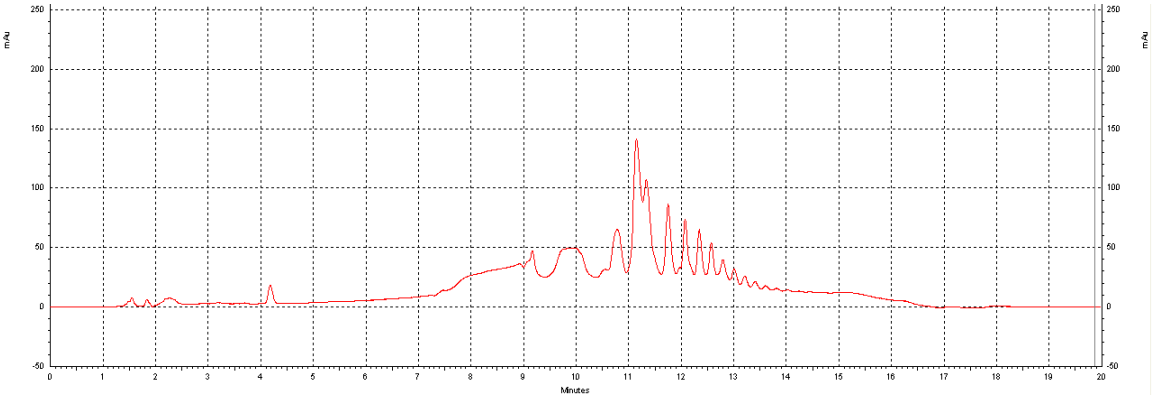

Figure F14: Chromatogram of time = 5 hr control aliquot of incubation of Δ^9-THCA with *P. putida.*

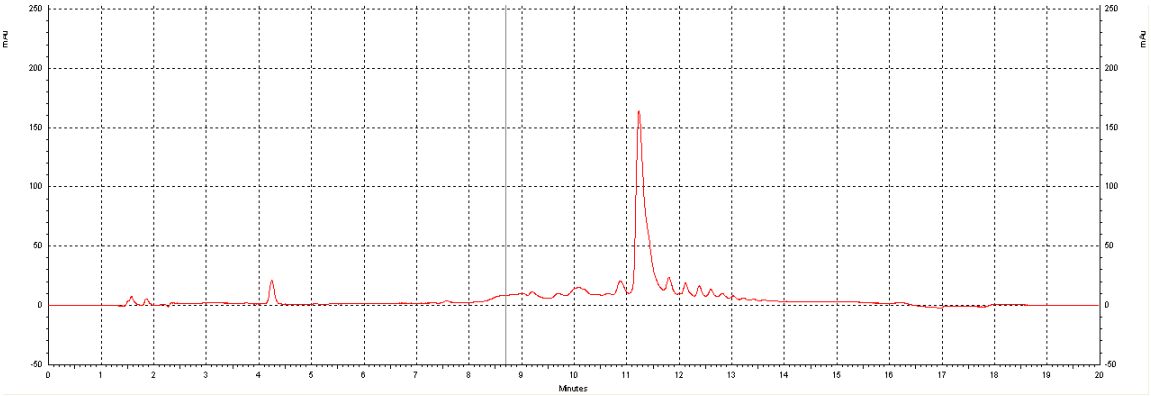

Figure F15: Chromatogram of time = 6 hr control aliquot of incubation of Δ^9-THCA with *P. putida.*

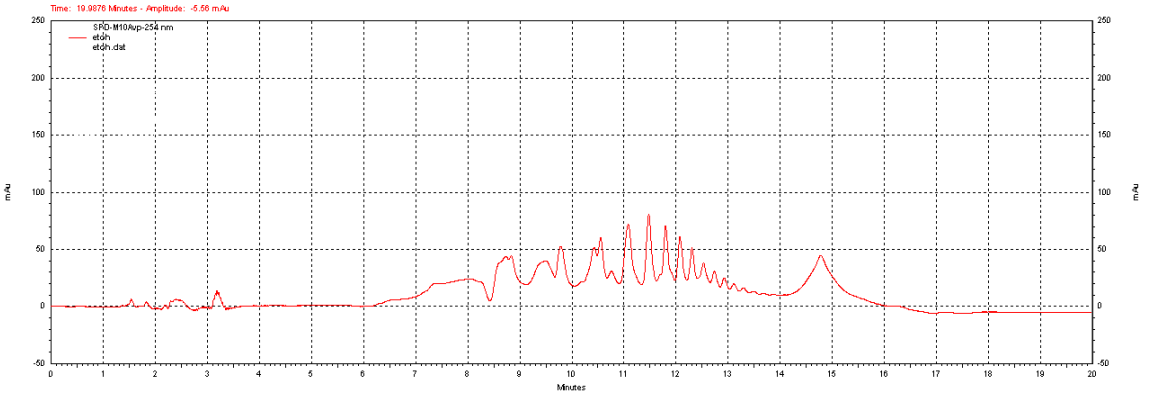

Figure F16: Chromatogram of absolute ethanol.

APPENDIX G

Fourth *P. putida* Assay

The fourth *Pseudomonas putida* assay was conducted using 16.0 mL of a 65.5 mg/mL microbial solution. The microbial cells were incubated with 0.1 mL of 2 mg/mL Δ^9-THCA isolated using the preparative HPLC method (Fig. 30). This was run alongside a control autoclaved microbial cell assay which consisted of 16.0 mL of a 37.5 mg/mL microbial solution which was incubated with 0.1 mL of 2 mg/mL Δ^9-THCA isolated using the preparative HPLC method (Fig. 30). The Δ^9-THCA isolated via preparative HPLC and the Δ^9-THC standard were analyzed via analytical HPLC before the aliquots for this assay to identify the peaks in the aliquot samples (Fig. G1 & G2).

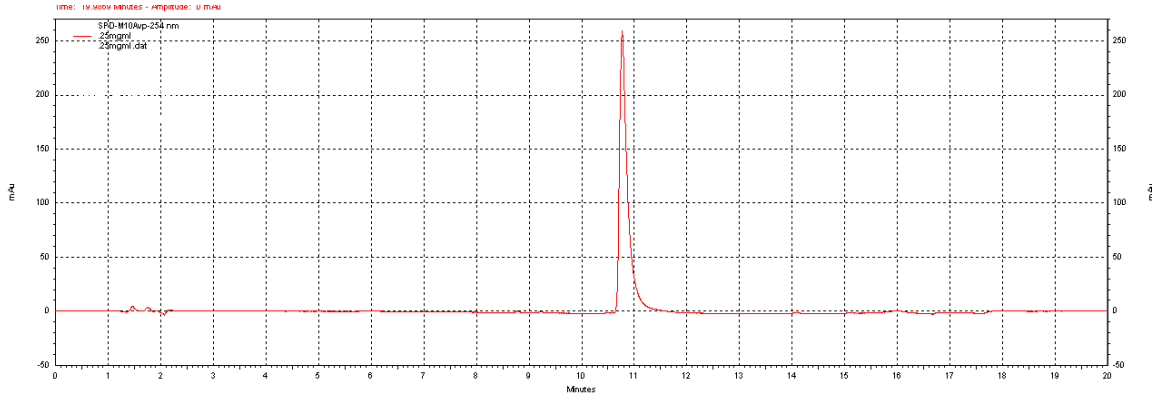

Figure G1: Analytical HPLC method chromatogram of Δ^9-THCA isolated via preparative HPLC (2 mg/mL in ethanol).

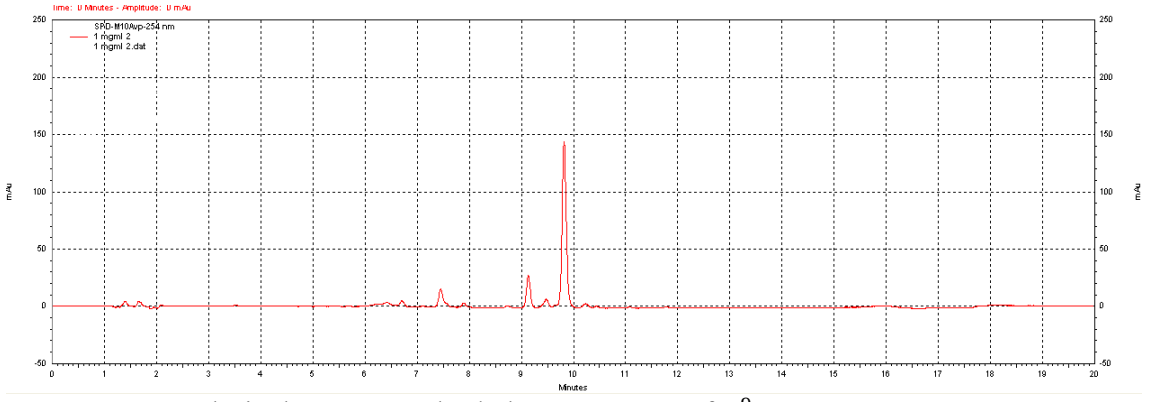

Figure G2: Analytical HPLC method chromatogram of Δ^9-THC standard (1.2 mg/mL in ethanol).

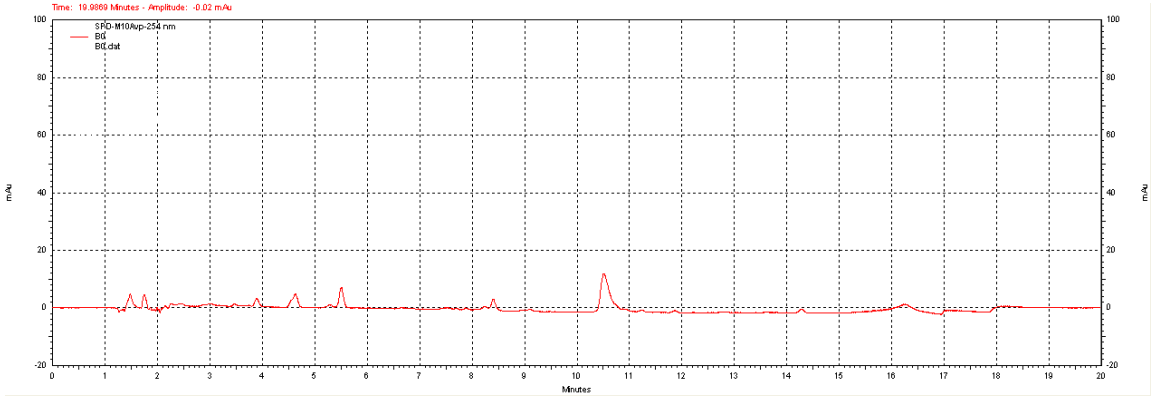

Figure G3: Chromatogram of time = 0 hr aliquot of incubation of Δ^9-THCA with *P. putida.*

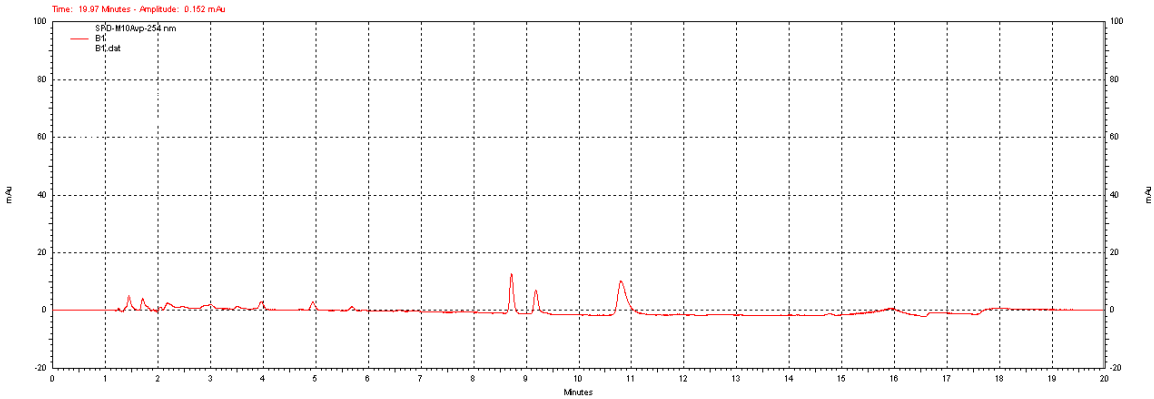

Figure G4: Chromatogram of time = 1 hr aliquot of incubation of Δ^9-THCA with *P. putida.*

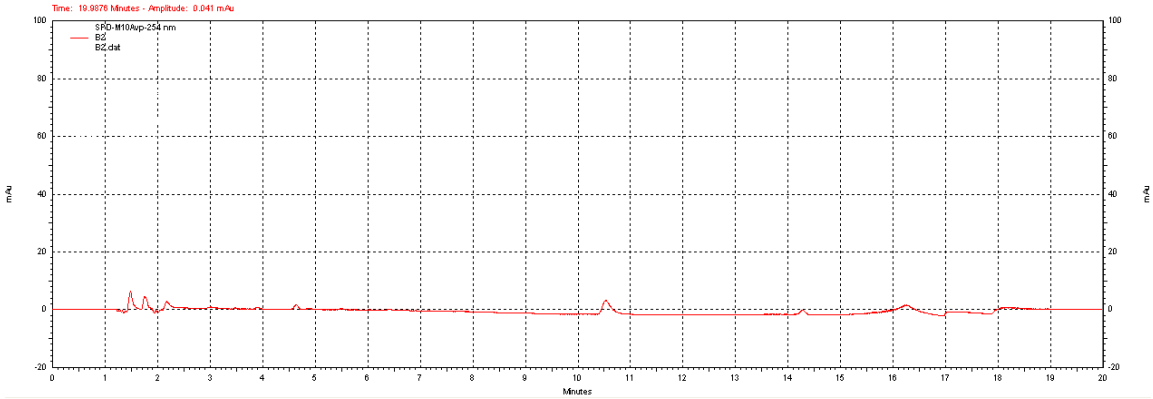

Figure G5: Chromatogram of time = 2 hr aliquot of incubation of Δ^9-THCA with *P. putida.*

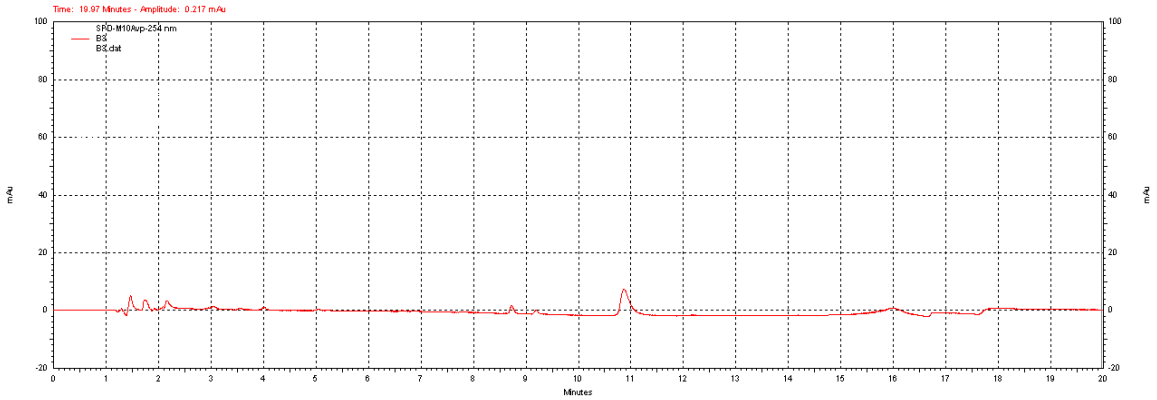

Figure G6: Chromatogram of time = 3 hr aliquot of incubation of Δ^9-THCA with *P. putida.*

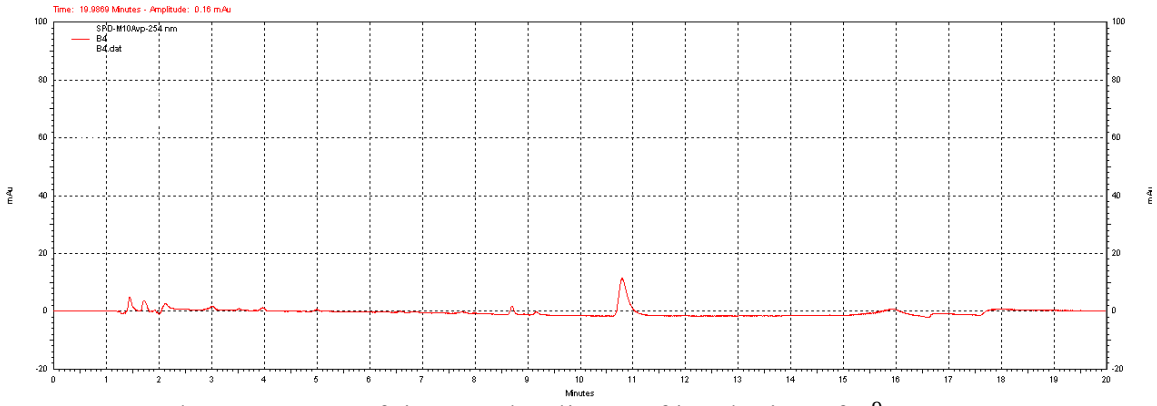

Figure G7: Chromatogram of time = 4 hr aliquot of incubation of Δ^9-THCA with *P. putida.*

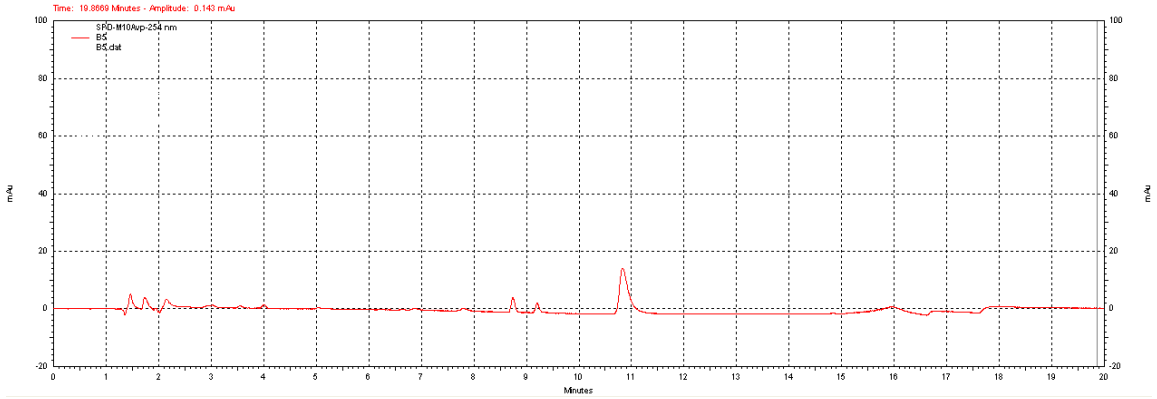

Figure G8: Chromatogram of time = 5 hr aliquot of incubation of Δ^9-THCA with *P. putida.*

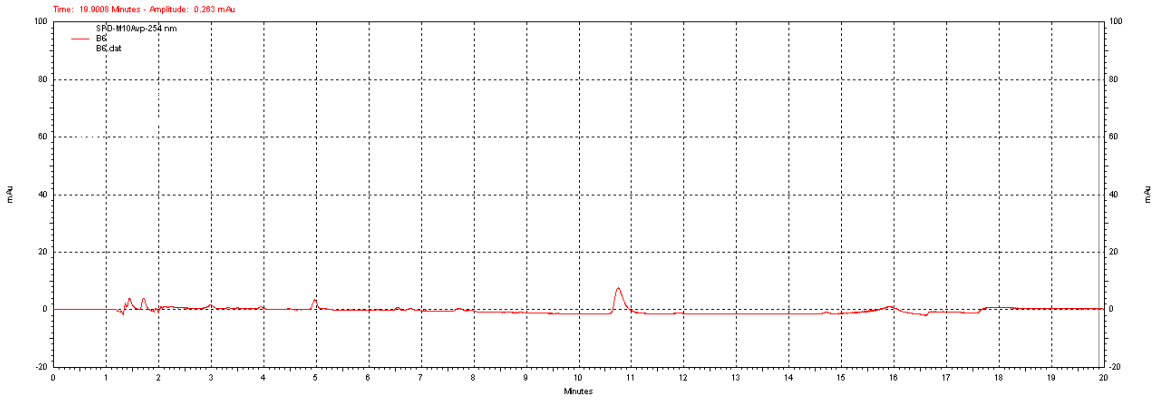

Figure G9: Chromatogram of time = 6 hr aliquot of incubation of Δ^9-THCA with *P. putida.*

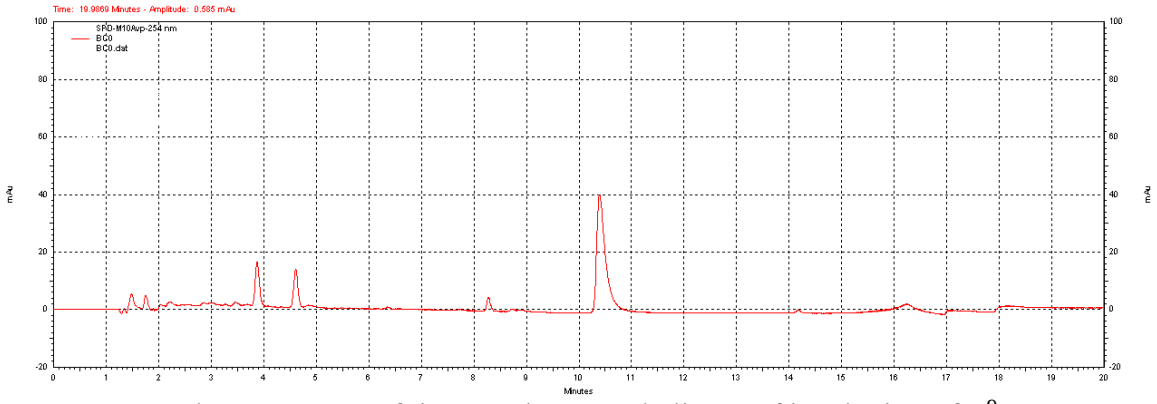

Figure G10: Chromatogram of time = 0 hr control aliquot of incubation of Δ^9-THCA with *P. putida.*

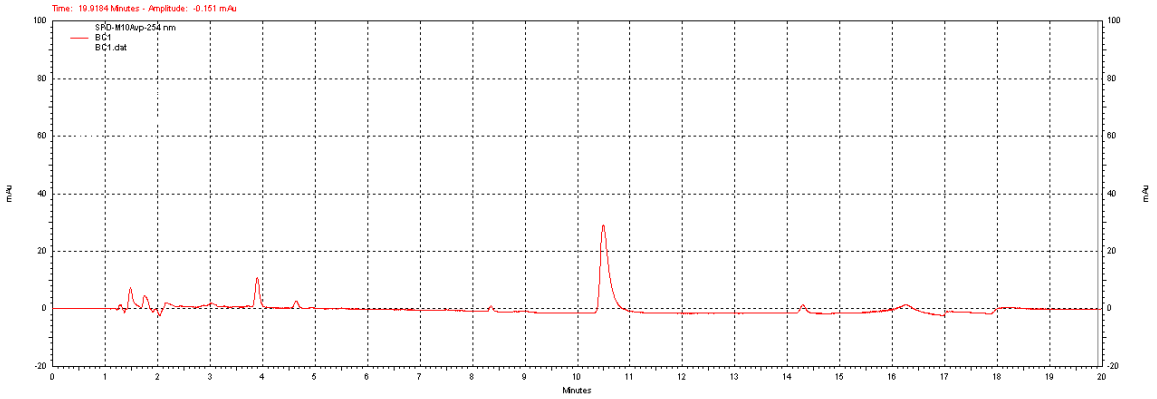

Figure G11: Chromatogram of time = 1 hr control aliquot of incubation of Δ^9-THCA with *P. putida.*

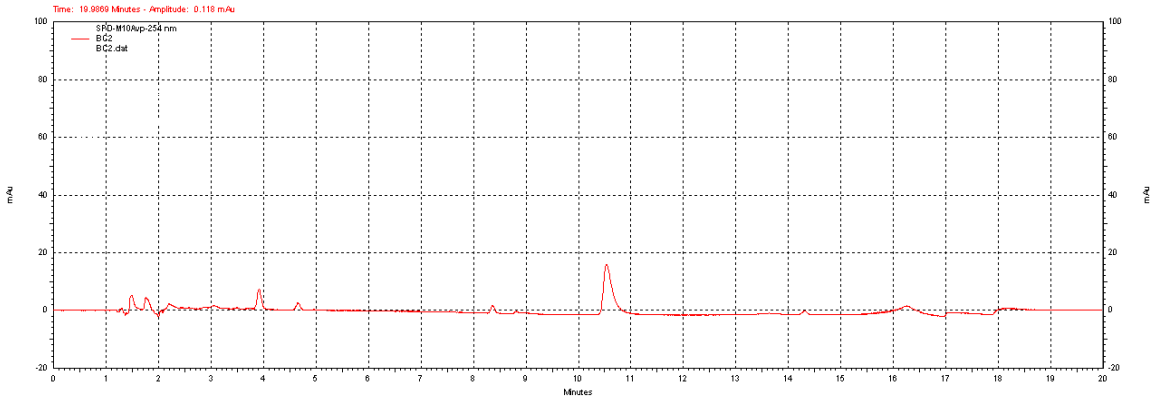

Figure G12: Chromatogram of time = 2 hr control aliquot of incubation of Δ^9-THCA with *P. putida.*

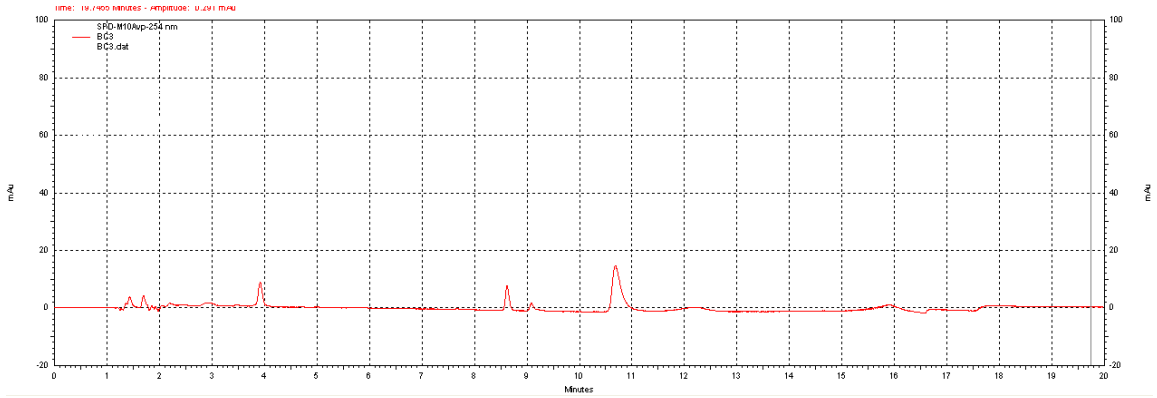

Figure G13: Chromatogram of time = 3 hr control aliquot of incubation of Δ^9-THCA with *P. putida.*

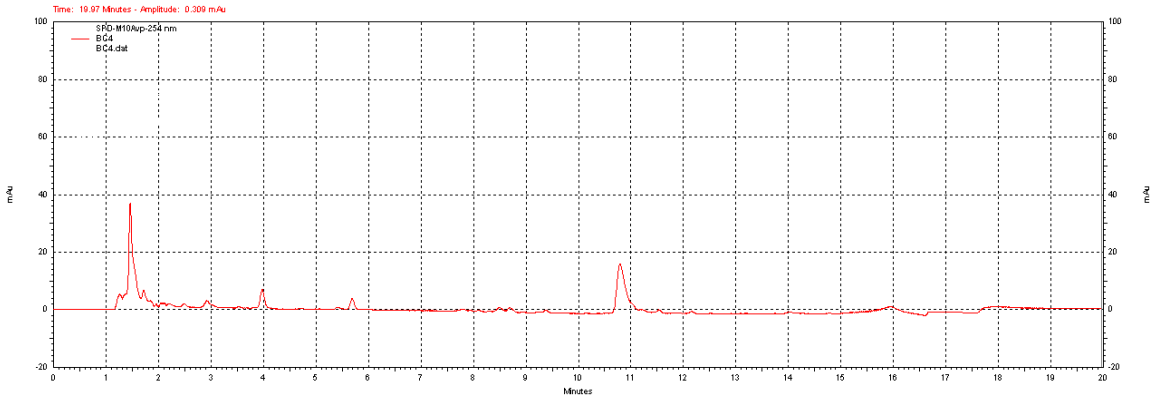

Figure G14: Chromatogram of time = 4 hr control aliquot of incubation of Δ^9-THCA with *P. putida.*

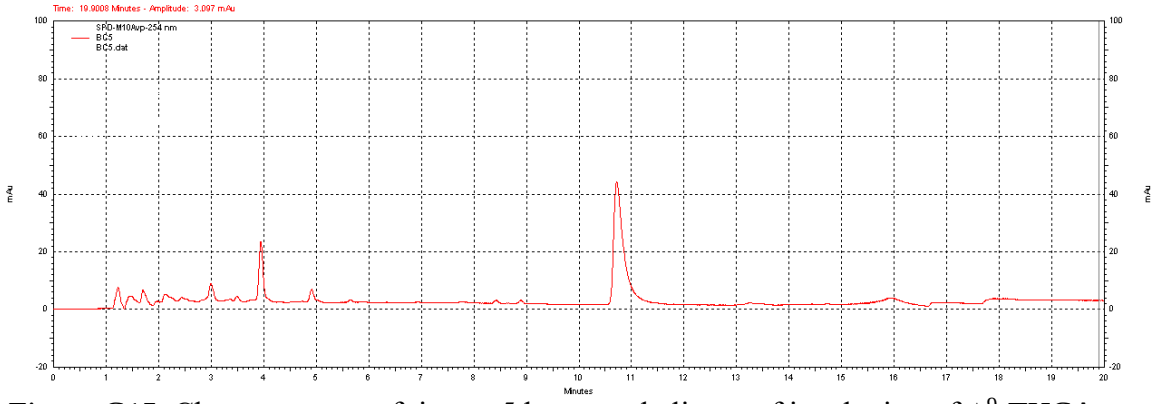

Figure G15: Chromatogram of time = 5 hr control aliquot of incubation of Δ^9-THCA with *P. putida.*

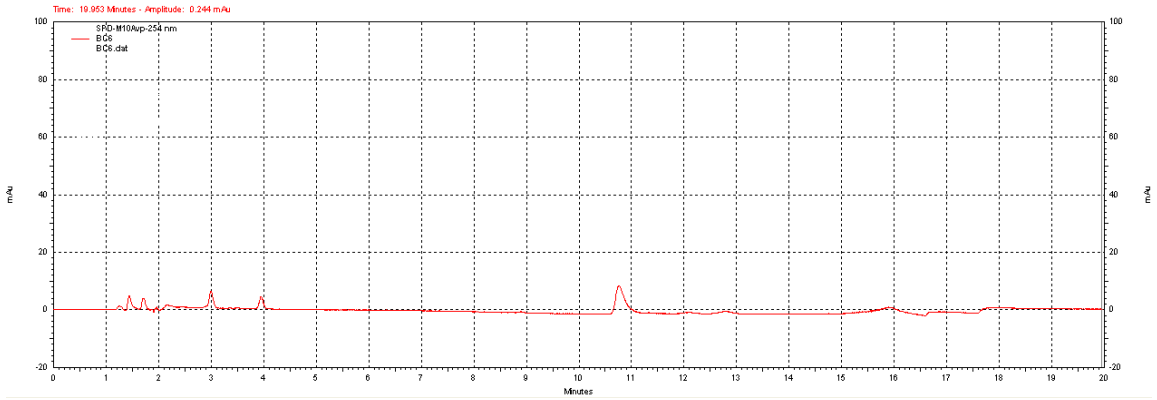

Figure G16: Chromatogram of time = 6 hr control aliquot of incubation of Δ^9-THCA with *P. putida.*

APPENDIX H

Fifth *P. putida* Assay

The fifth *Pseudomonas putida* assay was conducted using 16.0 mL of a 68.7 mg/mL microbial solution. The microbial cells were incubated with 0.1 mL of 4 mg/mL Δ^9-THCA isolated using the preparative HPLC method (Fig. 30). This was run alongside a control autoclaved microbial cell assay which consisted of 16.0 mL of a 60.60 mg/mL microbial solution which was incubated with 0.1 mL of 4 mg/mL Δ^9-THCA isolated using the preparative HPLC method (Fig. 30). The Δ^9-THCA isolated via preparative HPLC was analyzed via analytical HPLC, along with the Δ^9-THC standard, and the mixture of cannabinoids which contained CBDA, CBGA, CBG, CBD, THCV, CBN, Δ^9-THCA, Δ^9-THC, Δ^8-THC, and CBC (Fig. H1 – H3). This was done to identify the peaks in the aliquot samples. After all the aliquot samples from this assay were analyzed, 0.1 mg of Δ^9-THCA isolated via preparative HPLC was added to a 0.1 mL aliquot of the sample from time = 1 hr and analyzed via analytical HPLC again (Fig. H18). This was also repeated for the sample from time = 3 hr (Fig. H19). Additionally, 0.12 mg of Δ^9-THC standard was added to a 0.1 mL aliquot of the sample from time = 1 hr and analyzed via analytical HPLC (Fig. H20).

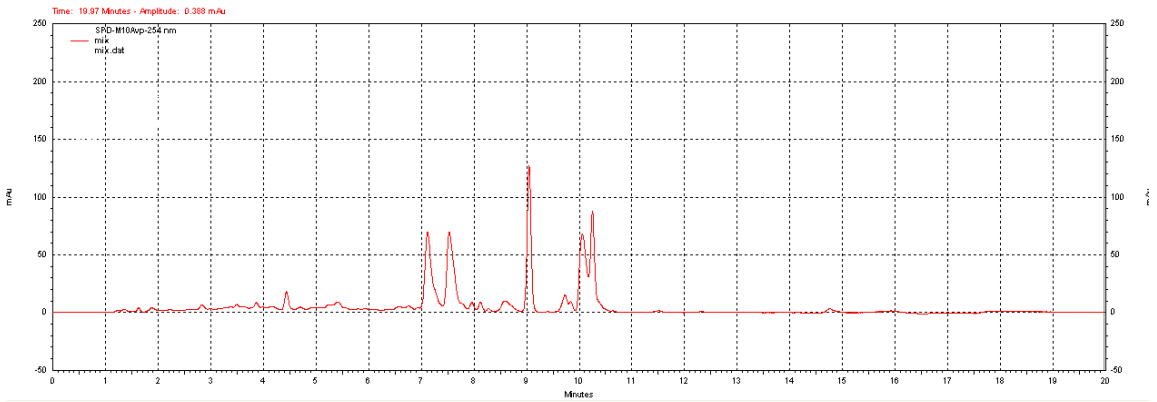

Figure H1: Analytical HPLC method chromatogram of cannabinoid mixture standard containing CBDA, CBGA, CBG, CBD, THCV, CBN, Δ^9-THCA, Δ^9-THC, Δ^8-THC, and CBC (100 µg/mL each in acetonitrile).

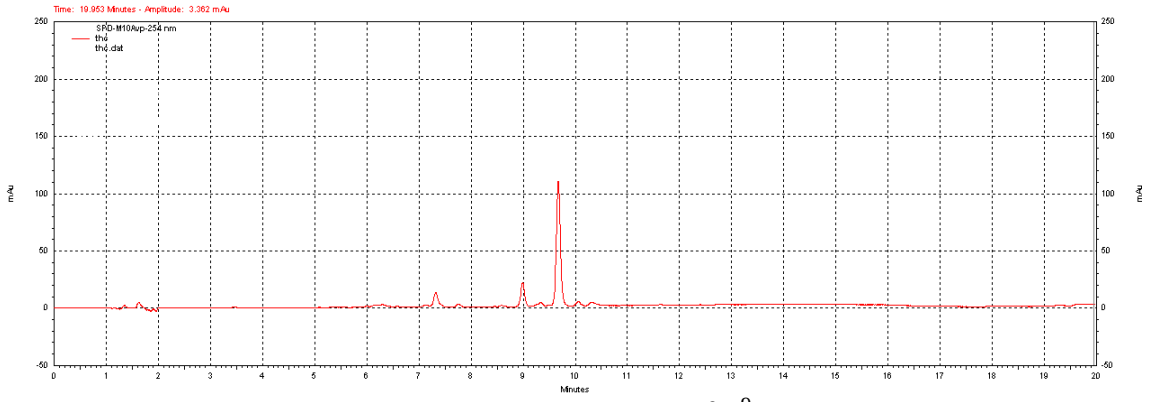

Figure H2: Analytical HPLC method chromatogram of Δ^9-THC standard (1.2 mg/mL in ethanol).

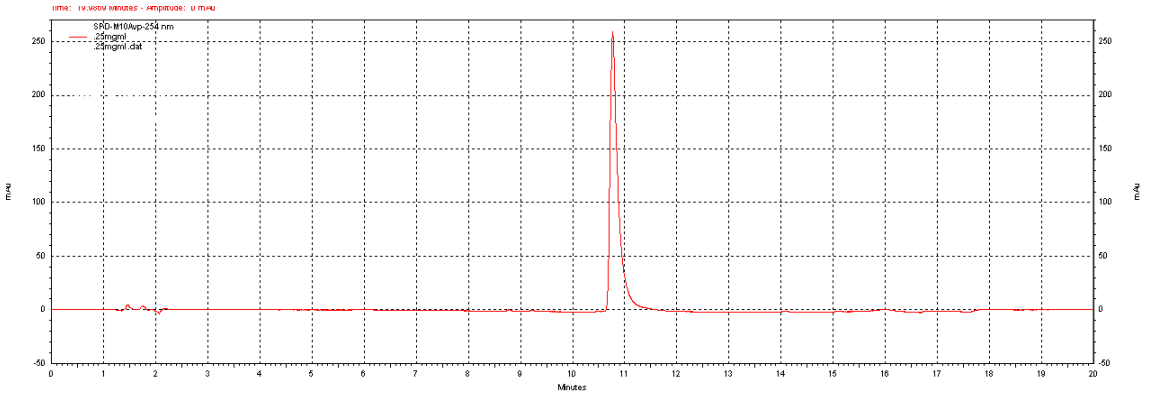

Figure H3: Analytical HPLC method chromatogram of Δ^9-THCA isolated via preparative HPLC (4 mg/mL in ethanol).

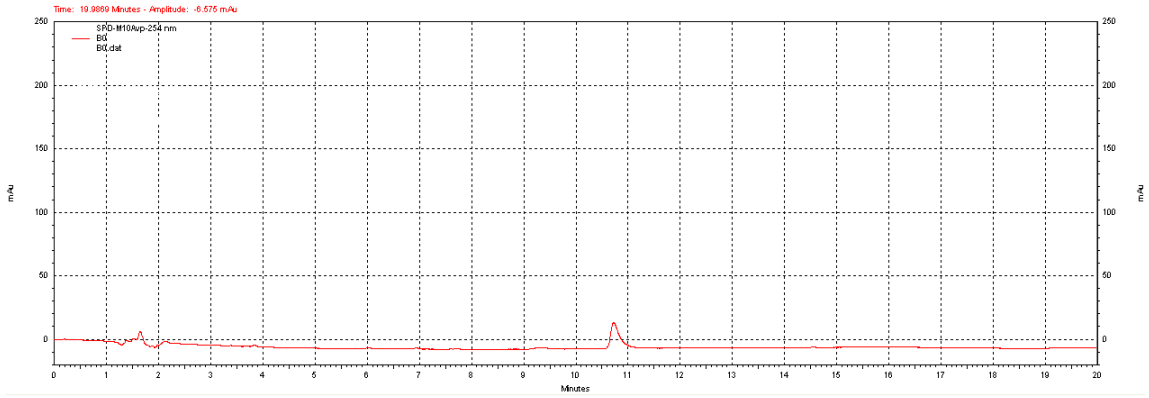

Figure H4: Chromatogram of time = 0 hr aliquot of incubation of Δ^9-THCA with *P. putida.*

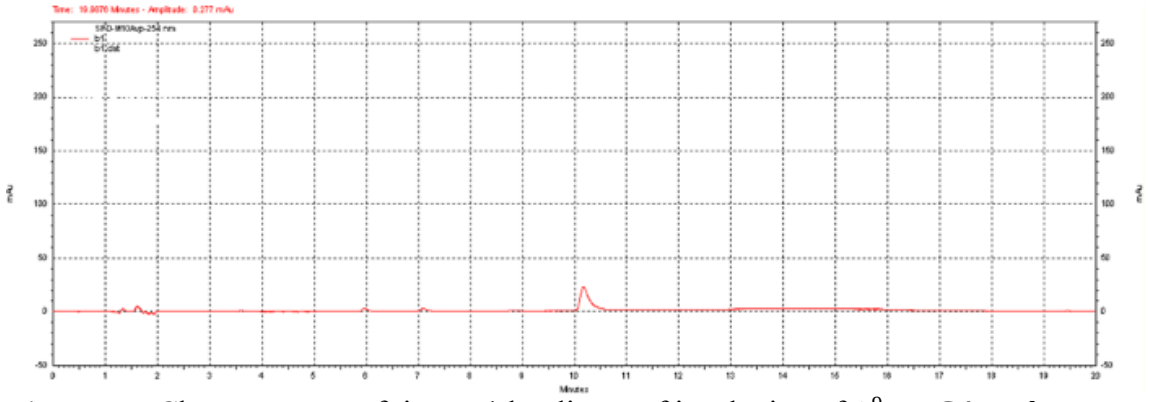

Figure H5: Chromatogram of time = 1 hr aliquot of incubation of Δ^9-THCA with *P. putida.*

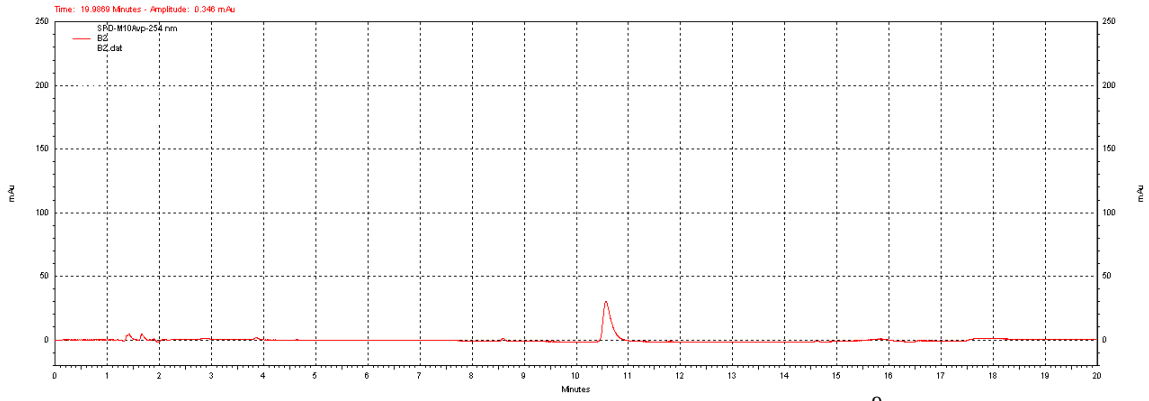

Figure H6: Chromatogram of time = 2 hr aliquot of incubation of Δ^9-THCA with *P. putida.*

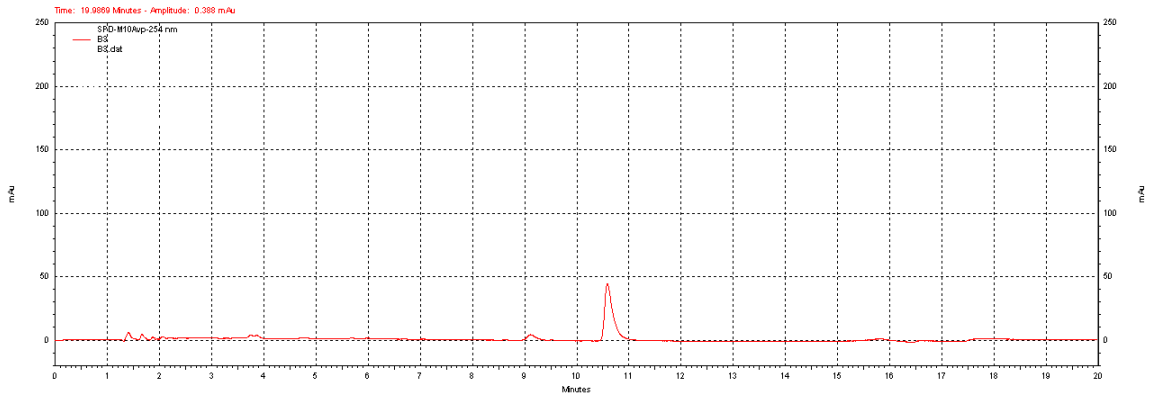

Figure H7: Chromatogram of time = 3 hr aliquot of incubation of Δ^9-THCA with *P. putida.*

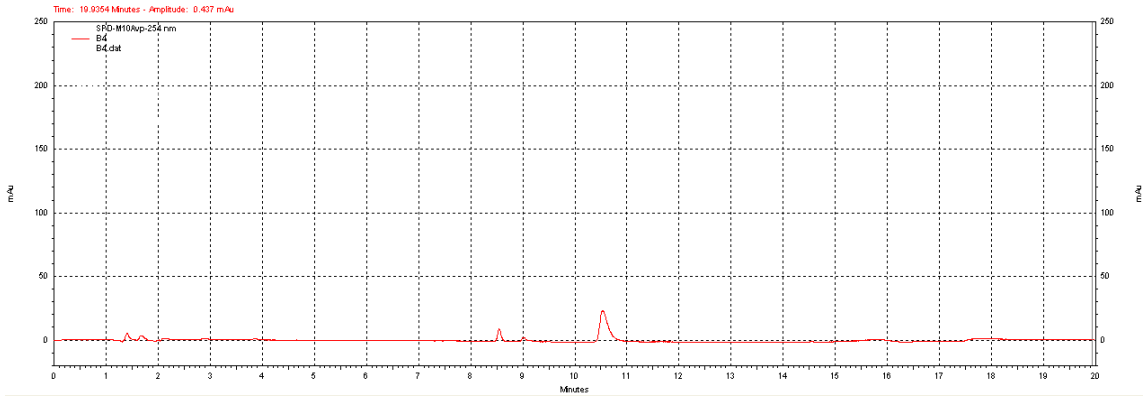

Figure H8: Chromatogram of time = 4 hr aliquot of incubation of Δ^9-THCA with *P. putida.*

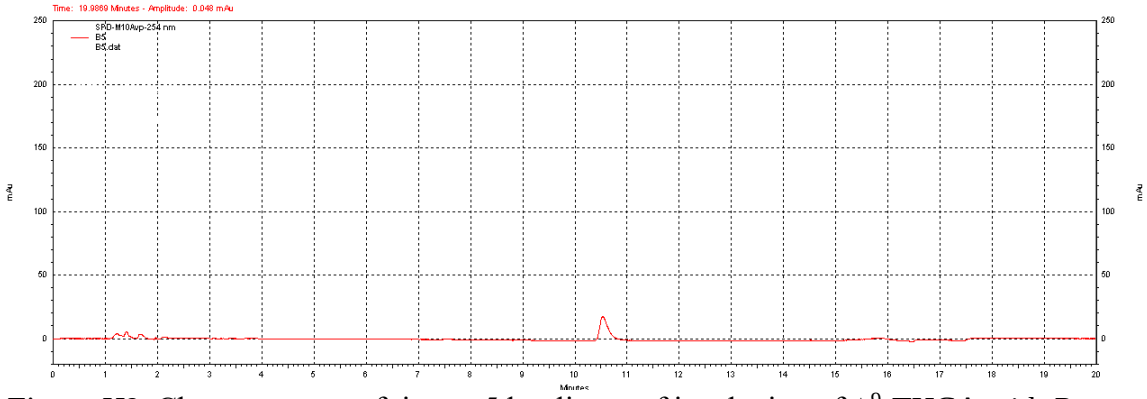

Figure H9: Chromatogram of time = 5 hr aliquot of incubation of Δ^9-THCA with *P. putida.*

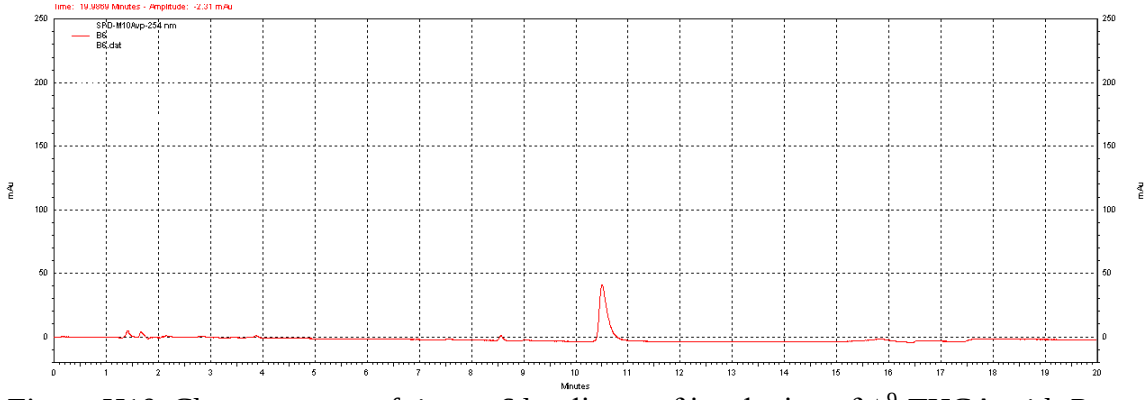

Figure H10: Chromatogram of time = 6 hr aliquot of incubation of Δ^9-THCA with *P. putida.*

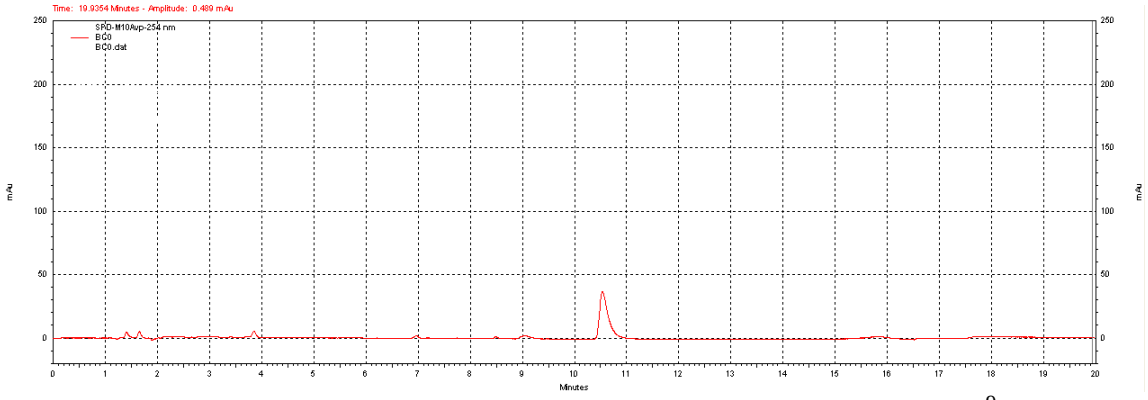

Figure H11: Chromatogram of time = 0 hr control aliquot of incubation of Δ^9-THCA with *P. putida.*

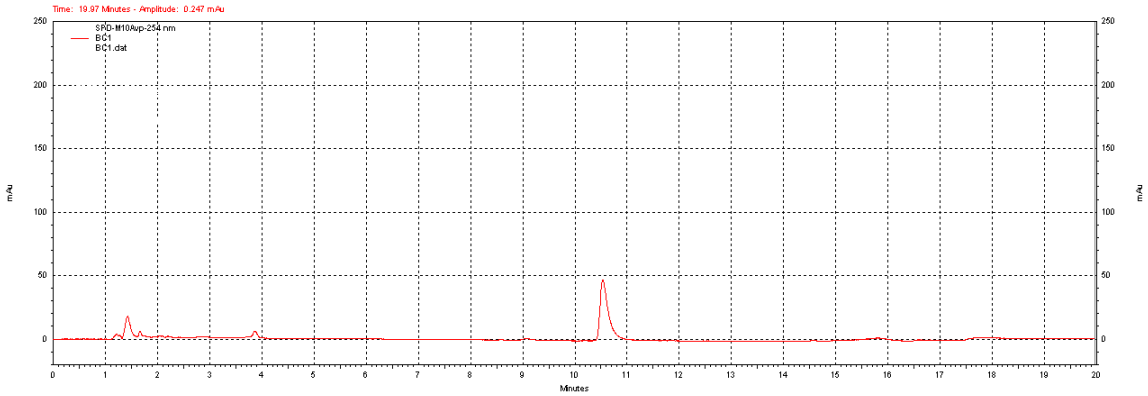

Figure H12: Chromatogram of time = 1 hr control aliquot of incubation of Δ^9-THCA with *P. putida.*

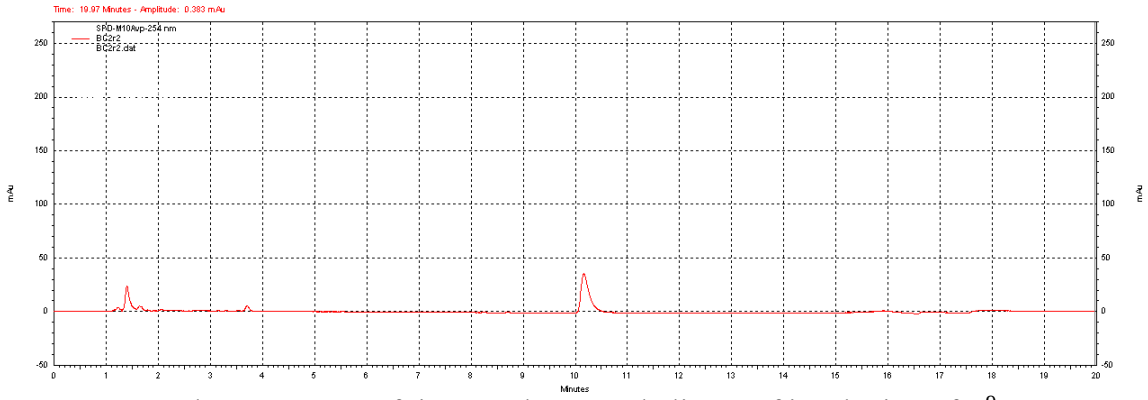

Figure H13: Chromatogram of time = 2 hr control aliquot of incubation of Δ^9-THCA with *P. putida.*

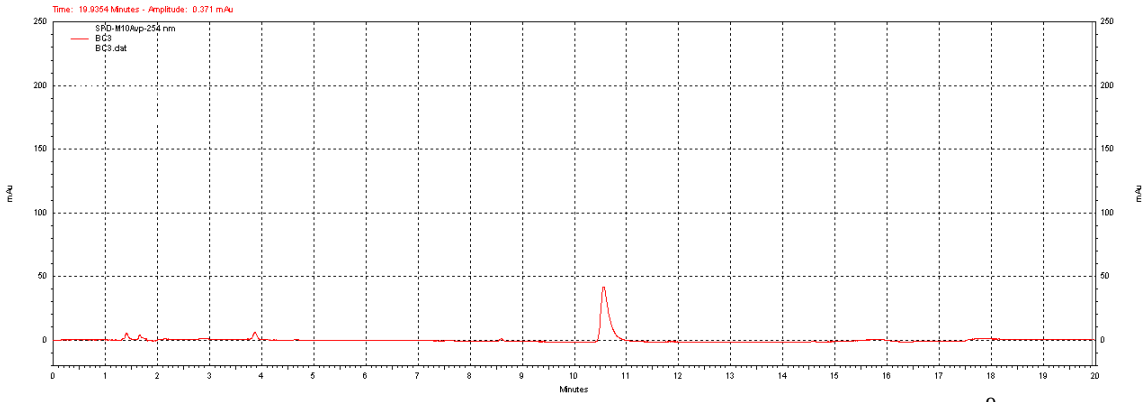

Figure H14: Chromatogram of time = 3 hr control aliquot of incubation of Δ^9-THCA with *P. putida.*

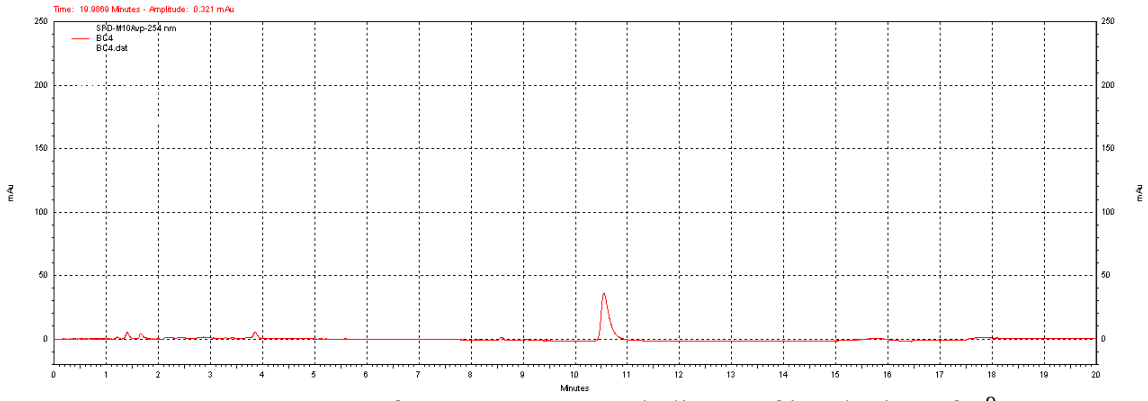

Figure H15: Chromatogram of time = 4 hr control aliquot of incubation of Δ^9-THCA with *P. putida.*

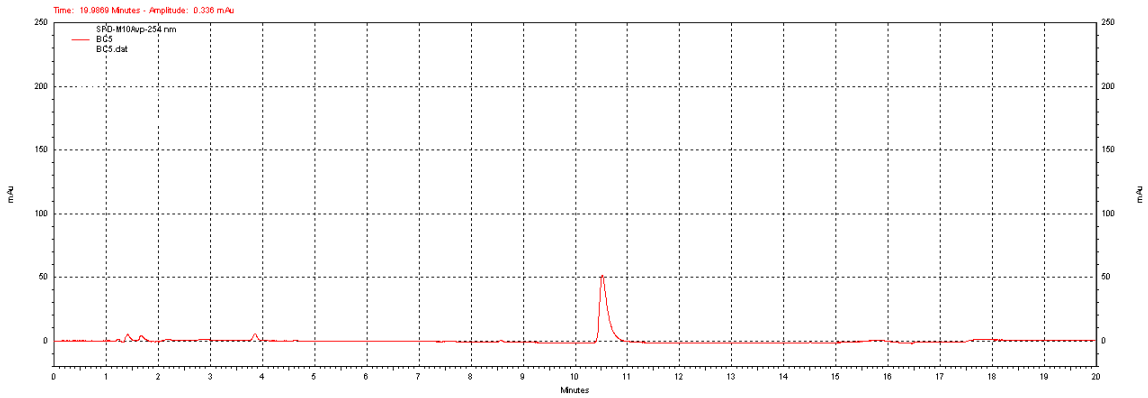

Figure H16: Chromatogram of time = 5 hr control aliquot of incubation of Δ^9-THCA with *P. putida.*

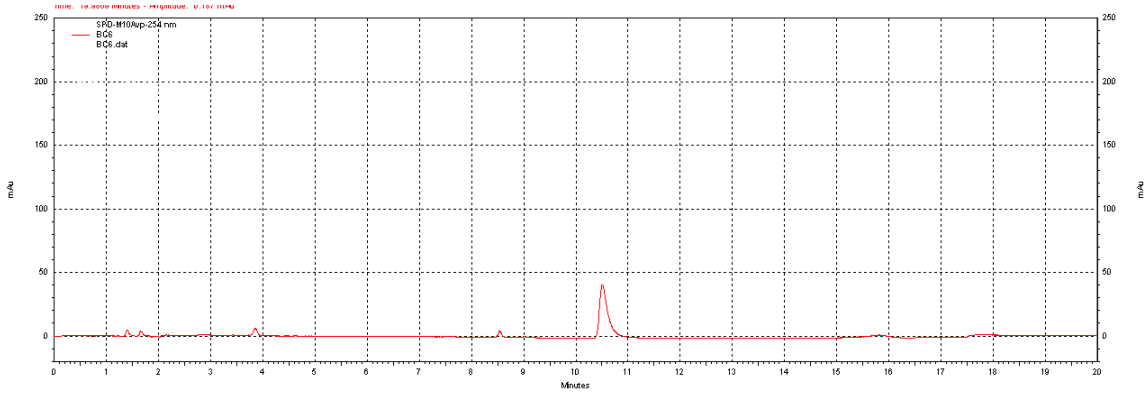

Figure H17: Chromatogram of time = 6 hr control aliquot of incubation of Δ^9-THCA with *P. putida.*

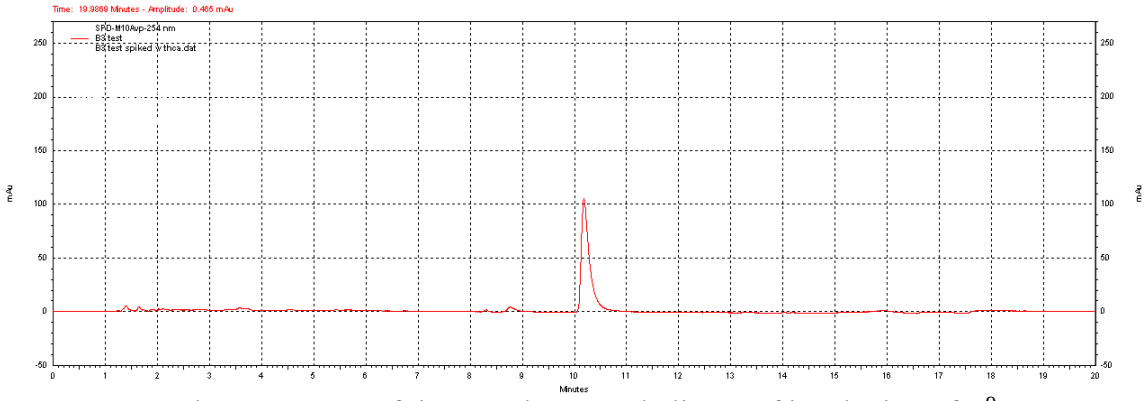

Figure H18: Chromatogram of time = 3 hr control aliquot of incubation of Δ^9-THCA with *P. putida* with 0.1 mg of added Δ^9-THCA.

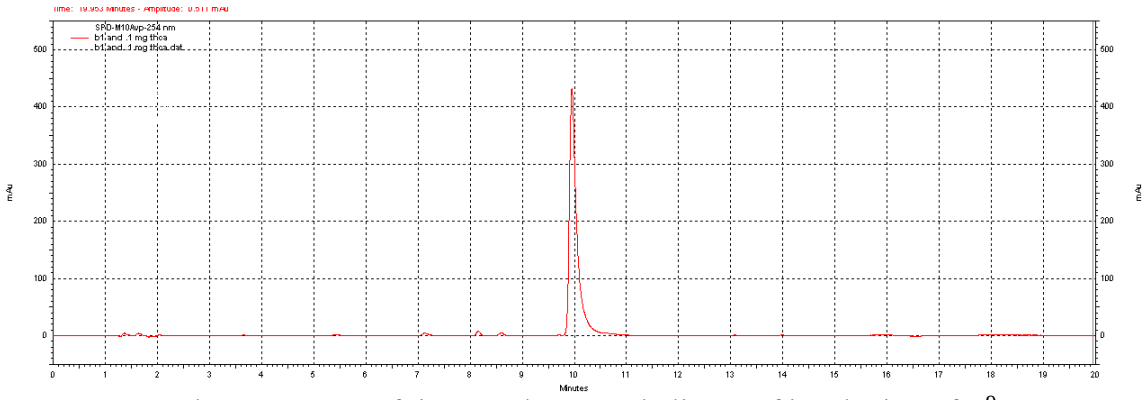

Figure H19: Chromatogram of time = 1 hr control aliquot of incubation of Δ^9-THCA with *P. putida* with 0.1 mg of added Δ^9-THCA.

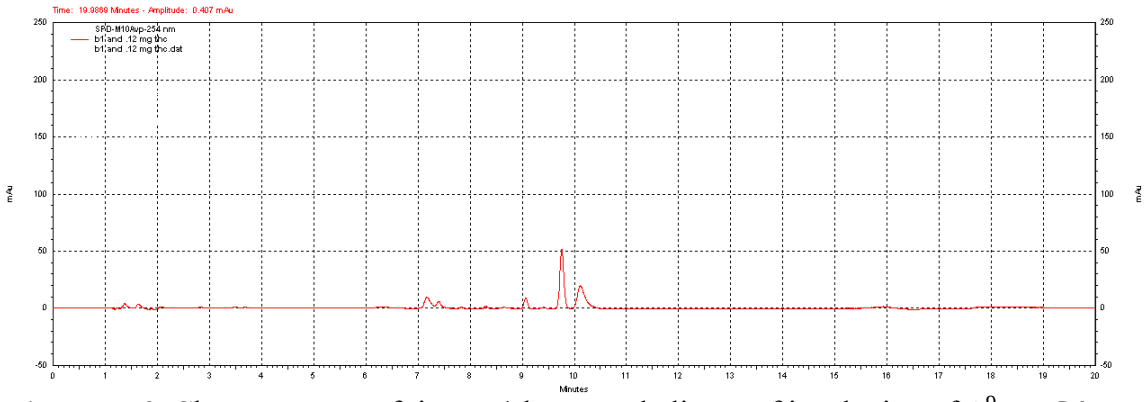

Figure H20: Chromatogram of time = 1 hr control aliquot of incubation of Δ^9-THCA with *P. putida* with 0.12 mg of added Δ^9-THC.